

ABSTRACT

NEVERS, BRANDON LEE. A Model of Saturation Flow Using Traffic Subgroups (Under the direction of Dr. Nagui M. Roupail).

This thesis presents a methodology for estimating saturation flow rates at signalized intersections by traffic subgroups. A subgroup is defined as a group of vehicles of a specific vehicle classification that make a single directional movement from one lane. The subgroup method is founded on the procedures described in the 1997 Highway Capacity Manual (HCM) (Transportation Research Board, 1997) but extends beyond the HCM's lane group model to provide results that can be aggregated at multiple levels. Rather than assuming homogeneous conditions within each lane or lane group as is the case with many capacity guides, the subgroup method decomposes a traffic stream into individual components, each of which have unique saturation headways. Comparisons with the HCM show that under similar assumptions, the subgroup method produces similar saturation flow rates when aggregated at the lane group level. This gives confidence for applying the subgroup approach to estimate individual lane performance.

The most critical element of the subgroup model is the estimation of lane volumes. Lane volume field data were gathered at four sites. Results of an evaluation of lane distribution strategies for estimating lane volumes when a choice is present indicate that the equal back of queue strategy best reflects driver behavior. Based on the observed field data, the equal back of queue strategy outperforms the equal delay strategy and the equal flow ratio strategy which are widely used in various international capacity guides.

A MODEL OF SATURATION FLOW USING TRAFFIC SUBGROUPS

by
BRANDON L. NEVERS

A thesis submitted to the Graduate Faculty of
North Carolina State University
in partial fulfillment of the
requirements for the Degree of
Master of Science

CIVIL ENGINEERING

Raleigh

2000

APPROVED BY:

Dr. Joseph E. Hummer

Dr. John R. Stone

Dr. Nagui M. Roupail
Chair of Advisory Committee

BIOGRAPHY

Brandon Nevers was born May 25, 1974 in Seattle, Washington. He was raised in Auburn, Washington and graduated from Auburn High School in 1992. Brandon attended the University of Idaho and received a Bachelor of Science degree in Civil Engineering in 1996. Following graduation Brandon went to work for Kittelson and Associates, Inc., a transportation engineering firm in Portland, Oregon. Following three years of work at Kittelson & Associates, Inc., Brandon took a leave of absence to pursue a Master of Science degree in Civil Engineering at North Carolina State University, focusing on transportation.

ACKNOWLEDGMENTS

First I would like to thank the Southeastern Transportation Center (STC) for providing partial funding for this work. Also, thanks to the National Institute of Statistical Sciences (NISS) for supplying video tapes that provided valuable field data.

I am indebted to my advisor, Dr, Nagui Roupail, for allowing me the opportunity to work with him and develop a product (this thesis) that began simply as a concept he had founded. His guidance, insight, desire and fellowship provided an invaluable experience and much enjoyment. Also, thanks to Dr. Joseph Hummer and Dr. John Stone for their involvement, review, and support of this work.

Lastly, thanks to all of my friends and family who have supported and encouraged me throughout my time at North Carolina State University.

TABLE OF CONTENTS

LIST OF TABLES	vi
LIST OF FIGURES	vii
1.0 INTRODUCTION	1
1.1 Background	1
1.2 Subgroup Saturation Flow Model	1
1.3 Problem Statement	2
1.4 Scope and Objectives	3
1.5 Organization	4
2.0 LITERATURE REVIEW	6
2.1 Non-Lane Based Saturation Flow Models	6
2.2 Lane Based Capacity Models	9
2.3 Lane Volume Prediction Models	14
2.4 Summary of Review	18
3.0 SUBGROUP-BASED METHODOLOGY	20
3.1 Glossary of Terms	20
3.2 Subgroup Definition	21
3.3 Basic Relationships	22
3.4 Ideal Saturation Flow	26
3.5 Binary Effect of Non-Ideal Conditions	27
3.6 Headway Equivalency Factors	27
3.7 Fraction of Total Flow in Each Subgroup	34
3.8 Lane Flow Allocation Process	39
3.9 Sample Calculation	43
3.10 Comparisons with HCM	48
4.0 LANE VOLUME FIELD DATA COLLECTION AND ANALYSIS	55
4.1 Purpose	55
4.2 Desired Criteria	55
4.3 Selected Sites	57
4.4 Data Collection Method	57
4.5 Summary of Observations	59
4.6 Limitations of the Data	62
4.7 Aggregated Field Data Results	63
4.8 Field Regression Model	72
4.9 Assessment of HCM Lane Utilization Factor	75
4.10 Summary	76
5.0 SUBGROUP LANE DISTRIBUTION MODEL EVALUATION	78
5.1 Evaluation of Lane Distribution Strategies	78
5.2 Implications of Selecting a Lane Distribution Strategy	86
5.3 Parametric Analysis	90
6.0 CONCLUSIONS AND RECOMMENDATIONS	96
6.1 Conclusions	96
6.2 Recommendations for Future Research	97

7.0	REFERENCES	100
APPENDIX A	SUBGROUP WORKSHEETS FOR HCM EXAMPLE	102
APPENDIX B	LANE VOLUME FIELD DATA PER INDIVIDUAL CYCLE.....	107
APPENDIX C	LANE VOLUME DATA PER 15 MINUTES	120
APPENDIX D	LANE DISTRIBUTION MODEL EVALUATION OUTPUT	124
APPENDIX E	RMSE/MAPE OUTPUT FOR INDIVIDUAL INTERSECTIONS.....	132

LIST OF TABLES

Table 3.01: Required Conditions for $U_j = 1$	27
Table 3.02: Detailed Subgroup Calculation: HCM Sample Calculation #1	46
Table 3.03: Lane Group Saturation Flow Rate Comparison - HCM #1.....	49
Table 3.04: Lane Group Saturation Flow Rate Comparison - HCM #2.....	51
Table 3.05: Lane Group Saturation Flow Rate Comparison - HCM #3.....	53
Table 4.01: Regression Output.....	72
Table 4.02: Statistical Evaluation of Empirical Model.....	75

LIST OF FIGURES

FIGURE 3.01. Illustration of Subgroups	23
FIGURE 3.02. Departure Pattern for Left Turning Vehicles	31
FIGURE 3.03. Departure Pattern for Through Vehicles from a Shared Through/Left Lane	33
FIGURE 3.04. Lane Flow Allocation Procedure	40
FIGURE 3.05. 1997 HCM Sample Calculation #1: Volume and Geometric Data	43
FIGURE 3.06. Lane Delay by Distribution Strategy – HCM Sample Calculation #1.....	44
FIGURE 3.07. 1997 HCM Sample Calculation #2: Volume and Geometric Data	50
FIGURE 3.08. 1997 HCM Sample Calculation #3: Volume and Geometric Data	52
FIGURE 4.01. Volume and Geometric Characteristics of Selected Sites Summary of Observations	59
FIGURE 4.02. Field Data Summary	64
FIGURE 4.03. Effect of Left Turn Flow on Through Traffic Distribution	67
FIGURE 4.04. Effect of Subject Approach Flow on Through Traffic Distribution	68
FIGURE 4.05. Effect of Opposing Flow on Through Traffic Distribution.....	69
FIGURE 4.06. Effect of Left Turn * Opposing Flow on Through Traffic Distribution	70
FIGURE 4.07. Effect of Right Turn Flow on Through Traffic Distribution.....	71
FIGURE 5.01. RMSE/MAPE Comparison for All Data Sets	80
FIGURE 5.02. Comparison of MAPE values by Left Turn Flow Regime	82
FIGURE 5.03. Comparison of MAPE values by Subject Flow Regime	83
FIGURE 5.04. Comparison of MAPE values by Opposing Flow Regime	84
FIGURE 5.05. Lane Distribution Strategy Comparison.....	85
FIGURE 5.06. Critical Lane Delay Comparison: Flow Ratio vs. Back of Queue Strategy	87
FIGURE 5.07. Critical Lane Delay Comparison: Delay vs. Back of Queue Strategy.....	88
FIGURE 5.08. Critical Lane Delay Comparison: Volume vs. Back of Queue Strategy	89
FIGURE 5.09. Effect of Opposing Traffic on Lane Distribution.....	91
FIGURE 5.10. Effect of Conflicting Pedestrians on Lane Distribution.....	92
FIGURE 5.11. Effect of Bus Stops on Lane Distribution.....	93
FIGURE 5.12. Effect of Green Time on Lane Distribution.....	94

1.0 INTRODUCTION

1.1 Background

The estimation of saturation flow is arguably the single most important element of a signalized intersection operational analysis. The calculation of performance measures such as average vehicle delay, level of service, capacity, and queue all require saturation flow as an input measure. Accurately predicting measures of effectiveness including delay and level of service require having a means for accurately estimating saturation flow.

The most commonly used guide for estimating saturation flow in the United States is the Highway Capacity Manual (Transportation Research Board, 1997). Transportation engineers utilize the procedures in the HCM to aid in the development of signal timing plans, storage-length requirements for turn bays, and benefit estimates for potential mitigation measures. Ideally, these applications all require the estimation of individual lane performance. In reality however, the Highway Capacity Manual does not provide performance at the individual lane level but rather at the lane group level. For approaches that include multiple shared through turn lanes, a lane group can include as many as two, three or four lanes. When traffic flow within a multi-lane lane group is not homogeneous as is assumed by the HCM lane group model, a more detailed approach for analyzing a traffic stream may be desired.

1.2 Subgroup Saturation Flow Model

An alternative to analyzing signalized intersection approaches by lane groups is to analyze approaches by subgroups. A subgroup is the smallest unit for which a saturation flow rate can be computed. A subgroup is defined as a group of vehicles of unique vehicle type making a single directional movement from a specific lane. The fidelity of the subgroup approach is between that of a microscopic (vehicle-by-vehicle) model and a macroscopic (lane/lane group) model. The strength of the subgroup approach lies in its

flexibility. A subgroup can be defined for any collection of vehicle groups, so long as the saturation headways for each unique vehicle group are known and identical. Subgroup results can be aggregated to provide performance measures at any level (lane, lane group, or approach), by any vehicle type (car or truck), and/or by any directional movement (left, through, or right). Moreover, the subgroup approach can be carried out using the same input that is required by a traditional HCM analysis.

The subgroup saturation flow model can be viewed as an extension of the 1997 HCM procedures. The Headway Equivalency Factors (HEF's) utilized by the subgroup model described in Chapter 3.0 are developed directly from the saturation flow adjustment factors described in Chapter 9 of the 1997 HCM. The major difference between the methods is that the subgroup method requires subgroup volumes as opposed to turning movement volumes for each approach.

For approaches where all movements occur from a single lane (exclusive or shared), the subgroup volumes can be determined assuming the percentage of each vehicle type is known. For cases where one or more movements can take place over multiple lanes (referred to as "choice" lanes), individual lane flows are required. In the absence of field data, which can be costly to obtain and are unknown for future year analyses, lane flows must be estimated.

1.3 Problem Statement

For the majority of practical applications involving "choice" lanes, individual lane flows are unknown. Herein lies the difficulty associated with implementing the subgroup methodology. An estimation of lane flows is required, either through the use of an empirical model or an operational-based performance criterion.

Three signalized intersection methodologies, including the Australian (Akcelik, 1981), Canadian (Teply, *et. al.*, 1995), and Swedish (Peterson, *et. al.*, 1995) methods, employ a lane-based model and estimate individual lane flow. These three methodologies apply an equal flow-ratio strategy across the lanes where a choice exists to

estimate individual lane flow. However, no field validation studies have been reported in any of the capacity guides that assess the accuracy of the flow-ratio strategy and whether it is the strategy used by motorists for lateral deployment.

The estimation of saturation flow at the lane level is highly dependent upon the amount of traffic in each individual lane. Thus, the accuracy of subgroup performance measures (i.e., delay, back of queue, etc.) is dependent not only on the estimation of saturation flow, but on the estimation of lane volume flow.

1.4 Scope and Objectives

This thesis provides a methodology for estimating saturation flow by subgroups and evaluates one of four parameters required by the subgroup method – the estimation of lane flows. The methodology described in Chapter 3.0 includes a comparison with the HCM to validate the results of the subgroup method at the lane group level when the same assumptions and input parameters are applied.

Six lane distribution strategies are evaluated against observed field data. The lane distribution strategies evaluated include equal back of queue, equal average queue, equal delay, equal flow ratio, equal volume, and the Bonneson method (1998). The Bonneson method is a closed-form procedure that estimates individual lane volumes and saturation flow using an equal flow ratio principle. The development of these strategies is based on a synthesis of the literature and the availability of performance measures calculated as part of the subgroup model.

Data were collected at four signalized intersections. Three of the intersections are located in Raleigh, North Carolina. The other is in Chicago, Illinois. The collected data consist of individual lane volumes by turning movement for the major-street approaches. All approaches include two lanes and have permissive, shared turns.

The analyses are based on 15-minute aggregations of the field data, although data were collected for each individual cycle. The data are representative of morning and evening peak hour conditions.

The following items outline the objectives of this thesis.

- Review existing methods used to estimate saturation flow and lane volumes.
- Develop a methodology for calculating saturation flow rates by subgroup.
- Analyze field data and examine the relationship between the distribution of through traffic across choice lanes. Use field data to predict the amount of through traffic across choice lanes.
- Compare the lane distributions observed in the field with those predicted using the 1997 HCM default lane utilization factor and with other lane distribution strategies found in the literature review.
- Determine the implications of using one strategy versus another in terms of the average control delay of the critical lane for a variety of operating conditions.
- Develop a recommended lane distribution strategy for use in the application of the subgroup approach.

1.5 Organization

This thesis is organized in seven chapters. Chapter 1.0 provides a definition of the problem statement and an outline of the scope and objectives. A literature review, provided in Chapter 2.0, summarizes the existing saturation flow models and lane distribution strategies for signalized intersections. Chapter 3.0 provides a detailed description of the subgroup model. Each component of the model is discussed, including the nine Headway Equivalency Factors and the potential lane distribution strategies. The Chapter presents a general procedure for estimating lane flow and includes an example using 1997 HCM Sample Calculation #1.

A discussion of the criteria used to select sites for data collection is provided in Chapter 4.0 along with a description of the chosen sites. Chapter 5.0 summarizes the results of the field data collection effort and presents a regression model for estimating individual lane flow. Chapter 6.0 provides the conclusions and recommendations.

Chapter 6.0 provides the evaluation results of the lane distribution strategies.
Lastly, Chapter 7.0 presents the conclusions and findings.

2.0 LITERATURE REVIEW

This chapter provides an overview of methods used to estimate saturation flow rates for signalized intersections. The 1997 *Highway Capacity Manual* (HCM) (Transportation Research Board, 1997) is the most commonly used methodology in the United States for analyzing signalized intersections; however, many other methodologies exist throughout the world including those published in the Canadian (Teply, *et al.*, 1995), Swedish (Peterson, *et al.*, 1995), and Australian (Akcelik, 1981) capacity guides. Of the four methodologies reviewed, the HCM is the only non lane-based procedure. The remaining three procedures provide performance measures for individual lanes and also include a lane distribution model to estimate the amount of traffic on each lane. In addition, a method developed by Bonneson (1998) is reviewed that estimates the proportion of turning movement traffic in a shared lane, thus yielding the distribution of traffic across each lane on a multi-lane approach.

2.1 Non-Lane Based Saturation Flow Models

The 1997 HCM (Transportation Research Board, 1997) is the only non-lane based analysis procedure that is included in the literature review of this thesis. In the 1997 HCM, saturation flow is calculated at the *lane group* level. A lane group is defined as “one or more lanes that accommodate traffic and have a common stop line and capacity shared by all vehicles.” The general form for estimating the saturation flow (s) of a lane group as provided in Equation 9-10 of the 1997 HCM follows.

$$s = s_o \cdot N \cdot f_w \cdot f_{HV} \cdot f_g \cdot f_p \cdot f_{bb} \cdot f_a \cdot f_{LU} \cdot f_{RT} \cdot f_{LT} \quad (2.01)$$

where: s_o = ideal saturation flow rate (vph),

N = number of lanes within the lane group, and

f_j = adjustment factors for lane width, heavy vehicles, grades, parking, bus blockage, area type, lane utilization, right-turn movements, and left-turn movements.

Analyzing approaches by lane groups simplifies the analysis process by eliminating the requirement for individual lane volumes. The lane group procedure inherently assumes that traffic conditions are homogeneous across all lanes within a lane group. This essentially implies that all vehicles within the lane group experience the same saturation flow rate and delay. This assumption is oftentimes not held true when the following conditions are present:

- pedestrians conflicting with right-turn movements,
- bus activity on the curb lane,
- parking on the curb lane,
- opposing traffic conflicting with permissive left-turn maneuvers, and
- upstream/downstream geometric effects such as lane drops, tapers, freeway on-ramps, etc.

To account for the effect that impedances have on the distribution of lane volumes, the HCM introduces a *Lane Utilization Factor* (LUF). According to the HCM, the LUF “accounts for the unequal distribution of traffic ... and provides an adjustment to the saturation flow rate to reflect the rate at which vehicles are discharged

from a lane group when variations in lane use exist.” The HCM equation for LUF (Equation 9-11) follows.

$$f_{LU} = \frac{v_g}{v_{g1} \cdot N} \quad (2.02)$$

where: v_g = lane group flow rate,

v_{g1} = highest lane flow, and

N = number of lanes.

Default values for the LUF range between 0.88 and 1.0. The default values are based on the approach type and number of lanes within a lane group, not the degree of impedance that intuitively causes traffic to shift.

Further, to determine the lane group saturation flow adjustment for curbside impedances such as bus stops and parking, the HCM averages the adjustment factor for the outside lane with the adjustment factor for the interior lane(s), which is 1.0 (no effect). For a lane group consisting of two lanes where the saturation adjustment factor due to the impedance on the outside lane is 0.9, the average adjustment factor is $\frac{.9+1.0}{2} = .95$. Averaging the adjustment factors implicitly assumes that the volumes in both lanes are equal. The assumption is oftentimes invalid since curbside impedances tend to result in a shift of through traffic to the inside lane. The reverse is true for cases where permissive left-turn movements block through movements from a shared lane.

Since the 1997 HCM analysis procedures are based on lane groups, the methodology does not include a lane distribution model, with one exception – permissive

left-turns from a shared through lane. In this case, the fraction of left-turn vehicles that depart from the shared through/left lane is calculated assuming an equal degree of saturation across the shared through/left lane and the adjacent lane. The equation for calculating the proportion of left turns in a shared lane (P_L) as provided in Equation 9-17 of the 1997 HCM follows.

$$P_L = P_{LT} \left[1 + \left(\frac{(N-1)g}{g_f + \frac{g_u}{E_{LI}} + 4.24} \right) \right] \quad (2.03)$$

where: P_{LT} = proportion of left turns in the lane group,

N = number of lanes in the lane group,

g = effective green time for the lane group (sec),

g_f = green time before the first left turn arrives (sec), and

g_u = unopposed green time (sec).

Knowing P_L and the left turn volume yields the amount of through traffic in the inside lane.

2.2 Lane Based Capacity Models

The Australian (Akcelik, 1981), Canadian (Teply, *et al.*, 1995), and Swedish (Peterson, *et al.*, 1995) Capacity Guides provide procedures for estimating individual lane performance. The general form of the equations for calculating adjusted lane saturation flows is similar to the multiplicative HCM model shown in Equation 2.01. In addition to

the standard adjustment factors shown in Equation 2.01, the Australian and Swedish methods provide an adjustment factor to account for the effect of short lanes.

Each method provides a means for estimating individual lane flow when a choice exists¹. The Canadian procedure is non-iterative and can be carried out by hand, whereas the Swedish and Australian methods apply an iterative approach that requires software. A description of the lane flow allocation procedure used in each method follows.

2.2.1 Canadian Procedure

The Canadian (Teply, *et al.*, 1995) method incorporates a five-step process to estimate the distribution of traffic across shared lanes. The underlying assumption is that equal flow ratios (v/s) will be achieved across the lanes where a choice exists. The manual states that the equal flow ratio principle is used as a “surrogate” to reflect the intention of drivers’ which is to join either the lane with shortest queue or the lane that affords the least delay. The first step in the lane allocation procedure is to estimate the saturation flow for each movement assuming that it operates from an exclusive lane. For cases where permissive left-turns exist, the initial saturation flow estimation can account for the opposing traffic, however the estimation assumes that the left-turn operates from an exclusive lane. The saturation flows for the left-turn and right-turn movements are divided into the saturation flow rate for the through movement to determine the through equivalency factor k for each movement. The example provided in the guide assumes a left-turn saturation flow of 600 vph and a right-turn saturation flow of 900 vph. Thus, the

¹ A choice lane refers to a case where a vehicle making a particular directional movement (left, through, or right) can choose between multiple lanes.

resulting k factor for the left-turn movement is $1800/600$ or 3.0 and the right-turn equivalency is $1800/900$ or 2.0.

The equivalency factors (k) are multiplied by the turning movement volumes to obtain equivalent through passenger car flows for each movement. The total equivalent through flows are summed across all movements and divided by the number of lanes to determine the equivalent through flow per lane. The through traffic is distributed such that the equivalent through flow rate of each lane is equal (equal flow ratio principle). Lastly, the turning movement flows are multiplied by the k factor to convert the flows back to normal passenger cars units from through passenger car units.

Once the volumes are assigned, the saturation flow rates are calculated for each lane based on the general form of the saturation flow rate model shown in Equation 2.01.

The five-step lane distribution procedure is non-iterative and can be carried out by hand. The shortcoming of the model is that the initial saturation flow estimates are developed assuming exclusive lanes. Thus, the effect that the proportion of turning traffic within a shared lane has on the lane's saturation flow is not accounted for in the lane flow allocation process. In reality, the saturation flow for movements within shared lanes is dependent upon the volume of the other movements in the lane.

2.2.2 Swedish Procedure

The Swedish method (Peterson, *et al.*, 1995) allocates traffic to lanes where a choice exists by assuming an equal degree of saturation (volume/capacity) across choice lanes. It should be noted that for lanes with equal effective green times, lanes with equal degree of saturation (v/c) will also have equal flow ratios (v/s).

The Swedish method uses an iterative procedure in order to achieve equal degree of saturation across choice lanes. The first step of the allocation process is to develop the non-ideal adjustment factors for each lane. Traffic is assigned to each lane such that the sum of the turning movement volumes in each lane equals the total turning movement volumes for the approach. Lane saturation flow rates are calculated based on the assigned volumes. The volumes are adjusted until equilibrium is achieved or a defacto turn lane results. The iterative procedure is necessary since the saturation flow rate of a lane is dependent upon the composition of traffic in that lane. The Swedish manual states that the assumption of equal degree of saturation has “not been validated as far as is known.”

2.2.3 Australian Procedure

The Australian lane allocation procedure (Akcelik, 1981), which is carried out in the SIDRA-2 (Akcelik, 1990) software program, uses an equal degree of saturation deployment strategy identical to that described for the Swedish (Peterson, *et al.*, 1995) method. Again, the equal degree of saturation strategy is identical to the equal flow ratio strategy for lanes that have the same effective green times.

A unique aspect of the Australian model is that it accounts for the under-utilization of a lane. Lane under-utilization may occur due to impedances at an intersection (bus, parking, pedestrian blockages, etc.) or due to downstream influences such as a lane drop or a heavily used freeway access. SIDRA-2 accounts for lane under-utilization through the use of a lane-utilization ratio (ρ_i) shown below.

$$r_i = \frac{y_i}{y} \quad (2.04)$$

where y_i is the flow ratio for lane i and y is the flow ratio of the critical lane. Thus, a lane utilization of 1 indicates that all “choice” lanes have equal flow ratios. A value less than one indicates that lane i is less utilized than the critical lane.

In the discussion of the Australian procedure, Akcelik describes the allocation of traffic across choice lanes as, in part, a behavioral issue (e.g., Why does a driver choose a lane?) (Akcelik, 1989). It is well stated in transportation literature that drivers attempt to minimize their travel time on a given link (Papacostas and Prevedouros, 2001). However, there are inherent differences in the decisions drivers make while traveling from point A to point B. Route choice decisions are typically based on the shortest perceived travel time. Intersection maneuvers, however, are more tactical and based not only on minimizing perceived travel time but also on avoiding impedances at the intersection (Akcelik, 1989). The Australian method applies the equal degree of saturation criterion to best represent the “tactical” behavior of drivers at signalized intersections. The equal degree of saturation method is applied assuming that drivers, in general, will choose lanes with minimum congestion. Akcelik found that the equal degree of saturation strategy gives a solution between the equal delay and equal queue strategies (1989). Thus, the equal degree of saturation criterion does not result in minimum delay (Akcelik, 1984).

2.3 Lane Volume Prediction Models

Bonneson (1998) presents a model that estimates individual lane volumes and saturation flow rates. Bonneson acknowledges that one factor that can reduce a lanes' saturation flow is the presence of turning movements in a shared through lane. The slower discharge rates of turning vehicles tend to discourage through vehicles from using the lane when given a choice. Bonneson developed a closed-form model that estimates the percentage of turning vehicles in a lane and the resulting saturation flow rate of the lane. His model is based on the work of Lieberman (1980) who hypothesizes that drivers will choose the lane that minimizes their perceived travel time. Bonneson, like Akcelik, uses the principle of equal flow ratio to model this behavior. Bonneson determines the percentage of turning traffic in a shared lane and its saturation flow based on the following relationship:

$$\frac{v_i}{s_i} = \frac{\sum_{i=1}^n v_i}{\sum_{i=1}^n s_i} \quad (2.05)$$

where: v_i = flow rate in lane i

s_i = saturation flow rate in lane i

n = number of through lanes on the approach

Bonneson notes in his paper that the equal flow-ratio approach is embedded in the HCM procedures for shared lanes (as discussed earlier in this paper). However, he points out that the HCM procedure does not account for the effect of right-turning traffic in the adjacent lane. Thus, the amount of through traffic in the left-turn lane is likely

underestimated since high volumes of right-turning traffic would encourage more through traffic to use the inside lane.

Bonneson developed a closed form solution that estimates the percentage of traffic in a shared lane. The assumption is that the percentage of turning traffic in a lane is independent of the level of subject and opposing volume. In addition, the Bonneson distribution model accounts only for the effect of turning traffic. Effects of buses, parking, pedestrians, etc. are not considered. The equations for calculating the proportion of left-turning vehicles (P_L) and right-turning vehicles (P_R) in each lane are shown below.

$$P_L = \frac{-b + \sqrt{(b^2 - 4ac)}}{2a} \leq 1.0 \quad (2.06)$$

with

$$a = R(E_L - 1) \frac{g_f}{g} \quad (2.07)$$

$$b = R \left(\frac{g_f}{g} + \frac{g_u}{g} \right) - P_{LT} (E_L - 1) \left[\frac{g_f}{g} + (n-1)f_s \right] \quad (2.08)$$

$$c = -P_{LT} \left[\frac{g_f}{g} + \frac{g_u}{g} + (n-1)f_s \right] \quad (2.09)$$

$$R = 1 + P_{RT}(E_R - 1) \quad (2.10)$$

and

$$P_R = P_{RT} \frac{\frac{s_1}{s_t} + (n-1)f_s}{f_s - P_{RT} \left[\frac{s_1}{s_t} + (n-2)f_s \right] (E_R - 1)} \leq 1.0 \quad (2.11)$$

where: E_L = through headway equivalency factor for left-turn movement,

E_R = through headway equivalency factor for right-turn movement, and
 f_s = maneuver factor (default = 0.91).

In addition to developing a closed-form solution, Bonneson introduces a lane change probability factor to account for the likelihood that drivers will maintain their lane position under low and high flow conditions. Bonneson theorizes that the probability of a lane change is a function of the motive for a lane change (which increases as subject flow increases) and the opportunity for a lane change (which decreases as subject flow increases). The function used to estimate the probability of a lane change (p_{lc}) is shown below:

$$P_{lc} = 1 - \left(2 \frac{v_a}{n s_{lc}} - 1 \right)^2 \geq 0.0 \quad (2.12)$$

where: v_a = approach flow rate

n = number of lanes on the approach

s_{lc} = maximum flow rate that will allow any lane changes.

The value s_{lc} is represented by $3600/h_{lc}$ where h_{lc} is the minimum acceptable time headway for a lane change. Bonneson assumes a value of 4.0 seconds per vehicle for the minimum acceptable headway factor in his analysis. Based on the function shown in Equation 2.12, the maximum probability of a lane change (1.0) occurs when the lane change flow ratio ($\frac{v_a}{n s_{lc}}$) is equal to 0.50. Assuming an h_{lc} factor of 4.0 sec/veh (thus, s_{lc} = 900 vph), the maximum lane change probability is achieved when the approach volume equals 450 vehicles per hour per lane. The theory behind this concept is that under low

flow conditions, drivers will maintain their lane position, irrespective of operating conditions, since both lanes likely are operating well within acceptable levels of service. However, under high flow conditions, drivers may want to change lanes but are unable to simply because of a lack of available gaps in the traffic stream. Thus, the optimum traffic level for lane changing occurs at a medium volume level (in this case, 450 vphpl) since under this condition drivers can reduce their delay by choosing an optimal lane and there are plenty of gaps available to make a lane change. The p_{lc} factor is applied to the right-turn and left-turn equivalency factors as shown below.

$$E_L^* = (E_L - 1)P_{lc} + 1 \quad (2.13)$$

$$E_R^* = (E_R - 1)P_{lc} + 1 \quad (2.14)$$

The result is that under extreme low volume and high volume conditions, the probability of a lane change approaches zero and the left-turn and right-turn equivalents approach 1.0. This implies that lane volumes are equal under these conditions.

Bonneson conducted a sensitivity analysis to test his model with field data; however, the data were only collected at unsignalized intersections. He also performed a sensitivity analysis using theoretical data and tested it versus the 1994 HCM method. The analysis shows that the HCM overestimates the amount of through traffic in the shared lane in comparison to the Bonneson method, thus underestimating the saturation flow of the inside lane in the range of 100-200 vph.

2.4 Summary of Review

The *Highway Capacity Manual* (Transportation Research Board, 1997) is the most widely used methodology in the United States for analyzing signalized intersections. Results are provided at the lane group level to avoid the need for obtaining individual lane volumes. In order to account for volume differences across lanes in a multi-lane lane group, a Lane Utilization Factor (LUF) is applied. The default values, which are used most exclusively, are based on the number of lanes and configuration of the approach. The default LUF values do not take into consideration impedances at the intersection nor the level of traffic on the subject and opposing approaches.

To date, there are three signalized intersection analysis models that provide individual lane performance: Canadian (Teply, *et al.*, 1995), Swedish (Peterson, *et al.*, 1995), and Australian (Akcelik, 1981). The Canadian is the simplest method as it is non-iterative and can be carried out in a single pass. The Swedish and Australian models are iterative and use an equal degree of saturation (volume-to-capacity ratio) strategy to allocate individual lane traffic. The equal degree of saturation strategy is identical to the equal flow ratio strategy (which is used in the Canadian method) when the effective green times for approach movements are equal.

Bonneson developed a closed-form model based on the work of Lieberman that estimates the percentage of turning traffic in a shared lane as well as the saturation flow rate of the shared lane. The model is based on the principle of equal flow ratio. The model assumes that the proportion of turning traffic in a shared lane is independent of the approach volumes. Bonneson introduces a lane change probability factor that accounts

for conditions of low and high traffic where drivers, theoretically, are not likely to change lanes.

Lastly, based on the literature review performed, there is no evidence of that field validation has been performed for any of the lane flow allocation models.

3.0 SUBGROUP-BASED METHODOLOGY

This chapter provides an overview of the subgroup saturation flow model for signalized intersections. In addition, this chapter provides a discussion of each parameter and includes an example that demonstrates how the subgroup method is applied. The lane group saturation flows predicted by the subgroup and HCM methods are compared for three examples. The comparison attempts to highlight the similarities and differences between the two methods when both are applied using the same assumptions.

3.1 Glossary of Terms

The following variables are used throughout this chapter:

f	traffic subgroup designation
F	total number of subgroups
j	index of a specific non-ideal condition related to traffic, geometry or control
J	total number of non-ideal conditions
l	lane designation
L	total number of lanes on an approach
p_f	proportion of total flow in F that occurs in subgroup f
h_f	average saturation headway for subgroup f
E_f	through passenger car equivalent for subgroup f
h_F	average saturation headway for the entire traffic group F
h_i	ideal through passenger car saturation headway
E_j	through passenger car equivalent for non-ideal condition j
U_{fj}	binary variable – equal to 1 if subgroup f is effected by non-ideal condition j , zero otherwise
E_{fj}	through passenger car equivalent for subgroup f under non-ideal condition j
M_l	number of turning movements serviced in lane l
C_l	number of vehicle types serviced in lane l
g_p	effective green time for a protected turn (s)
g	effective green time for a through movement or permitted turn (s)
E_{lo}	left turn passenger car equivalent in protected phasing (default = $1/0.95$)
g_q	time it takes to clear the opposing queue in a permitted phase (s)
g_f	time until the first left turn arrives in the subject lane (s)
E_{ll}	left turn passenger car equivalent in permitted phasing

- $u_s =$ 1 if the approach opposing the left turn subgroup is in a single lane, zero otherwise
- $g_{diff} =$ opposing queue green time remaining after the first left turn on the subject approach arrives
- $E_{l2} =$ left turn passenger car equivalent during opposing queue discharge from a single opposing lane
- $E_R =$ right turn passenger car equivalent
- $E_L =$ left turn passenger car equivalent
- $E_{LT}^T =$ through passenger car equivalent for a through movement in a shared through/left turn lane
- $S_F =$ prevailing saturation flow rate
- $S_i =$ ideal saturation flow rate
- $E_{r0} =$ right turn passenger car equivalent in protected phasing (default = $1/0.85$)

3.2 Subgroup Definition

A traffic stream is composed of individual vehicles that have unique time headway characteristics. Attributes that influence the time headway of vehicles at signalized intersections include the vehicle type, directional movement, and lane the vehicle is traveling in. As discussed in Chapter 2, the *Highway Capacity Manual* develops saturation flow estimations at the lane group (macroscopic) level. While this method is simple to carry out, it essentially treats a group of lanes as a single traffic stream in which every vehicle has the same headway. For cases where more fidelity is desired, a user could apply a microsimulation model such as CORSIM (Federal Highway Administration, 1996). Microscopic simulation models provide, arguably, the most realistic representation of traffic flow. However, the benefits gained from using a microsimulation model, particularly for a single, isolated intersection, are generally offset by the costs of coding the model.

The subgroup model provides performance measures at a level between a microsimulation model and a macrosimulation model. By definition, a subgroup represents the smallest unit for which a saturation flow rate can be computed. Thus, a subgroup consists of a group of vehicles of unique type (car or truck) making a single directional movement (left, through, or right) from one lane. The basic assumption is that

each traffic subgroup within the approach has a fixed average headway at saturation. This headway is formed from the inherent properties of each subgroup and is affected by the non-ideal conditions that the subgroup is exposed to (e.g., parking, pedestrian conflicts, opposing traffic, buses, etc.).

3.3 Basic Relationships

Based on the number of turning movements allowed in each lane (M_l), the number of vehicle types in each lane (C_l), and the number of lanes on an approach (L), the maximum number of subgroups (F) on a single intersection approach can be estimated as follows:

$$F = \sum_{l=1}^L M_l \times C_l \quad (3.01)$$

For example, a three lane approach serving passenger cars and trucks in which the middle lane contains through-only vehicles, while the inner and outer lanes contain a combination of through and turning vehicles will have $F = (2 \cdot 2) + (1 \cdot 2) + (2 \cdot 2) = 10$ subgroups (see Figure 3.01). It should be noted that F can be defined in any arbitrary manner chosen by the user. For example, it could include only the through vehicle subgroups, in which case $F = (1 \cdot 2) + (1 \cdot 2) + (1 \cdot 2) = 6$ subgroups in this example.

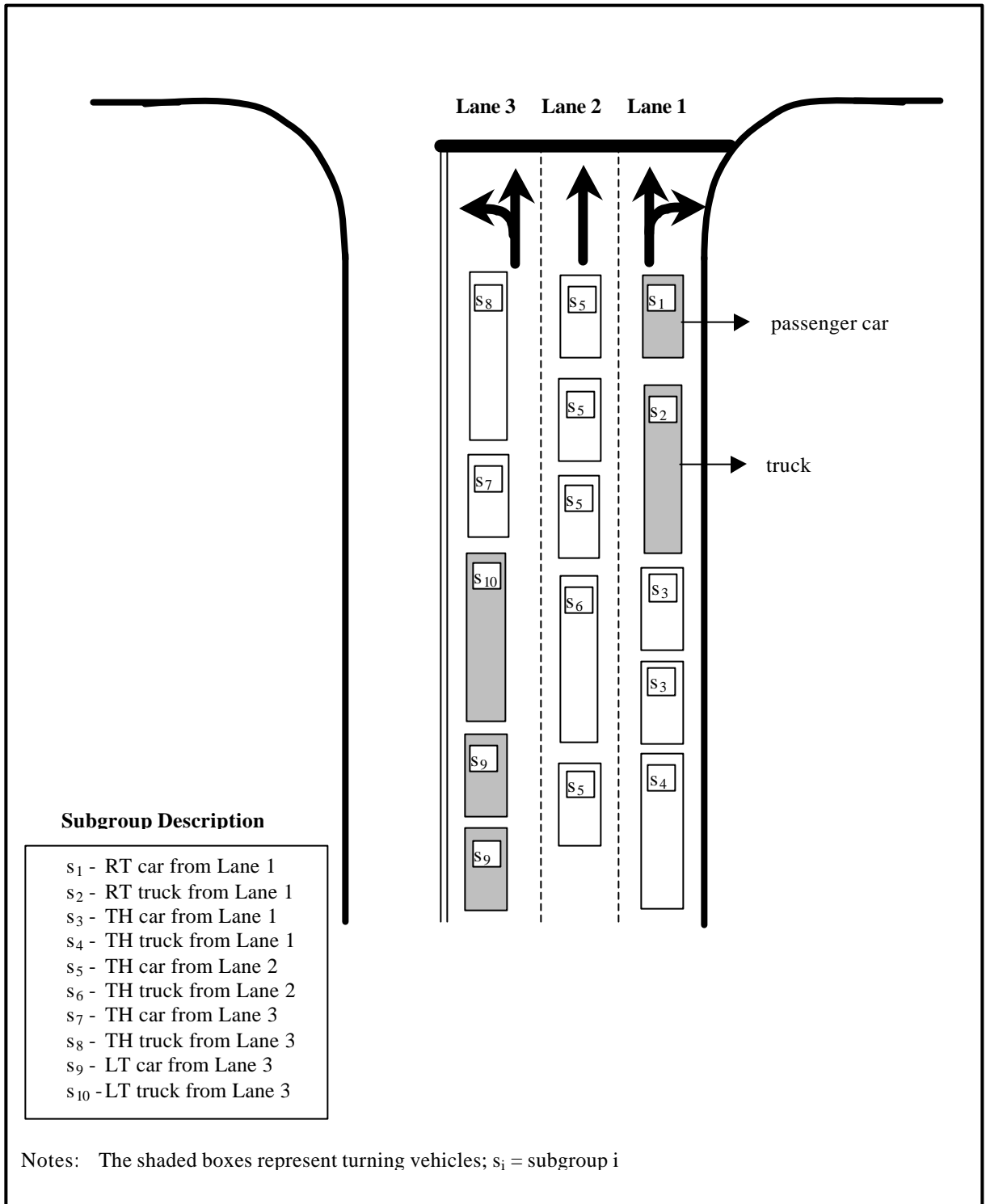


FIGURE 3.01. Illustration of Subgroups

The through passenger car equivalent for any subgroup f , is defined as:

$$E_f = \frac{h_f}{h_i} \quad (3.02)$$

The average saturation headway for the combined subgroups $1,2,\dots,f,\dots,F$ is computed from Equation (3.03).

$$h_F = \sum_{f=1}^F p_f \times h_f \quad (3.03)$$

Substituting (3.02) in (3.03) gives:

$$h_F = \sum_{f=1}^F p_f \times E_f \times h_i \quad (3.04)$$

Dividing both sides in Equation (3.04) by h_i gives the through passenger car equivalent for the subgroup combination, E_F as shown in Equation (3.05) below.

$$E_F = \frac{h_F}{h_i} = \sum_{f=1}^F p_f \times E_f \quad (3.05)$$

The through passenger car equivalent for each subgroup, E_f is normally estimated as the product of the individual equivalency factors due to the non-ideal conditions effecting each subgroup. For example, if a subgroup consists entirely of left turning trucks in a protected phase (assuming all other conditions are ideal), then E_f for that subgroup will be the product of E_T and E_L , the through passenger equivalents for trucks and for protected left turns, respectively. This approach assumes that the interaction effects of non-ideal conditions are independent ($E_{jk} = E_j \times E_k$). This rather strong assumption needs further investigation and invites future research into the relationship between the average subgroup passenger-car equivalent and the individual effects of non-ideal conditions. Nevertheless, the framework presented in this paper is not technically dependent on any particular functional form of E_{jk} , which can be described in any appropriate manner consistent with empirical evidence. For the sake of consistency with

the 1997 HCM however, the multiplicative model form is retained in this model, resulting in the following estimate for E_f .

$$E_f = \prod_{j=1}^J E_{fj} \quad (3.06)$$

where, E_{fj} is the through passenger car equivalent for subgroup f under non-ideal condition j . Since a subgroup will either be affected or unaffected by a non-ideal condition, (e.g., left turns in exclusive pockets are unaffected by parking on the curb lane), this binary relationship can be best expressed as follows:

$$E_{fj} = U_{fj} \times E_j + (1 - U_{fj}) = 1 + U_{fj}(E_j - 1) \quad (3.07)$$

where U_{fj} is a binary variable that is equal to 1 if non-ideal condition j affects the saturation headway for subgroup f (zero otherwise) and E_j is the through passenger car equivalent for non-ideal condition j (e.g. grade, lane width or parking, etc.).

Substituting (3.06) and (3.07) into (3.05) gives:

$$E_F = \sum_{f=1}^F p_f \prod_{j=1}^J \{1 + U_{fj}(E_j - 1)\} \quad (3.08)$$

Finally, by definition $S_F = I/h_F$ where $S_F =$ prevailing saturation flow rate and $S_i = I/h_i$ is the ideal saturation flow rate, and thus:

$$S_F = \frac{S_i}{E_F} = \frac{S_i}{\sum_{f=1}^F p_f \prod_{j=1}^J \{1 + U_{fj}(E_j - 1)\}} \quad (3.09)$$

Equation (3.09) provides the means for estimating the prevailing saturation flow rate for any combination (F) of traffic subgroups $f=1,2,\dots, F$ that are subjected to the effect of non-ideal conditions $j=1,2,\dots,J$. It is important to note that the collection of all subgroups (F) could be defined in any manner chosen by the user. This could be at the lane, lane group, or approach level. The structure of the saturation flow rate model in (3.09) is seemingly simple, requiring the measurement or estimation of only four principal parameters:

- 1) the ideal saturation flow rate, or S_i .
- 2) whether a given non-ideal condition (j) has an effect on subgroup (f), or U_{fj} .
- 3) the through passenger car equivalent for non-ideal condition (j), or E_j .
- 4) the fraction of total flow (F) which occurs in subgroup (f), or p_f .

The first three parameters are derived from the 1997 HCM and can be applied using the same input data required by the HCM. The fourth parameter (fraction of total flow in each subgroup) is the critical element to the model; it is the point where the subgroup model extends beyond the 1997 HCM procedures. Without the presence of field data, lane flow must be estimated for lanes where a choice exists.

3.4 Ideal Saturation Flow

Ideal saturation flow represents the average departure rate for through passenger cars under ideal conditions. Typical values for ideal saturation flow vary from 1800-2100 pcphpl (Transportation Research Board, 1997)(Akcelik, 1981)(Peterson, *et al.*, 1995)(Teply, *et al.*, 1995). The ideal saturation flow rate provides the foundation for estimating saturation flow. The headway equivalency factors (discussed in the following sections) are applied to the ideal saturation headway to estimate saturation flow of non-ideal conditions.

3.5 Binary Effect of Non-Ideal Conditions

The parameter U_{fj} is a binary variable that is set to one if a non-ideal condition exists (such as bus, parking, etc.) or zero otherwise. The term $\{1 + U_{fj}(E_j - 1)\}$ from Equation 3.09 equals 1 if a saturation effect does not exist and E_j if an effect does exist. Thus, for interior lanes that do not experience effects due to curb-lane impedances such as parking maneuvers and bus stops, U_{fj} is equal to 0 and the equivalency factor E_j is not accounted for. This is an improvement to the 1997 HCM procedures that apply a weighted average of the curb-side effect to an entire lane group (which implicitly assumes that the volume in each lane is equal). Table 3.01 provides the conditions required for U_j to be equal to 1.0.

Table 3.01: Required Conditions for $U_j = 1$

Non-Ideal Condition j	The condition $U_j = 1$ applies to the following subgroups
Lane Width	All subgroups in the lane
Heavy Vehicles	Truck subgroups
Grade	All subgroups
Parking	Subgroups in the outer (curb) lane
Bus Blockage	Subgroups in the outer (curb) lane
Area Type	All subgroups
Left-Turn Movements	Left turn subgroups
Right-Turn Movements	Right turn subgroups
Through Movements in Shared Through/Left-Turn Lanes	Through subgroups in a shared through/left lane

3.6 Headway Equivalency Factors

The non-ideal through passenger car equivalents (also referred to as Headway Equivalency Factors) are derived directly from the saturation adjustment factors in the 1997 HCM. These non-ideal effects include: lane width, heavy vehicles, approach grade, on-street parking, bus blockage, area type, left-turn movements, right-turn movements, and through movements in shared through/left lanes.

The following sections provide the equivalency factors for each effect. Note that the equivalency factors presented below are time headway factors, not saturation flow

factors as are used in the HCM. Thus, an equivalency factor of 1.5 represents a time headway that is 1.5 times greater than that of a through passenger car.

3.6.1 Lane Width

The lane width equivalency factor accounts for the detrimental effect that narrow lanes have and the positive effect that wide lanes have on saturation flow. The equivalency factor for lane width, E_w , is as follows:

$$E_w = \frac{30}{18 + w} \quad (3.10)$$

where w is the lane width in feet. The input value of w ranges between 8 and 16 feet.

3.6.2 Heavy Vehicles

By definition, a subgroup consists of a group of vehicles of a single vehicle type. Two vehicle types, cars and trucks, are used in the subgroup model discussed in this section, although more could be considered. The heavy vehicle equivalency factor, E_{hv} , for passenger cars is 1.0 (meaning no effect) and for trucks is 2.0.

3.6.3 Grade

The effects of approach grade are accounted for in the equivalency factor for grades (E_G) as shown below.

$$E_G = \frac{200}{200 - G} \quad (3.11)$$

where G = grade in percent. The input value of G ranges between -6 and $+10$.

3.6.4 Parking

The effect of parking applies only to the lane adjacent to the parking space. The parking equivalency factor (E_p) typically is applied to the outside lane, although in the case of one-way streets parking could be allowed adjacent to the inside lane. The parking equivalency factor is applied if the presence of parking affects traffic flow in the adjacent

lane. Therefore, the binary term U should be set to 1 (effect exists) even if no parking maneuvers take place during the time period of the analysis, and the number of parking maneuvers, N_m , should be entered as 0. The general form of the parking equivalency factor is:

$$E_p = \frac{200}{180 - N_m} \quad (3.12)$$

where N_m = the number of parking maneuvers per hour. The allowable range for N_m is 0-180 parking maneuvers per hour, subject to $E_p \leq 20$.

3.6.5 Bus Blockage

The bus equivalency factor (E_b) accounts for bus blockage that takes place at either the near side or far side of the intersection. Similar to the parking equivalency factor, the bus equivalency factor is applied only to the curb lane. Thus, all interior lanes have a U factor equal to 0 (no effect). The equivalency factor for buses follows:

$$E_b = \frac{250}{250 - N_b} \quad (3.13)$$

where N_b = number of buses stopping per hour. The allowable range of N_b is 0-250, subject to $E_b \leq 20$.

3.6.6 Area Type

The area type equivalency factor (E_{AT}) is either 1.11 ($\frac{1}{.9}$) for intersections located in Central Business Districts and 1 for all other intersections.

3.6.7 Right-Turn Movements

A generalized parametric model has been developed for right turn equivalency factors. It covers all combinations of lane use (exclusive or shared) and right turn protection (protected or permissive). By substituting the appropriate values, the model

generates all 7 right turn cases given in Table 9-11 of the 1997 HCM. The general model form is given below and applies to the right turn movement subgroups in the curb lane.

$$E_R = \frac{g_p + g}{\frac{g_p}{E_{ro}} + g \cdot \left(\frac{1}{E_{ro}} - \frac{PEDS}{2100} \right)} \text{ where,} \quad (3.14)$$

- g_p = effective green time in the protected phase (sec)
 E_{ro} = right-turn passenger car equivalent in protected phasing ($\frac{1}{0.95}$)
 g = effective green time in the permitted phase (sec)
 $PEDS$ = pedestrians per hour conflicting with the right-turn movement (≤ 1700).

The right-turn equivalency factor is not to exceed 20 ($E_R \leq 20$).

3.6.8 Left-Turn Movements

Similar to the right-turn model, a generalized parametric model has been developed for left turn equivalency factors based on the 1997 HCM. In the left turn equivalency model the green period is divided into various ‘time-slices’ to represent the unique departure rates that occur over the entire period. Figure 3.02 illustrates three of these periods: the protected green period (g_p), the opposing queue clearance period (g_q); and the permitted (unsaturated) green period (g_u). Note that in this example, the opposing queue clearance time is greater than the time until the first left turner arrives ($g_q > g_f$).

During the g_p period, vehicles depart at headways equal to the protected left-turn phasing equivalency ($\frac{1}{0.95}$) times the ideal headway h_i . Period #2 (g_q) represents the initial permitted portion of the phase when the opposing queue is clearing. Thus, no left-turn departures occur during this period.

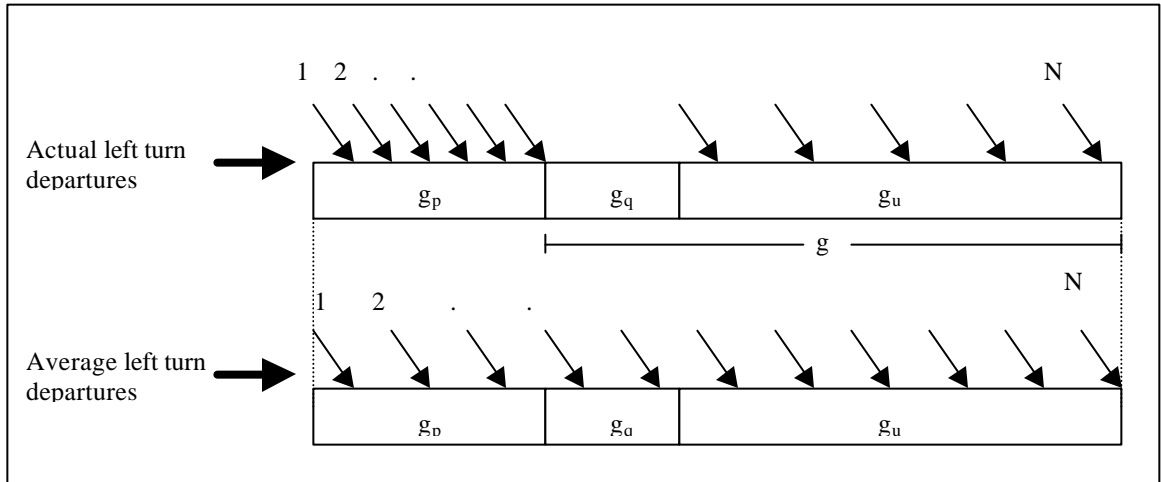


FIGURE 3.02. Departure Pattern for Left Turning Vehicles

During the unsaturated opposed period (g_u), vehicles depart at headways equal to the permitted left turn equivalency rate (E_{l1}) times the ideal through headway.

The left-turn equivalency model converts the actual departure headways for left turns (shown in the top portion of Figure 3.02) into a single equivalent departure headway (shown in the bottom portion of Figure 3.02).

From Equation 3.02, the equivalency factor for a non-ideal condition is determined by dividing the average headway h_a by the ideal headway h_i as shown in Equation 3.15.

$$E = \frac{h_a}{h_i} \quad (3.15)$$

The average headway is the time during which vehicle departures can occur divided by the number of vehicle departures N as shown below.

$$h_a = \frac{g_p + g}{N} \quad (3.16)$$

Expressing the number of departures in terms of green time divided by headway for each period yields the following:

$$N = \frac{g_p}{h_p} + \frac{g_u}{h_{g_u}} \quad (3.17)$$

Combining Equations 3.17 into 3.16 gives:

$$h_a = \frac{g_p + g}{N} = \frac{g_p + g}{\frac{g_p}{h_p} + \frac{g_u}{h_{g_u}}} = \frac{g_p + g}{\frac{g_p}{h_i \cdot E_{l0}} + \frac{g_u}{h_i \cdot E_{l1}}} \quad (3.18)$$

Finally, substituting Equation 3.16 into 3.15 yields the left-turn equivalent factor for this example.

$$\frac{h_a}{h_i} = E_L = \frac{g_p + g}{\frac{g_p}{E_{l0}} + \frac{g_u}{E_{l1}}} \quad (3.19)$$

Equation 3.19 represents the left-turn equivalency factor for a case where the left-turn movement is opposed by a multi-lane approach and the opposing queue clearance time is greater than the time it takes until the first left turn arrives. To account for the effect that a single-lane opposing approach has on the left-turn movement, the following term is added to the denominator:

$$\left(\frac{u_s \cdot g_{diff}}{E_{l2}} \right) \quad (3.20)$$

where: $u_s = 1$ if the opposing flow occurs from a single lane (0 otherwise)

g_{diff} = opposing queue green time remaining after the first left turn arrives (sec)

E_{l2} = through passenger car equivalent for left turns when opposing queue discharges from a single lane.

Additionally the $\frac{g_u}{E_{L1}}$ term is represented by $\left(\frac{g - \text{Max}(g_q, g_f)}{E_{L1}} \right)$ to account for cases

where $g_f > g_q$. The complete form of the left-turn equivalency model is given below.

$$E_L = \frac{g_p + g}{\frac{g_p}{E_{l0}} + \frac{g - \text{Max}(g_q, g_f)}{E_{l1}} + \frac{u_s \times g_{diff}}{E_{l2}}}, \text{ where} \quad (3.21)$$

3.6.9 Through Movements in Shared Through/Left-Turn Lanes

The presence of left turn vehicles in a shared lane affects the rate of discharge of through traffic in that lane. Until the first left turn arrives (g_f period), through traffic discharges at its normal rate which is equal to the ideal saturation headway h_i (through passenger car headway). From the time the first left turn vehicle arrives to the time the opposing queue clears, through traffic is blocked reducing the effective saturation flow of the through movement to 0 for that period. After the opposing queue clears and left turning vehicles wait for gaps in the opposing stream (g_u period) through vehicles depart at their ideal headway h_i . Figure 3.03 illustrates the departure pattern for through vehicles.

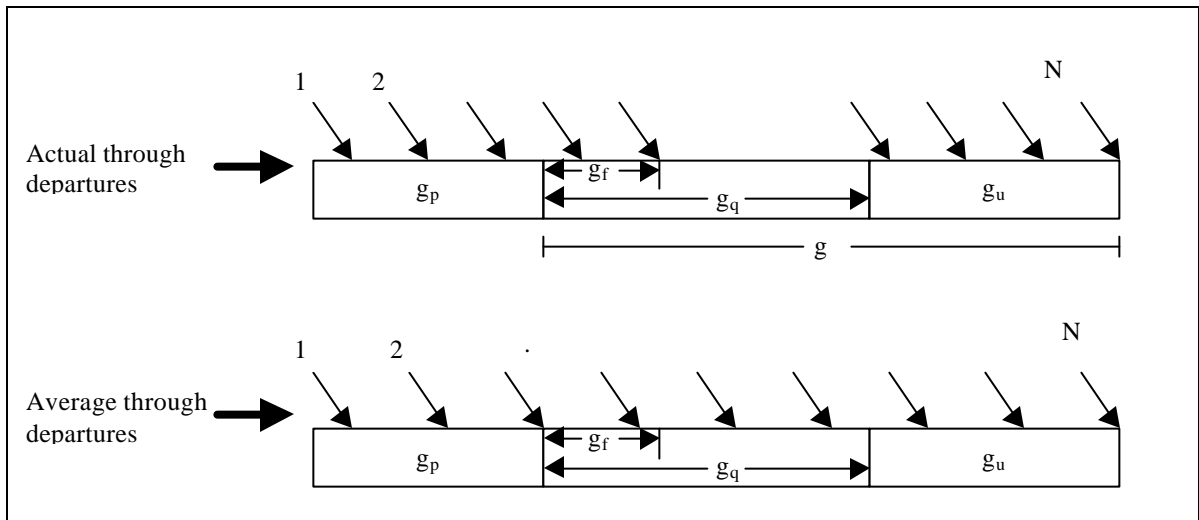


FIGURE 3.03. Departure Pattern for Through Vehicles from a Shared Through/Left Lane

The equivalency factor for through vehicles in a shared through/left lane is derived similar fashion to the left turn equivalency factor. The average headway for through vehicles h_a is determined by dividing the available green time by the number of departures N as shown in Equation 3.16. The number of through vehicle departures N from a shared through/left lane is represented as follows.

$$N = \frac{g_p}{h_i} + \frac{g - \text{Max}(g_q - g_f, 0)}{h_i} \quad (3.22)$$

Combining Equations 3.22, 3.16 and 3.15 yields the equivalency factor for through movement subgroups in shared through/left lanes, as shown below.

$$E_{LT}^T = \frac{g_p + g}{g_p + g - \text{Max}(g_q - g_f, 0)} \quad (3.23)$$

Note from (3.23) that if $g_f > g_q$, $E_{LT}^T = 1.0$, meaning that left turns do not block through movements at all.

3.7 Fraction of Total Flow in Each Subgroup

The ability to acquire or estimate subgroup-level traffic data is critical to the success of the subgroup method. By definition, a subgroup flow consists of a lane-volume count by turning movement and vehicle type. The fraction of subgroup flow (p_x) is required in order to estimate saturation flow from Equation 3.09. Normally, such detailed count data are not available and would be expensive to collect. Further, in the case of future year analyses these data are unknown. For a simple case (e.g., an approach that consists of one left-turn lane, one through lane, and one right-turn lane), subgroup flows can be determined if the turning movement volumes and percentage of heavy vehicles are known. For a more complicated approach that includes choice lanes (two or more lanes that accommodate one turning movement), individual lane flow are required.

The selection of lanes when given a choice is largely a behavior issue. As drivers approach an intersection they are faced with two options: stay in the lane they are in or change lanes. A driver may choose to stay in a lane because:

- the benefit of changing lanes is negligible;
- a downstream maneuver needs to be performed from the current lane; or
- the approach is too congested to change lanes.

On the other hand, a driver may choose to change lanes to:

- avoid congestion and/or impedances, or
- perform a downstream maneuver.

These behavioral choices can be generalized as a function of three factors: approach congestion, downstream effects, and lane impedances. Developing a mathematical model to simulate driver behavior proves difficult. Calculations of approach congestion can be performed, but at what level do vehicles find it necessary to change lanes? Likewise, the effect that lane impedances have on lane flow distribution can be observed in the field, but again, at what point do drivers feel that changing lanes is beneficial? This thesis attempts to answer these questions.

3.7.1 Mathematical Lane Distribution Model

Mathematically, the flow across lanes can be estimated by minimizing the objective function (Z) which is the squared difference of the selected objective criterion (χ) between lanes l and j for all choice lanes L' . The general form of the objective function is shown below.

$$\text{Min} \left(Z = \sum_{j=1}^{L'-1} \sum_{l=j+1}^{L'} \left(\frac{c_j}{a_j} - \frac{c_l}{a_l} \right)^2 \right) \quad \text{where,} \quad (3.19)$$

α is an under-utilization factor that ranges from 0 (no one uses the lane) to 1.0 (the lane is fully utilized). By definition, at least one of the choice lanes on an approach must have an under-utilization value of 1.

The model shown in Equation 3.19 accounts for two factors that affect the distribution of traffic across choice lanes: downstream effects (represented by lane under-utilization) and lane impedances. Based on the literature review performed, only the Bonneson model attempts to account for the effect that approach congestion has on the probability that a vehicle will change lanes. Although this effect is not accounted for in the subgroup model, the field data analyzed in this thesis provide insight into the behavioral characteristics of drivers at various levels of congestion.

A general discussion of lane under-utilization and lane impedances is provided, followed by a presentation of the lane flow distribution process. The section concludes with a numerical example.

3.7.1.1 Lane Under-Utilization

The under-utilization factor accounts for pre-positioning effects due to downstream influences. Downstream influences include freeway on-ramps, lane drops, turn-only lanes, and heavily used access roads or driveways. The under-utilization factor (α) provides an adjustment to the lane distribution criterion (χ). To demonstrate the effect of the lane under-utilization factor, consider a two-lane approach where:

- the saturation flow rates in both lanes is equal to 1,600 vph,
- the total approach volume is 1,200 vph,
- the under-utilization factor of lane 1 is 1.0,
- the under-utilization factor of lane 2 is 0.6, and
- a lane distribution criterion of equal flow ratio is used.

In this example, the objective function Z would be formulated as follows:

$$Z = \min \left(\frac{v_1/1600}{1.0} - \frac{v_2/1600}{0.6} \right)^2 \text{ subject to: } v_1 + v_2 = 1200, v_1 \geq 0 \text{ and } v_2 \geq 0$$

Minimizing Z (which goes to zero in this case) results in $v_1 = 750$ and $v_2 = 450$. The resulting flow ratio for lane 1 is $750/1600 = 0.469$ and the flow ratio for lane 2 is $450/1600 = 0.280$. Thus, an under-utilization ratio of 0.6 indicates that lane 2 experiences a flow ratio that is 60% of the flow ratio of lane 1.

Field data are required to determine the effects that a downstream condition has on the pre-positioning of traffic at the upstream intersection. Some calibration of lane utilization factors have been developed in SIDRA (Akcelik, 1990). In addition, Bonneson has collected field data at interchanges to demonstrate the effect that pre-positioning has at ramp terminals (1997). It should be noted that the effect of pre-positioning, or lane under-utilization, was not analyzed as part of this thesis. The difficulty with developing under-utilization factors is that the degree of under-utilization due to a downstream effect is largely dependent upon the characteristics of the effect (e.g., the percentage of traffic that uses an on-ramp or turns into a driveway access). Development of an effort to determine under-utilization factors is recommended as part of future development of the subgroup model.

3.7.1.2 Lane Flow Distribution Criteria

A factor that affects the distribution of traffic across choice lanes is the presence of non-ideal saturation flow effects. On the outer (curb) lane, these include the presence of conflicting pedestrians, on-street parking, and bus stops. If there is a noticeable presence of either pedestrians, parking, or bus stops, through traffic on a multi-lane approach will often shift to an inside lane to avoid the high delay that is incurred on the curb lane.

Permitted left-turn movements that occur from shared lanes also impede lane flow. Through traffic at an approach with a shared through/left lane and a through-only

lane will likely shift to the through-only lane to avoid potential lane blockage caused by the left-turning vehicles that are waiting for a gap in the opposing traffic stream. In the case of high opposing volumes, all through traffic may shift to the through-only lane resulting in a de-facto left-turn lane.

The lane distribution effects described above are a function of the operational characteristics of the intersection. The distribution of traffic across choice lanes due to intersection impedances can be estimated by stipulating that an operational criterion is met across the choice lanes (referred to as a lane distribution strategy). Five potential lane distribution strategies are:

- 1) equal back of queue,
- 2) equal lane delay,
- 3) equal lane cycle-average queue,
- 4) equal lane volume, and
- 5) equal lane-flow ratio.

As discussed in the Chapter 2, the Australian, Canadian, and Swedish methods all employ an equal flow ratio strategy.

Although the effect of lane impedance is described in terms of intersection operations, the choice that drivers make remains behavioral. Thus, one question worth asking when choosing a lane distribution strategy is “Do drivers actually behave according to the chosen strategy?” Short of performing a human factors experiment, this question is difficult to answer. Field data can be collected and statistical analyses can determine the best fitting model; however, do drivers approaching an intersection interpret the delay or flow ratio of each choice lane? Based on the five strategies listed above, the most instinctive choice perhaps is the equal back of queue strategy since queues are distinguishable to drivers.

As mentioned in Chapter 2, there have been, to the author’s knowledge, no verification studies of lane distribution strategies performed with field data. A goal of

this thesis is to provide justification based on a field evaluation as to the lane distribution strategy that best represents actual driver behavior.

3.8 Lane Flow Allocation Process

The lane flow allocation process can be carried out in a nine-step process as illustrated in Figure 3.04 and is described below.

Step #1: Specify Lane Deployment Criterion

The first step in the allocation process is to specify a lane deployment criterion. The following criteria are evaluated in this thesis: equal back of queue, equal delay, equal flow ratio, equal cycle-average queue, equal lane volume, and the Bonneson method. A goal of this thesis is to evaluate the performance of all six criteria under various operating conditions.

Step #2: Set Initial Lane Volume Distribution

Before lane saturation flow rates can be calculated, it is necessary to develop a set of initial lane volumes. Although various initial assumptions could be used, the analyses performed as part of this thesis all assume an initial condition of equal lane volumes.

Step #3: Define Subgroups

Once an initial volume distribution is made, the subgroup for each approach is defined. As discussed earlier in this section, a subgroup is defined as a single vehicle type (car or truck) making a directional movement (left, through, or right) from a single lane.

Step #4: Calculate Subgroup HEF's

Using the volume and geometric characteristics of the intersection, the headway equivalency factors for each of the nine non-ideal conditions discussed in Section 3.6 are calculated for each approach. The equivalency factors are derived directly from the 1997 HCM saturation flow adjustment factors.

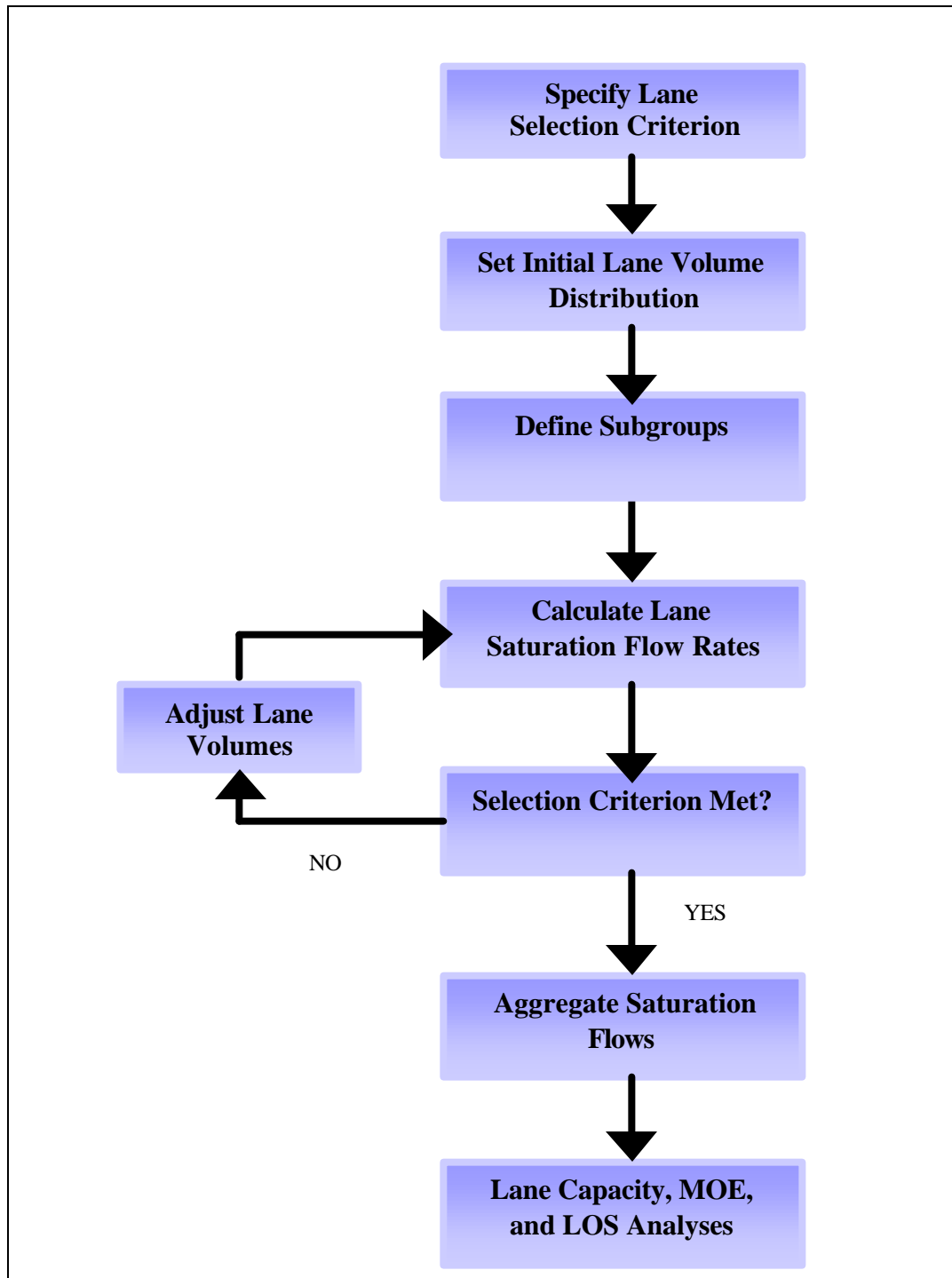


FIGURE 3.04. Lane Selection Procedure

Step #5: Calculate Lane Saturation Flow Rates

Using Equation 3.09, the saturation flow rate for each choice lane is calculated. It should be noted that this step is identical to Step #8, with the exception that it is only performed for choice lanes. The initial lane volume distribution from Step #2 is used to calculate the proportion of subgroup flow in each lane (p_f) and the Headway Equivalency Factor's calculated in Step #4 are applied to all subgroups when the effect of the non-ideal condition is present ($U = 1$). In addition, an ideal saturation flow rate is required in this step. The analyses presented in this thesis all assume an ideal saturation flow rate of 1900 vph.

Step #6: Is Selection Criterion (Equilibrium) Met?

Once the saturation flow rate for each lane is known, the measure of effectiveness relating to the lane distribution criterion chosen in Step #1 (e.g., delay, flow ratio, back of queue, etc.) is calculated for all choice lanes. This step is identical to Step #9, with the exception that it is only performed for the choice lanes. If the criterion is met, no adjustment to the lane volumes is required and the analyst can proceed to Step #8. If the criterion is not met, an iterative is required beginning in Step #7.

Step #7: Adjust Lane Volumes – Repeat Step #5

The iterative approach between Steps #5-7 is required because of the non-linear form of the solution. In this step, the movement with choice (typically the through) is increased in the lane that “over performs” (the lane with a lower delay, flow ratio, queue, etc. than the other choice lane) and decreased in the lane that “under performs.” This is subject to the constraint that the sum of the volumes in each lane equals the through volume for the approach. After each increment, new lane volumes are determined and a new saturation flow for each choice lane is calculated. This process continues until the lane distribution criterion is met, meaning equilibrium has been achieved. Software is required in order to efficiently carry out this process.

Step #8: Aggregate Saturation Flows at the Lane/Lane Group Levels

Once the lane distribution criterion is met for the choice lanes, the saturation flow rates for all lanes are calculated. The lane saturation flows can be aggregated at the lane group level by calculating the fraction of subgroup flow in the lane group as opposed to the lane. The example provided in this section demonstrates how lane and lane group saturation flows are calculated.

Step #9: Calculate Capacity, MOE's and LOS

The capacity for each lane/lane group is calculated based on Equation 9-3 of the 1997 HCM ($c_i = s_i \left(\frac{g_i}{C} \right)$). The average control delay for each lane/lane group is determined based on Equation 9-22 of the 1997 HCM:

$$d = d_1 PF + d_2 + d_3 \quad (3.20)$$

where: d_1 = uniform control delay (1997 HCM Equation 9-23)

PF = uniform delay progression adjustment factor (1997 HCM Equation 9-24)

d_2 = incremental delay (1997 HCM Equation 9-25)

d_3 = residual demand delay

The level of service for each lane/lane group is determined based on the criteria set in Table 9-1 of the 1997 HCM.

Other measures calculated include the cycle-average queue which is a product of the delay and volume of the lane/lane group. In addition, the average back of queue and 95th percentile back of queue is calculated based on the procedures described in Appendix G of the 2000 HCM.

It is important to note that delays calculated at the lane level and aggregated at the lane group level may be greater than lane group level delays due to the capacity term in d_2 .

3.9 Sample Calculation

The numerical example that follows demonstrates how the subgroup method and flow distribution procedure (shown in Figure 3.04) is implemented. The example is taken directly from Sample Calculation #1 of the 1997 HCM.

3.9.1 Description of HCM Calculation #1

Sample calculation #1 involves a four-legged intersection with shared lanes on each approach in a CBD area (Figure 3.05). There are no effects of grade or parking on any of the approaches. Each right-turn movement has a conflicting pedestrian volume of 100 pedestrians per hour. All left-turn movements are permitted and each approach is treated as one lane group.

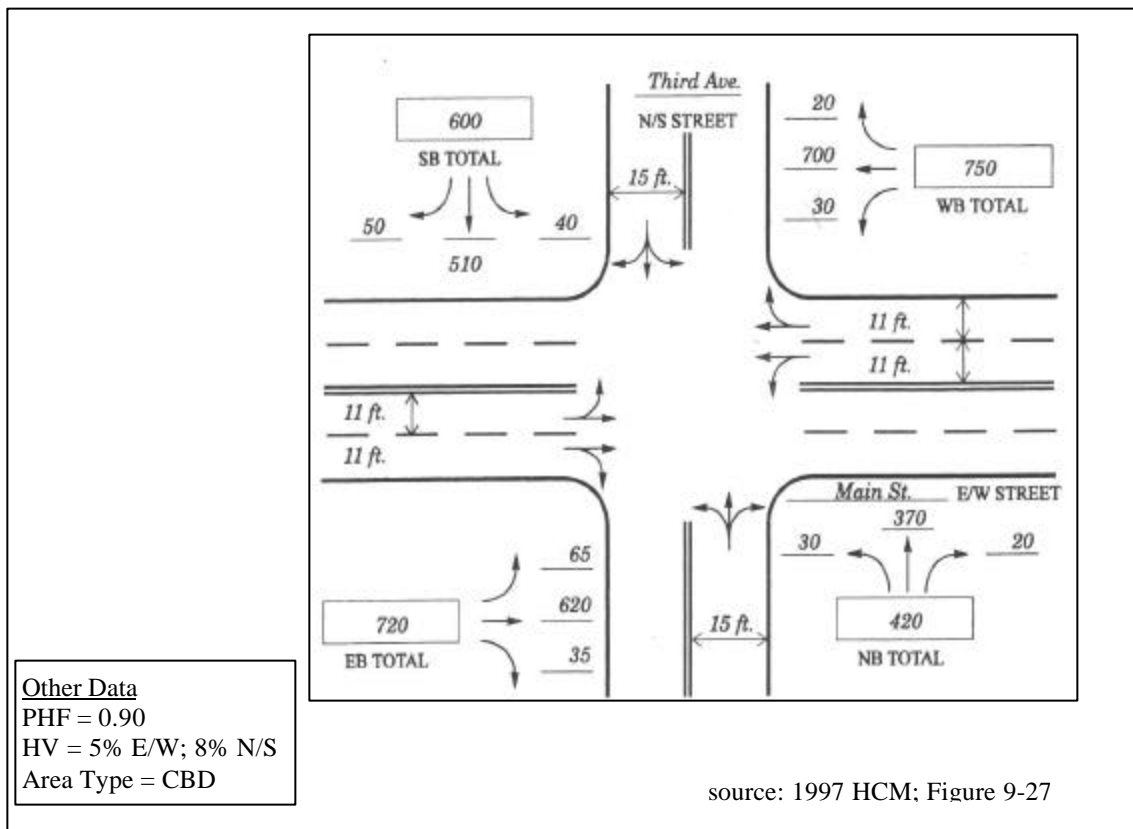


FIGURE 3.05. 1997 HCM Sample Calculation #1: Volume and Geometric Data

The eastbound and westbound approaches each include a shared through/right-turn lane and a shared through/left-turn lane. Thus, since the through traffic on these approaches has the option of using either lane, these are referred to as “choice” lanes.

3.9.2 Step #1: Select Lane Distribution Strategy

The first step of the analysis is to choose a lane distribution strategy in order to allocate the through traffic on the eastbound and westbound approaches. As part of this analysis, four lane distribution criteria were evaluated to determine the strategy that appears most appropriate for this example. The four strategies include: equal lane delay, equal cycle-average queue, equal lane volume, and equal flow ratio. The objective function Z , shown in Equation 3.19 was minimized under all four cases assuming an under-utilization factor of 1.0. The resulting lane delays for the eastbound approach of HCM Calculation #1 are provided for each of the four distribution strategies in Figure 3.06.

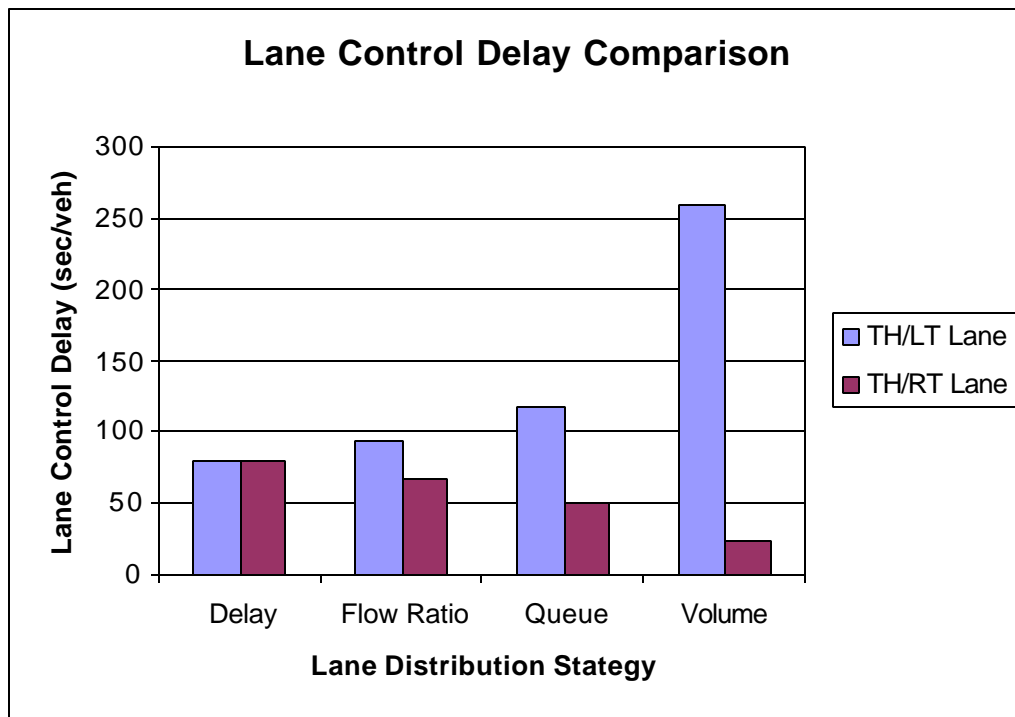


FIGURE 3.06. Lane Delay by Distribution Strategy – HCM Sample Calculation #1

As shown in Figure 3.06, the equal volume strategy results in the largest discrepancy of lane delays. By definition, the equal delay method results in equal lane delays. From the figure, the equal-flow ratio method appears to be a reasonable strategy as it represents roughly an average of the equal queue and equal delay strategies. Further, the equal flow-ratio strategy is used in the Australian, Canadian, and Swedish capacity guides. Thus, the equal flow ratio analysis is used to estimate the lane flows for this example.

3.9.3 Step #2: Set Initial Lane Volumes

The second step involves setting an initial lane volume distribution for the eastbound and westbound approaches. For this case, the initial volumes are set so that the lane volumes on each approach are equal. Thus, for the eastbound approach, the volume for each lane is the total adjusted volume ($\frac{720}{0.90} = 800$) divided by two, or 400 vph.

3.9.4 Step #3: Define Subgroups

Table 3.02 provides a description of all subgroups for this example. The eastbound and westbound approaches each consist of 8 subgroups and the northbound and southbound approaches each consist of 6 subgroups.

Table 3.02: Detailed Subgroup Calculation: HCM Sample Calculation #1

Approach	Lane	Subgroup	TM	Vehicle	Adj. Volume	SG Fraction	Equivalency Factor	Saturation Flow Rate	Percentile Group Factor	Sat Flow
EB	1	1	RT	Car	37	0.062	1.432	1327	0.089	1549
		2	RT	Truck	2	0.003	2.863	664	0.010	
		3	TH	Car	528	0.887	1.149	1654	1.020	
		4	TH	Truck	28	0.047	2.298	827	0.108	
	2	5	TH	Car	126	0.615	1.560	1218	0.959	533
		6	TH	Truck	7	0.034	3.121	609	0.107	
		7	LT	Car	68	0.332	6.748	282	2.238	
		8	LT	Truck	4	0.020	13.496	141	0.263	
EB APPROACH SUMMARY					800	-	-	-	-	2081
WB	1	9	RT	Car	21	0.0436	1.432	1327	0.062	1558
		10	RT	Truck	1	0.0021	2.863	664	0.006	
		11	TH	Car	437	0.9066	1.149	1654	1.042	
		12	TH	Truck	23	0.0477	2.298	827	0.110	
	2	13	TH	Car	302	0.8604	1.149	1654	0.989	1132
		14	TH	Truck	16	0.0456	2.298	827	0.105	
		15	LT	Car	31	0.0883	5.875	323	0.519	
		16	LT	Truck	2	0.0057	11.750	162	0.067	
WB APPROACH SUMMARY					833	-	-	-	-	2690
NB	1	17	RT	Car	20	0.0428	1.259	1510	0.054	1364
		18	RT	Truck	2	0.0043	2.517	755	0.011	
		19	TH	Car	378	0.8094	1.010	1881	0.818	
		20	TH	Truck	33	0.0707	2.020	941	0.143	
		21	LT	Car	31	0.0664	4.642	409	0.308	
		22	LT	Truck	3	0.0064	9.283	205	0.060	
NB APPROACH SUMMARY					467	1.0000	-	-	-	1364
SB	1	23	RT	Car	52	0.0780	1.259	1510	0.098	1475
		24	RT	Truck	4	0.0060	2.517	755	0.015	
		25	TH	Car	522	0.7830	1.010	1881	0.791	
		26	TH	Truck	45	0.0675	2.020	941	0.136	
		27	LT	Car	40	0.0600	3.441	552	0.206	
		28	LT	Truck	4	0.0060	6.883	276	0.041	
SB APPROACH SUMMARY					667	1.0000	-	-	-	1475

3.9.5 Step #4: Calculate Headway Equivalency Factors

The Headway Equivalency Factors are summarized for each subgroup in Table 3.02. Note that the “Fixed” factors include the product of the lane width, bus, parking, area type, grade, and heavy vehicle factors. The “Overall” HEF represent the product of the individual fixed, right-turn, left-turn, and through equivalency factors. As Table 3.02 shows, Subgroup #1 has an overall HEF of 1.432 and Subgroup #2 has an overall HEF of 2.863.

3.9.6 Steps #5-#7: Calculate Lane Saturation Flow Rates, Iterate until Deployment Criterion (Equilibrium) is Met

The iterative process that is required to achieve equilibrium (Steps #5, 6, and 7) is not shown since each iteration includes a separate saturation flow calculation for each lane. In this process, the through traffic is incremented in the lane that has the lower flow ratio (thus reducing the through traffic in the other lane) until the flow ratio in each lane is equal. The subgroup volumes shown in Table 3.02 represent the “equilibrium” state.

The flow ratio for lane 1 of the eastbound approach is $\frac{37 + 2 + 528 + 28}{1549} = 0.384$, and the flow

ratio for lane 2 of the eastbound approach is $\frac{126 + 7 + 68 + 4}{534} = 0.384$.

3.9.7 Step #8: Aggregate Saturation Flows at the Lane/Lane Group Levels

The saturation flow rates for each lane (Step #8) are calculated as follows. For the case of Subgroup #1, the proportion of subgroup flow (p_f), or the Subgroup Fraction is the subgroup volume divided by the lane volume ($\frac{37}{595} = 0.062$). The subgroup fraction is multiplied times the product of the headway equivalency factors ($1.149 \cdot 1.246 \cdot 1.0 \cdot 1.0 = 1.432$) to obtain the percentile group factor ($0.062 \cdot 1.432 = 0.089$). The percentile group factors for all subgroups in Lane 1 are summed and divided into the ideal saturation flow rate (1900 vph) to arrive at the adjusted lane saturation flow rate (1549 vph) per (3.09). Subgroup saturation flow rates are determined simply by dividing

the ideal saturation flow rate by the Overall Headway Equivalency Factor. The lane group saturation flow rates are calculated similarly to the lane saturation flows, except that the subgroup fraction is calculated based on the amount of subgroup traffic in the lane group rather than the lane.

3.10 Comparisons with HCM

The saturation flow rates developed using the subgroup method (shown in Table 3.02) are aggregated at the lane group level and compared with results produced using the 1997 HCM method. In addition, a comparison of lane group saturation flows is provided for Sample Calculation #2 and #3 of the HCM (the detailed subgroup worksheets for these examples are located in the Appendix A). The purpose of these comparisons is to show the similarities and differences between the subgroup and HCM methods when they are applied using the same assumptions. Under ideal conditions, both methods should give similar results. With the presence of impedances such as bus stops and parking, it is expected that the two methods will produce slightly different results due to the equal lane volume assumption that is implicit with the HCM adjustment factors (see Chapter 2.1).

3.10.1 HCM Sample Calculation #1

Table 3.03 provides a comparison of lane group saturation flows developed using the subgroup and HCM methods for the first HCM sample calculation.

Table 3.03: Lane Group Saturation Flow Rate Comparison - HCM #1

<i>Intersection Characteristics</i>											
Approach	#of Lanes			LW (ft)	HV %	PHF	Grade	Parking Man./Hour	Bus Stops/ Hour	Peds/ Hour	Left Turn Phasing
	L	T	R								
EB	s	2	s	11	5	0.90	0	N	0	100	Perm.
WB	s	2	s	11	5	0.90	0	N	0	100	Perm.
NB	s	1	s	15	8	0.90	0	N	0	100	Perm.
SB	s	1	s	15	8	0.90	0	N	0	100	Perm.

<i>Lane Group Saturation Flow Rate Comparison (vph)</i>				
Lane Group	Subgroup Method	1997HCM Method	% Difference	
EB LT/TH/RT		2081	2118	-1.75%
WB LT/TH/RT		2690	2681	0.34%
NB LT/TH/RT		1364	1454	-6.19%
SB LT/TH/RT		1475	1466	0.61%

s – shared lane

As shown in Table 3.03, the subgroup method produces saturation flows within two percent of the HCM method for all lane groups, with the exception of the Northbound lane group. A review of the saturation flow calculation for the northbound approach reveals that the differences in saturation flow are attributable to differences in the right-turn and left-turn factors of both models.

Conceptually, the adjustment factors for turning movements are quite different between the two models. The HCM applies a single adjustment factor for left- and right-turn factors to the entire lane group. The subgroup method, on the other hand, applies the effect of turning movements in proportion to the volume within each turning movement subgroup. Fundamentally, the subgroup method is superior since the effect of a turning movement is dependent on the volume of the turning movement.

For shared lanes, such as the northbound approach in this example, the effects of left- and right-turn movements are interdependent. This is not accounted for in the HCM model. Thus changes in the proportion of turning movements can lead to great variations in saturation flow estimation.

An analysis was performed assuming zero right-turning traffic for the northbound approach of Sample Calculation #1 to test the sensitivity of the right-turning movement

factor of the two models. In this case, the HCM method predicts that the elimination of the right-turn traffic will result in a 12% increase in saturation flow. On the contrary, the subgroup method predicts that the saturation flow will remain approximately the same. Because the right turns make up only 5% of the approach traffic, it seems unreasonable that eliminating the movement would improve the saturation flow by 12% as the HCM predicts. This example demonstrates one of the weaknesses of the HCM model which is the overestimation of the impact of right-turning traffic from a single lane.

3.10.2 HCM Sample Calculation #2

The second example involves the intersection of a one-way street in the northbound direction and a two-way street in the east-west direction. Figure 3.07 shows the lane configurations and volumes for this example.

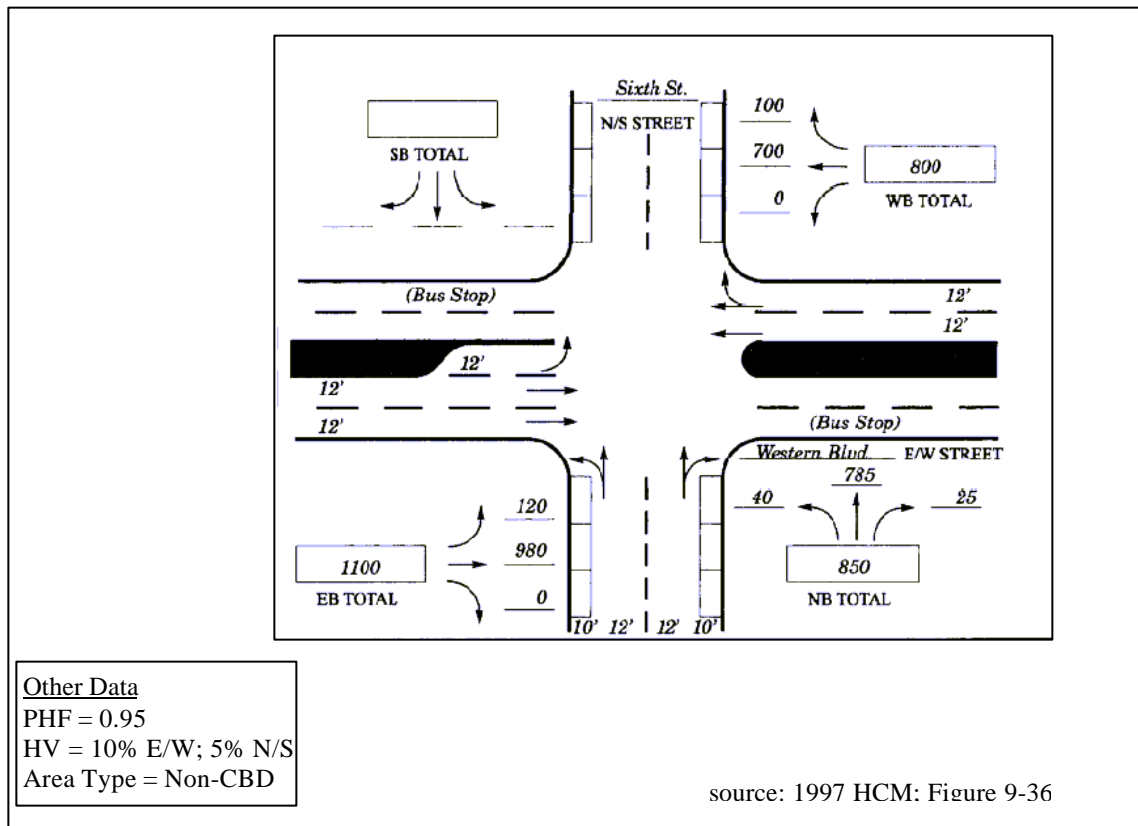


FIGURE 3.07. 1997 HCM Sample Calculation #2: Volume and Geometric Data

The east-west approaches have bus stops and conflicting pedestrians. The phasing for the eastbound left-turn movement was analyzed under three scenarios: (a) protected + permitted, (b) protected, and (c) permitted + protected. Table 3.04 provides the intersection characteristics and saturation flow rate summaries.

Table 3.04: Lane Group Saturation Flow Rate Comparison - HCM #2

<i>Intersection Characteristics</i>											
Approach	# of Lanes			LW (ft)	HV %	PHF	Grade	Parking Man./Hr	Bus Stops/Hour	Peds/ Hour	Left Turn Phasing
	L	T	R								
EB	1	2	-	12	10	0.95	0	N	20	50	*
WB	-	2	s	12	10	0.95	0	N	20	50	-
NB	s	2	s	12	5	0.95	-2	20	0	50	Prot.

<i>Lane Group Saturation Flow Rate Comparison (vph)</i>				
Lane Group	Subgroup Method	1997HCM Method	% Difference	
EB TH		3316	3151	5.24%
EB – LT (case a)		546	-	-
EB – LT (case b)		1641	1641	0.00%
EB – LT (case c)		735	-	-
WB TH/RT		3231	3082	4.83%
NB LT/TH/RT		3058	3084	-0.84%

s = shared lane

* The eastbound left-turn movement was analyzed under three phasing scenarios: (a) protected + permitted, (b) protected and (c) permitted + protected.

Table 3.04 shows that the calculated saturation flow rates under the subgroup method are within one percent of the HCM values for two of the four lane groups. The eastbound through and westbound through/right lane group saturation flow rates are approximately 5 percent higher than the calculated HCM values. These differences are attributable to the fact that the HCM assumes equal lane volume when applying the bus adjustment factor to multi-lane lane groups.

3.10.3 HCM Sample Calculation #3

The third sample calculation in Chapter 9 of the HCM involves an intersection in a CBD of two five-lane streets, each with an exclusive left-turn lane, a through lane, and a shared through right-turn lane. Figure 3.08 illustrates this example.

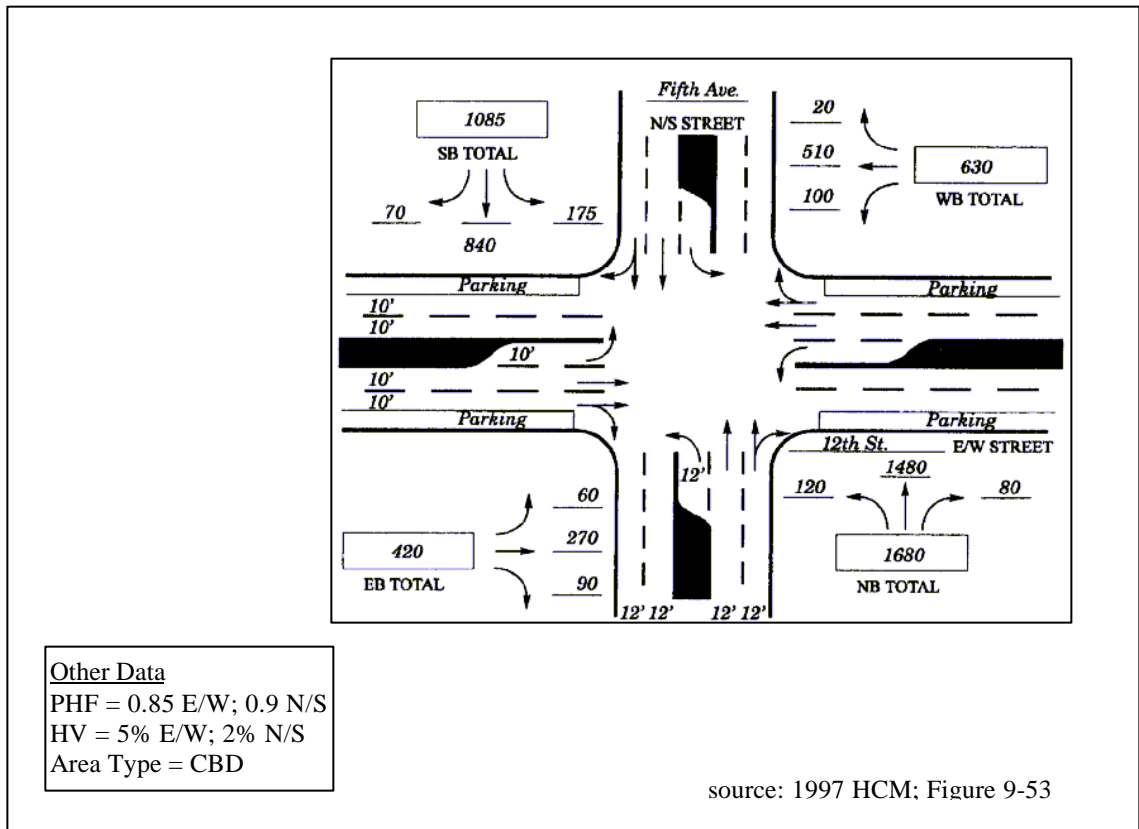


FIGURE 3.08. 1997 HCM Sample Calculation #3: Volume and Geometric Data

Parking is allowed on the eastbound and westbound approaches and all right turns experience conflicting pedestrian movements. No other non-ideal conditions exist. Table 3.05 provides the intersection characteristics and the saturation flow rates for all lane groups using the subgroup and HCM methodologies.

Table 3.05: Lane Group Saturation Flow Rate Comparison - HCM #3

<i>Intersection Characteristics</i>												
Approach	# of Lanes			LW (ft)	HV%	PHF	Grade	Parking Man./Hr	Bus Stops/ Hour	Peds/ Hour	Left Turn Phasing	
	L	T	R									
EB	1	2	s	10	5	0.85	0	5	0	200	Perm.	
WB	1	2	s	10	5	0.85	0	5	0	200	Perm.	
NB	1	2	s	12	2	0.90	0	N	0	50	Prot +Perm.	
SB	1	2	s	12	2	0.90	0	N	0	50	Prot +Perm.	

<i>Lane Group Saturation Flow Rate Comparison (vph)</i>				
Lane Group	Subgroup Method	1997HCM Method	% Difference	
EB TH/RT		2600	2675	-2.80%
EB LT		317	317	0.00%
WB TH/RT		2777	2823	-1.63%
WB LT		561	561	0.00%
NB TH/RT		3317	3323	-0.18%
NB LT		519	*	-
SB TH/RT		3300	3302	-0.06%
SB LT		278	*	-

s – shared lane

* The 1997HCM procedures do not calculate saturation flow movements for protected + permitted movements

Table 3.05 shows that the saturation flow rates for all lane groups using the subgroup methodology fall within 3-percent of the HCM saturation flow rates. This similarity is expected because of the lack of curbside impedances at the intersection and that the assumption of homogeneous conditions appears valid for this example.

3.10.4 Summary of HCM Comparisons

A comparison of three examples shows that the subgroup method produces saturation flows within 6% of the HCM method when aggregated at the lane group level. This gives credibility to the subgroup approach for estimating saturation flow. The benefit of applying the subgroup method is that additional insight is provided beyond a standard HCM analysis. In particular, the subgroup method provides results at the individual lane level.

Slight differences were found between the methods regarding the right- and left-turn factors for single lane approaches and the bus adjustment factor for multilane approaches. The differences in the turning factors are due primarily to the fact that the HCM applies the effects of non-ideal conditions to the entire approach, not just the proportion of traffic that is affected by it. The differences due to the bus factor are a result of the Highway Capacity Manual's assumption of equal lane volume across lanes within a lane group.

4.0 LANE VOLUME FIELD DATA COLLECTION AND ANALYSIS

A key element of the subgroup method is the estimation of lane volumes. To date, there has been no field validation studies of lane distribution strategies. In order to evaluate the lane distribution strategies however, individual lane volume data must be collected from the field. This chapter summarizes the effort that was undertaken to collect lane volume data and provides an analysis of the field data.

4.1 Purpose

The purpose of the data collection effort was to obtain field data that can be used to evaluate various lane distribution strategies as part of the subgroup lane distribution model. As mentioned throughout this report, three countries have developed lane-by-lane analysis procedures (Australia, Canada, and Sweden), each of which apply an equal flow-ratio strategy. None of the countries, though, have undertaken a data collection effort to validate the flow-ratio strategy against field data. Data collected as part of this thesis will attempt to validate various lane distribution strategies and provide insight into the level of accuracy that can be achieved in the estimation of individual lane flows. The data will also be used to develop an empirical field data model to estimate lane volumes.

4.2 Desired Criteria

The data collection effort focuses on sites where lane distribution is affected by non-homogenous, non-ideal conditions. These effects can include bus stops, parking maneuvers, conflicting pedestrians, right-turn movements from shared lanes, and (permitted) left-turn movements from shared lanes. Of these effects, left-turn movements from shared lanes appear to consistently have the most significant effect on the distribution of traffic. Thus, the data collection effort focus exclusively on intersections that include permissive-shared left-turn lanes.

Further, the data collection effort focus on two-lane approaches in order to simplify the data collection process and because there are fewer intersections with three and four lane approaches that include shared turns (particularly shared-permissive left turns).

In order to obtain unbiased lane distribution data it is necessary that the selected intersections operate in isolation from the remainder of the system. The intersection must be free of upstream or downstream effects that may cause drivers to favor one lane over the other. It is also desired that platooning at each site is minimal since under these conditions drivers are likely to stay in the lane they are currently in.

Intersections that operate with pre-timed signal control are preferred. Comparing lane distribution data at sites with pre-timed controllers eliminates the effect that variations in signal timing may have on distribution. Further, intersections with “fixed” operations simplify the data collection and analysis process.

It is also desired to choose sites that include impedances aside from permissive left-turning vehicles, such as pedestrians, bus stops and parking maneuvers. Ideally, a portion of the sites chosen would include pedestrian, bus and/or parking effects while the remainder do not. Data from these sites would also provide insight into the validity of the HCM-based right-turn, bus and parking equivalency factors that are utilized in the subgroup method.

Lastly, it is desired to collect data at approaches that experience moderate to high levels of congestion. The signalized intersection analyses typically focus on peak hour operations. It is during these highly congested periods that analysts are most interested in evaluating lane performance (including queues and delays). The effect of lane distribution and lane impedances on traffic operations during non-peak periods is less critical and oftentimes not an issue since the delay (and frustration) experienced by drivers during this time is minimal. Further, the implication of using one lane distribution strategy over another is likely going to be most significant under high volume conditions.

4.2.1 Summary of Desired Criteria

In summary, the following intersection conditions and characteristics are desired when selecting sites for collecting lane volume distribution data:

- two-lane approaches,
- shared, permissive left-turn movements,
- pre-timed controller,
- isolated operations,
- effects of pedestrians, and
- moderate to high congestion levels.

4.3 Selected Sites

Four sites were selected for data collection based on the desired criteria described above. Three of the sites are located in Raleigh, North Carolina and the other site is located in downtown Chicago, Illinois. Data at the three Raleigh sites were gathered in the field while data from the Chicago site were collected from observations of video tape provided by the National Institute of Statistical Sciences (NISS).

4.4 Data Collection Method

Individual turning movement volumes were recorded by individual lane for each cycle at the selected sites. Data were collected using a laptop computer with a spreadsheet program. The program allows the user to cumulatively record counts for each lane movement for each cycle. In addition, the program allows the user to record a timestamp at the beginning and end of the green period. A summary of the peak-hour turning movement volumes, geometric configurations, and intersection characteristics are provided in Figure 4.01 for all four intersections. Appendix B includes all raw count data and Appendix C provides a summary of the volumes aggregated every 15 minutes and converted to hourly volumes.

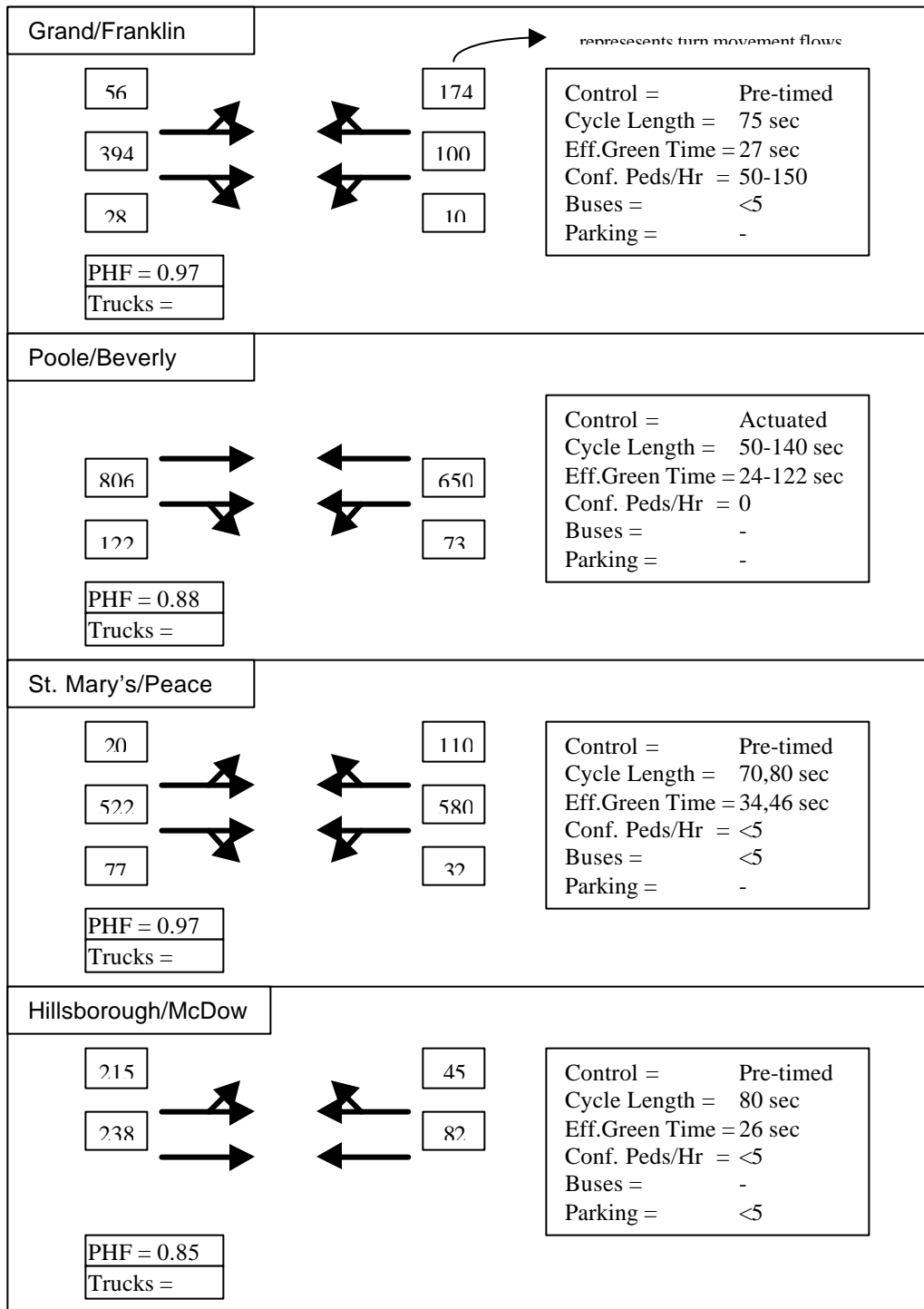


FIGURE 4.01. Volume and Geometric Characteristics of Selected Sites

4.5 Summary of Observations

W Grand Avenue/N Franklin Street Intersection – Chicago, Illinois

The Grand/Franklin intersection is located west of downtown Chicago in a Central Business District. Grand Avenue is a four-lane roadway with a speed limit of 35 miles per hour. Data collection focused on the eastbound and westbound approaches at the intersection. At the intersection of Franklin Avenue, Grand Avenue has a shared through/right-turn and shared through/left-turn lane. The major movements at the intersection are the through movements on Grand Avenue. There is a moderate to low percentage of truck traffic on Grand Avenue (~5%). Both left-turn movements on Grand Avenue operate in permissive phasing. The intersection is pre-timed and during the peak periods the intersection operates with a cycle length of 75 seconds.

The intersection includes moderate levels of pedestrians that block right-turning traffic during portions of the cycle. There is a bus stop prior to the Grand/Franklin intersection in the eastbound direction.

Video of the Grand/Franklin intersection was collected on May 25, 2000. A total of six hours of data were collected (7-10 a.m. and 3:30-6:30 p.m.). The weather for the day was overcast and dry. A total of 285 cycles were observed in the a.m. and p.m. periods combined. Throughout the observational period there were low to moderate levels of pedestrian crossings in the eastbound and westbound directions. For both morning and evening periods, there were approximately 50 pedestrian crossings per hour (~ one per cycle) conflicting with the eastbound right-turning movement, and approximately 150 pedestrians per hour (~ three per cycle) conflicting with the westbound right-turning movement. In addition, the rate of bus stops that blocked traffic in the eastbound direction was less than two per hour. Approach congestion was predominately at a moderate level. No cycle failures were observed.

Poole Road/Beverly Drive – Raleigh, North Carolina

Poole Road is a four lane road located east of downtown Raleigh, North Carolina. Poole Road runs east-west, has a speed limit of 35 mph, and serves as an arterial for traffic traveling between downtown Raleigh and the Beltline (I-440). Beverly Road serves predominately residential traffic and intersects Poole Road from the south to form a “T” intersection. Data collection focused on the eastbound and westbound approaches at the intersection. The eastbound approach of Poole Road consists of a through lane and a shared through/right-turn lane. The westbound approach of Poole Road includes a through lane and a shared through/left-turn lane. The left-turn movement on Poole Road operates with a permissive phase. The Poole/Beverly intersection operates with actuated control. No pedestrian crossings were observed. Poole Road does not include bus stops and does not allow on-street parking in the vicinity of Beverly Drive.

Data were collected at the Poole/Beverly intersection between 4-6 p.m. on September 19, 2000. The weather was overcast with light rain. Data were discarded for all cycle with cycle lengths less than 50 seconds and greater than 140 seconds. A total of 77 cycles were observed, 17 of which were excluded from the analysis because of the cycle length constraints. The green times for the eastbound and westbound approaches were recorded for each cycle. An average was taken in order to determine the effective green time and cycle length for 5- and 15-minute periods. No pedestrian or bus activity was observed. Traffic volumes were light to moderate. No cycle failures were observed.

St. Mary’s Street/West Peace Street – Raleigh, North Carolina

Peace Street is located north of downtown Raleigh and serves as a connector between US-401 and Oberlin Road. Peace Street maintains a four-lane cross section and has a speed limit of 35 mph in the vicinity of St. Mary’s Street. Data collection focused on the eastbound and westbound approaches of the intersection. At its intersection with St. Mary’s, Peace Street includes a shared through/right-turn lane and a shared through/left-turn lane on both eastbound and westbound approaches. Both the right-turn and left-turn movements operate with permissive phasing. The intersection operates with

a two-phase pre-timed signal. The cycle length at the intersection during peak periods is 80 seconds and during non-peak periods is 70 seconds. Bus stops are located on Peace Street in both directions just west of St. Mary's Street.

Data were collected at the Peace/St. Mary's intersection on September 21, 2000 between 3:45-5:30 p.m. and on November 16, 2000 between 4:30-6:30 p.m. During the September count, a total of 81 cycles were observed. The weather was overcast and dry. Less than five pedestrian crossings occurred in the eastbound and westbound directions. A total of 4 bus stops were observed during the 1:45 minute observation period, two of which did not block traffic. Overall, traffic congestion was light to moderate. No cycle failures were observed.

During the November count 88 cycles were observed. A total of three pedestrian crossings were observed. One bus blockage took place in the westbound direction on Peace Street. Congestion levels were light to moderate.

During both observations at Peace/St Mary's, through vehicles traveling in the eastbound direction appeared to favor the outside lane regardless of the level of left-turning traffic.

Hillsborough Street/North McDowell Street – Raleigh, North Carolina

The Hillsborough/McDowell intersection is located one block west of the State Capitol near downtown Raleigh, North Carolina. Hillsborough Street runs east-west and is a major arterial between the Beltline (I-440) to the west and the State Capitol to the east. In the vicinity of McDowell Street, Hillsborough Street is a four-lane roadway with a posted speed of 35 mph. At the intersection of Hillsborough/McDowell, McDowell is a one-way street in the northbound direction. Data collection at this intersection focused on the eastbound and westbound approaches. The eastbound (Hillsborough Street) approach to the intersection includes a through lane and a shared through/left-turn lane. The left-turn movement operates with permissive phasing. The westbound approach includes a through lane and a shared through/right-turn lane. The intersection operates as a two-phased, pre-timed signal. The intersection has a cycle length of 80 seconds. On-

street parking is allowed on the eastbound and westbound approaches. There are no bus stops on Hillsborough Street in the vicinity of McDowell Street.

Lane volumes at the Hillsborough/McDowell intersection were recorded on September 25, 2000 between 4:15-5:30 p.m. A total of 68 cycles were observed. The weather was cloudy with rain. Vehicle arrivals in the eastbound direction are heavily platooned. Field observations revealed that there is a heavy southbound left-turn movement at the upstream signal that turns onto Hillsborough Street. The majority of these vehicles travel in the inside through lane on Hillsborough Street. In addition, there are very low volumes on the westbound approach. Overall, traffic congestion at Hillsborough/McDowell is very light. Vehicles park along Hillsborough Street in both directions, although there were less than five parking maneuvers that took place during the period of observation. In addition, less than five pedestrian crossings were observed.

4.6 Limitations of the Data

In total, 13 hours of data were collected at the four sites combined. Although lane volume data are provided for 580 cycles, this results in only 100 observations over a 15-minute aggregation period.

Furthermore, the observations are limited to approaches that include two-lanes with permitted-shared turns. Lane distribution effects were not observed for approaches with three and four lanes or with protected turns.

The primary lane distribution effect observed was permissive left-turning movements blocking through vehicles. The effect of pedestrian crossings was only seen at the Grand/Franklin intersections. None of the other three intersections experienced any level of pedestrian impedance. Likewise, none of the observations included effects due to bus stops or parking maneuvers. The effect that bus blockages have on lane distribution, particularly on a per-cycle basis, are of particular interest.

Lastly, each of the approaches operate under relatively low congestion levels. This is primarily due to the fact that each approach selected for data collection is a major-street approach that receives more than adequate green time.

4.7 Aggregated Field Data Results

Prior to analyzing the field data, it is necessary to review the data for ambiguities and to develop measures for analyzing the data. The following two sections provide a description of the data and the analysis measures.

4.7.1 Data Extraction

Review of the field data collected for the Hillsborough/McDowell intersection revealed that drivers heavily favor the inside lane in the eastbound direction. The biased selection of lanes occurs because of the heavy southbound left-turn movement that takes place at the upstream intersection (Hillsborough/Dawson). The majority of the left-turning vehicles stay in the inside through lane on Hillsborough Street after making the left-turn movement. Because of the low volumes on Hillsborough Street, vehicles continue to stay in the inside lane since there is little motivation to change lanes. As discussed in Chapter 3, one of the criteria for collecting data is that intersections operate in isolation from the remainder of the system. Because of this, data collected at the Hillsborough/McDowell intersection were not included in the analysis.

Likewise, traffic in the eastbound direction at the Peace/St Mary's intersection heavily favors the outside travel lane. Review of the field data confirmed that between 60-70% of through traffic uses the outside lane, regardless of the number of left-turning or right-turning vehicles. Thus, these data were also eliminated from analysis.

Figure 4.02 graphically depicts all the field data including the extracted data.

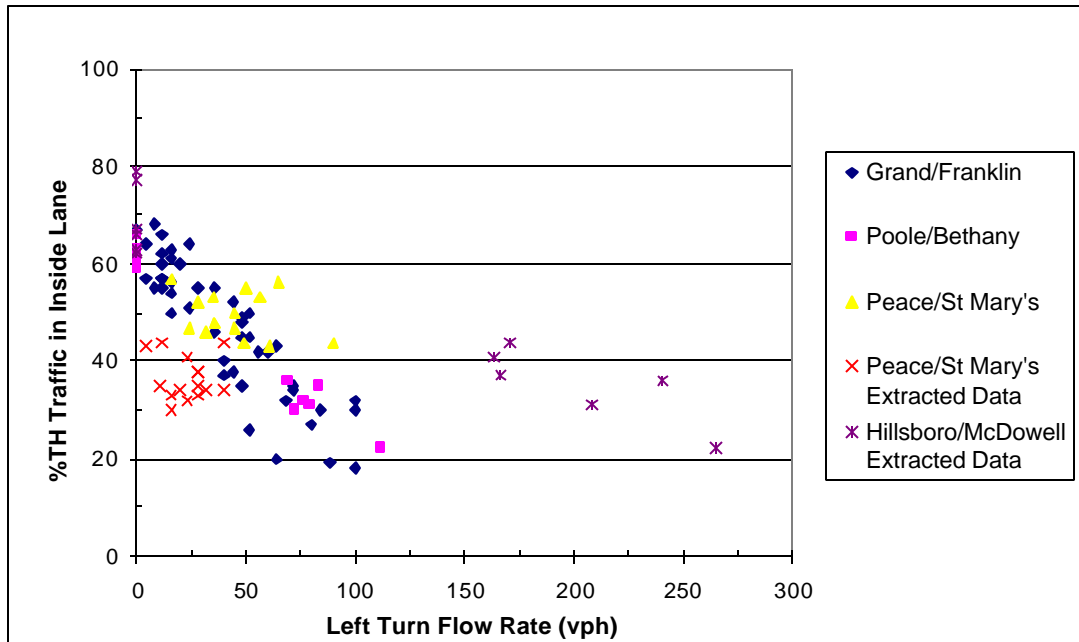


FIGURE 4.02 Field Data Summary

As shown in the figure, the data collected at the eastbound approach of Peace/St Mary's and at the Hillsborough/McDowell intersection clearly lie outside of the remaining observations.

4.7.2 Discussion of Analysis Measures

To provide consistency with the HCM methodology, the field data were aggregated every fifteen minutes (or close to fifteen minutes based on the cycle length) and converted to hourly flow rates. Based on the 15-minute aggregations, a total of 73 data points are available. Each data point includes the right-turn volume in the outside lane, the through volume in the outside lane, the through volume in the inside lane, and the left-turn volumes in the inside lane *for each approach*. Of the 73 data points, 46 represent Grand/Franklin (63%), 12 represent Poole/Beverly (16%), and 15 represent Peace/St. Mary's (21%).

The focus of the analysis presented in this chapter is on the distribution of through traffic across the two choice lanes. The measure chosen to represent the distribution of traffic is the percentage of through traffic that is in the inside (shared left-turn) lane, as represented by the equation below.

$$\% \text{THVol in the Inside Lane} = \frac{THVol_{\text{InsideLane}}}{THVol_{\text{InsideLane}} + THVol_{\text{OutsideLane}}} \quad (4.01)$$

Note that this measure is not to be confused with the percentage of traffic in the inside lane that consists of through traffic!

Other potential measures include the percentage of traffic in the inside lane that turns left (used by Bonneson and Lieberman) and the percentage of total approach flow in the inside lane. The percentage of left-turning traffic in the inside lane was avoided for two reasons:

- 1) it is an indirect means of estimating the variable condition which is the amount of through traffic in each lane, and
- 2) the resulting through volumes for each lane that are determined by using the percentage of left-turn traffic in the inside lane and the percentage of right-turn traffic in the outside lane do not always produce the total through traffic flow.

The latter measure (percentage of total approach flow in the inside lane) will produce similar trends to the percentage of through traffic in the inside lane measure. However using the total lane flows accounts for the right-turn and left-turn traffic which, in the cases analyzed in this thesis, are fixed. Thus, the effect of lane distribution strategies is less evident for cases where high turning movement flows exist.

The percentage of through traffic in the inside lane is used to relate data of all flow levels. If the actual flow rate of through traffic in the inside lane were used as a measure of comparison (as opposed to the percentage of through traffic) it would be nearly impossible to compare results for sites that experience different levels of traffic

flow. Nonetheless, caution should be exercised when evaluating percentages at low traffic flows since values with small denominator terms tend to have a greater variance.

The percentage of through traffic in the inside lane is analyzed against the hourly flow rates for the left-turn movement, subject approach, and opposing approach. An alternative to analyzing the data in terms of hourly flow rates is to analyze the data in terms of vehicles per cycle. The units of vehicles per cycle were not used in this analysis, though, primarily for the sake of simplicity. In addition, because the cycle lengths for 90% of the data points are within 10 seconds of each other, analyzing the data in terms of vehicles per hour will produce similar results to analyzing them in vehicles per cycle.

4.7.3 Observation Summaries

Figures 4.03-4.07 provide the results of the field data collection for the three sites. The y-axis for all figures represents the percentage of through traffic in the inside lane. A percentage of 100 indicates that all through traffic use the inside lane; a percentage of zero indicates that no through traffic uses the inside lane (thus resulting in a defacto left-turn lane). In addition, the vertical bars in the graphs represent division lines for the flow regimes that are evaluated in Chapter 5.0.

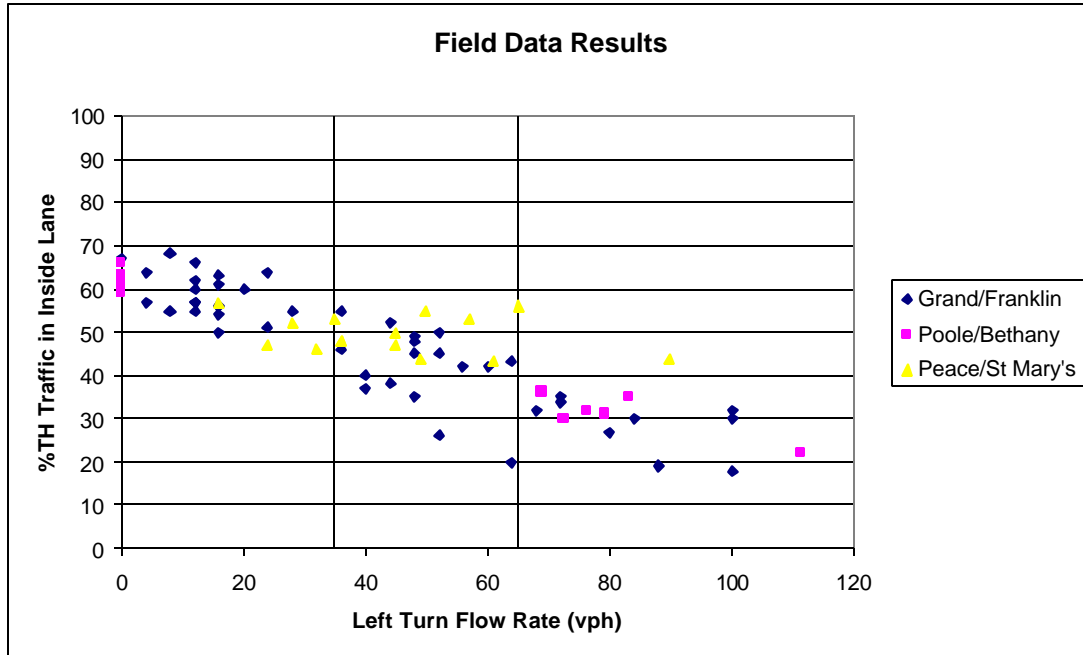


FIGURE 4.03. Effect of Left Turn Flow on Through Traffic Distribution

Figure 4.03 shows that the through traffic in the inside lane decreases as left-turn flow increases. This is expected, since left-turning vehicles that are waiting for a gap in the opposing traffic stream block through vehicles in the inside lane. Thus, the lane becomes less desirable as the left-turning traffic increases and through traffic begins to shift to the outside lane. For cases where the left-turn flow rate is zero (either because the left-turn movement does not exist or no left-turning vehicles were observed), the percentage of through traffic in the inside lane is approximately between 60-70%. This shows that vehicles tend to favor the inside lane when no left-turners are present, likely because the outside lane experiences impedances caused by right-turning vehicles and conflicting pedestrians.

Figure 4.03 also shows that no defacto left-turn lanes were observed for any of the 15-minute observations although some appeared in individual cycles. In addition, the left-turn flow rates ranged from 0 – 110 vehicles per hour. This relatively low left-turn

volume (which corresponds roughly to 2-2.5 vehicles per cycle) is reasonable given that the left-turn movements operate with permissive phasing in a shared lane.

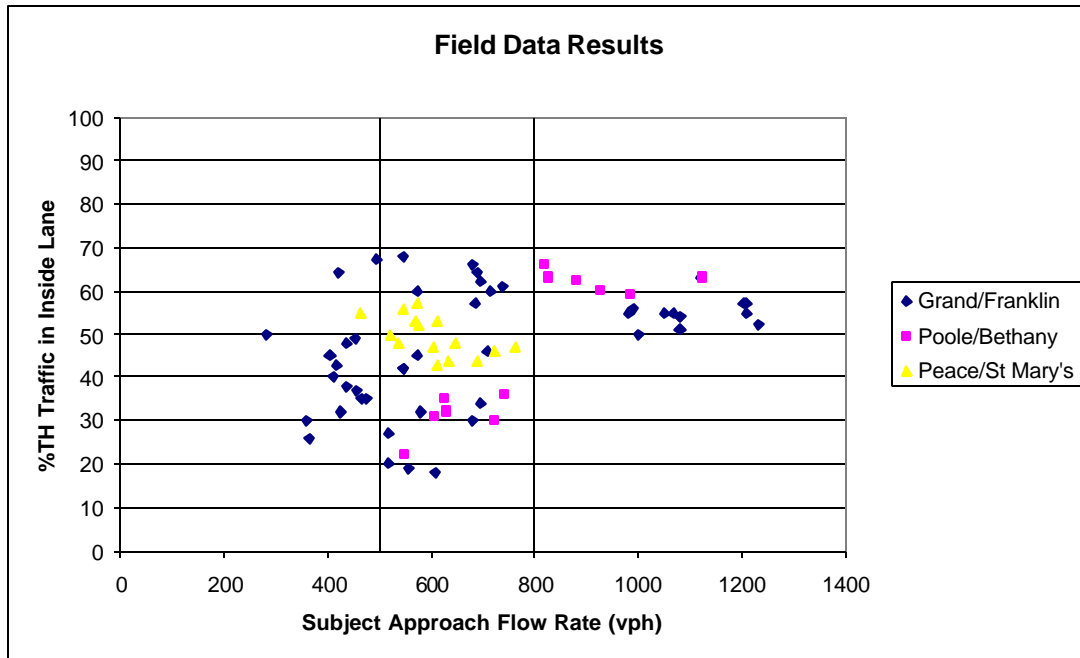


FIGURE 4.04. Effect of Subject Approach Flow on Through Traffic Distribution

Figure 4.04 indicates that at higher subject flow rates, the percentage of traffic in the inside lane tends to stabilize between 50-65%. At flow rates less than 800 vph, the amount of subject approach flow does not greatly influence the percentage of through traffic in the inside lane and the percentage varies between 20-70%.

The results shown in Figure 4.04 give some credence to Bonneson’s lane change probability model. The model states that the likelihood of a driver changing lanes is low under low flow and high flow conditions. Although there does not appear to be a “favored” lane for through traffic under low flow conditions, the variability in the selection of lanes under high flow conditions is distinctly lower than under lesser flow conditions.

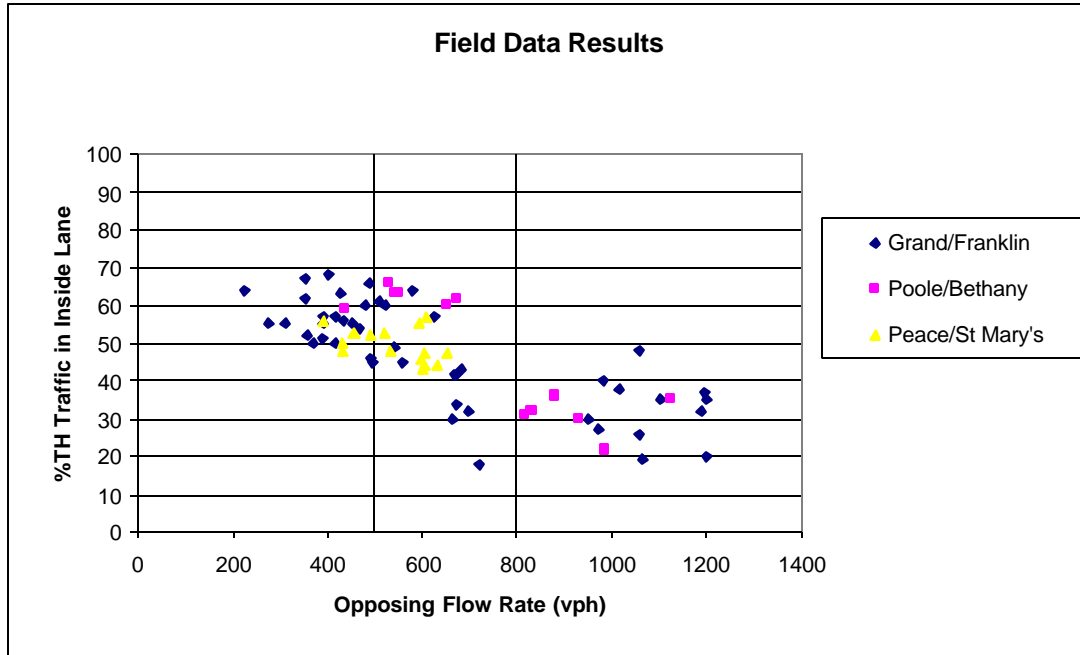
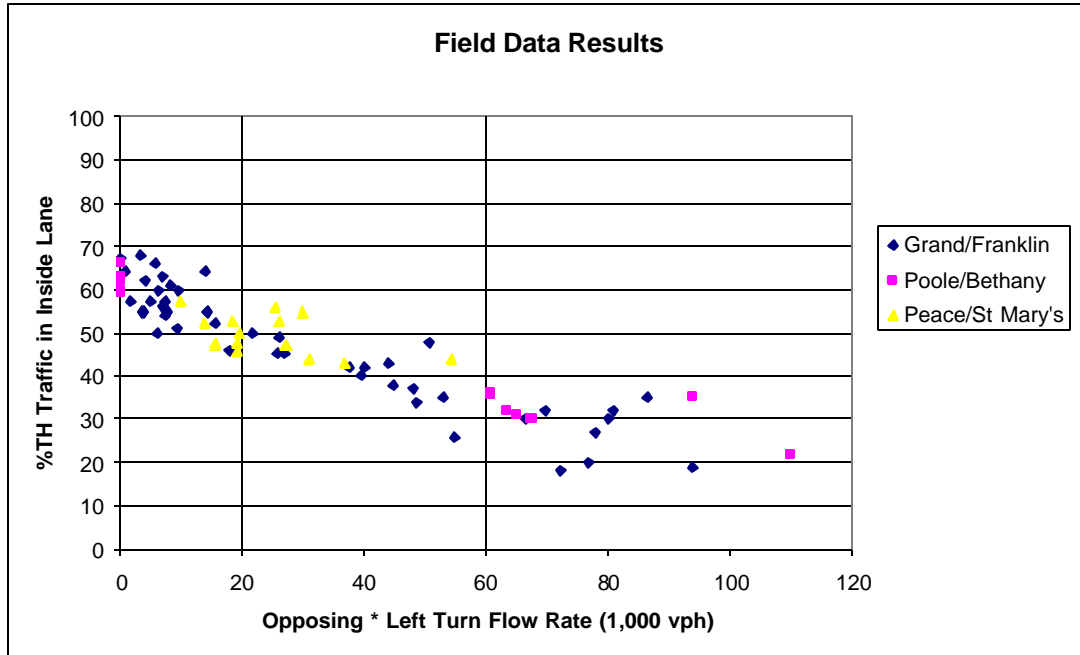


FIGURE 4.05. Effect of Opposing Flow on Through Traffic Distribution

The effect that opposing traffic has on the percentage of through traffic in the inside lane (shown in Figure 4.05) is similar to the effect that left-turning traffic has on the distribution of through traffic (4.03). In general, the percentage of through traffic in the inside lane decreases linearly as opposing flow increases. An increase in the opposing flow results in an increase in the delay for left-turning vehicles which, in turn, blocks through traffic in the inside lane. Thus, under conditions of high opposing flow, through traffic tends to shift to the outside lane.



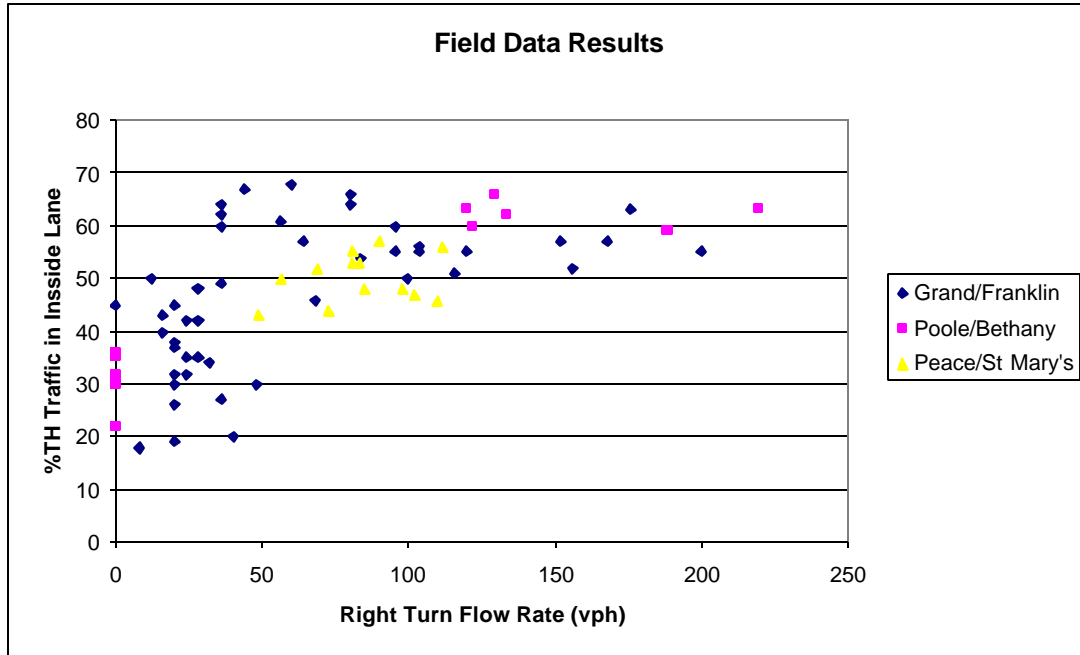


FIGURE 4.07. Effect of Right Turn Flow on Through Traffic Distribution

Figure 4.07 shows the relationship between the right-turn flow rate and the percentage of through vehicles in the inside lane. In general, the outside lane is attractive under low right-turn volumes and less attractive under higher right-turn volumes. In the lower ranges of right-turn volume (< 100 vph) the distribution of through traffic appears highly variable. The distribution of through traffic appears to stabilize between 50-65% under high right-turn flow conditions.

In summary, the graphs depicted in Figures 4.03-4.07 indicate that data from the three sites correlate well. The figures also show that the level of opposing and left-turn traffic has the greatest effect on the distribution of through traffic. Lastly, it is important to note that no defacto left-turn lanes were observed over any of the 15-minute periods.

4.8 Field Regression Model

A regression analysis was performed using the field data collected to predict the volume of through traffic (not the percentage) in the inside lane. It is important to note that the regression model is based on data collected at two-lane approaches that include shared/permitted turns. Effects due to pedestrians, bus stops, and parking are not included in the model. The general form of the regression equation is as follows:

$$TH_{Inside} = a \cdot (TH + RT)^{b1} \cdot (LT)^{b2} \cdot (Opp)^{b3} \quad (4.02)$$

where TH_{Inside} = through flow rate (vph) in the inside lane, $(TH + RT)$ = sum of through and right-turn flow rates (vph), LT = left-turn flow rate (vph), Opp = opposing flow rate (opposing through + right-turning flow rates, vph). For a two-lane approach, the through flow rate in the outside lane is computed by subtracting TH_{Inside} from the total through traffic.

It should be noted that the through and right-turn volumes were combined into one variable to account for the effect that right-turning traffic has on lane distribution while still maintaining the ability to use the model when the right-turn volume is zero.

Results from the regression analysis are shown in Table 4.01.

Table 4.01: Regression Output

<i>Regression Statistics</i>		
R^2		0.89
Standard Error		0.195
Observations ¹		73
<i>Coefficient Statistics</i>		
Variables	Coefficient	P-Value
α	9.561	0.005
β_1	0.980	0.000
β_2	-.067	0.001
β_3	-.437	0.000

The R^2 value for the regression model is 0.89. As shown in the table, the coefficients β_2 and β_3 of the regression model are negative. This indicates that as left-turn flow and opposing flow increase, the amount of through traffic in the inside lane decreases. Lastly, the p-value for each of the variables is less than 0.05 which implies that all variables are significant.

The final form of the field regression model is thus:

$$TH_{Inside} = \frac{9.561 \cdot (TH + RT)^{0.98}}{(LT)^{0.067} \cdot (Opp)^{0.437}} \quad (4.03)$$

A comparison of the predictions from the regression model (Equation 4.03) with field data is provided in Figure 4.08.

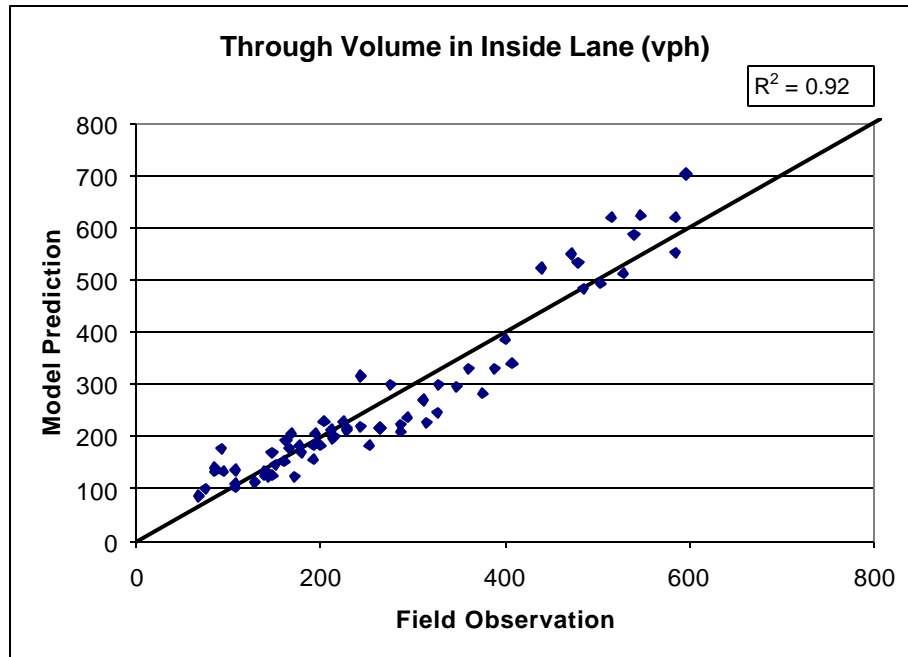


FIGURE 4.08. Evaluation of Regression Model against Field Data

In general, the regression model tends to slightly underestimate the through volume in the inside lane for volumes ranging between 250-400. Conversely, the regression model tends to overestimates the amount of through traffic in the inside lane for volumes greater than 400 vph.

Two statistical tests are used to evaluate the performance of the empirical model: the Root Mean Squared Error (RMSE) test (add reference ...) and the Mean Absolute Percentage Error (MAPE) test (add reference ...). The equations for calculating the RMSE and MAPE error values follow.

$$RMSE = \sqrt{\frac{1}{N} \sum_{i=1}^N (x_i - \hat{x}_i)^2} \quad (4.03)$$

$$MAPE = \left(\frac{1}{N} \sum_{i=1}^N \frac{|x_i - \hat{x}_i|}{x_i} \right) \cdot 100 \quad (4.04)$$

where x_i = observed value of measure,

\hat{x}_i = forecast value of measure, and

N = number of observations.

The measure used in the comparison of the empirical model prediction and the observed field data is the number of through vehicles in the inside lane (in vehicles per hour). Thus, the RMSE test provides the average error, in vehicles per hour, of the prediction of through vehicles in the inside lane versus the observed field values. The MAPE test calculates the percentage error between the predicted and observed values. The results of the RMSE and MAPE tests for the empirical field model are shown in Table 4.02.

Table 4.02: Statistical Evaluation of Empirical Model

Test	Error
RMSE	44.68
MAPE	15.09

As shown in Table 4.02, the RMSE error is approximately 45, indicating that on average the empirical model prediction for through traffic in the inside lane is 45 vph different than the observed field value. Likewise, the MAPE value shows that the percentage error of the empirical model prediction is, on average, 15%.

Although the field model provides a relatively high R-squared value and on average is within 15% of the observed field data, the model is limited for use only for two-lane approaches that include shared through left- and right-turn lanes that operate with permissive phasing. Because of these limitations, the empirical model provided in Equation 4.03 is not included in the lane distribution strategy analysis presented in Chapter 5.0. Upon further data collection however, an empirical model similar to the one shown in Equation 4.04 could provide a means for estimating individual lane flow when no other parameters other than turning movement flows are known.

4.9 Assessment of HCM Lane Utilization Factor

A Lane Utilization Factor (LUF) was calculated for each observation using Equation 9-11 of the 1997 HCM, as shown below.

$$f_{LU} = \frac{v_g}{v_{g1} \cdot N} \tag{4.05}$$

where v_g = the total lane group flow (or in this case, approach flow) (vph), v_{g1} = the highest lane flow (vph), N = the number of lanes (2). From Table 9-4 of the 1997 HCM, The default lane utilization factor for two-lane approaches with shared turns is 0.95.

Figure 4.09 shows the computed lane utilization factors for each observation versus the product of opposing and left-turn flow.

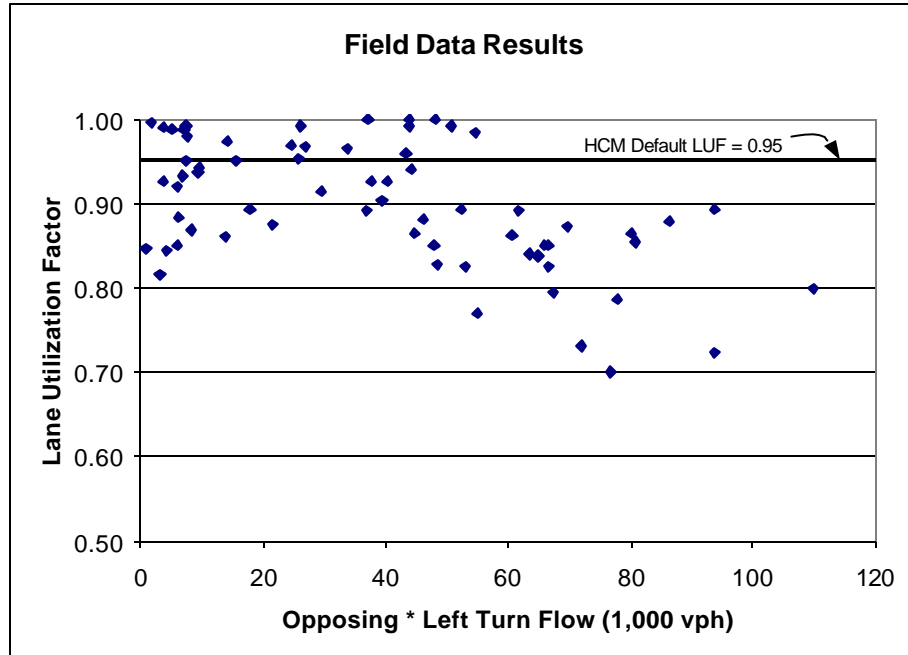


FIGURE 4.09. Effect of Opposing * Left Turn Flow on HCM Lane Utilization Factor

As shown in the figure, the default HCM Lane Utilization Factor of 0.95 is reasonable under cases where the product of opposing and left-turn flows is less than 50,000 vph. At higher levels, the LUF factor ranges between 0.70 and 0.90. This shows that the distribution of traffic on a two-lane approach is not represented well by a single, constant factor, such as is used as a default in the HCM.

4.10 Summary

The following items summarize the results of the field data analysis:

- The distribution of through traffic is affected most by the opposing flow and the left-turn flow (particularly the product of both), and to a lesser degree the subject flow and right-turn flow (which is included in the subject flow).
- Data from the three sites correlate well.

- The Bonneson model for lane change probability appears valid for cases of high subject flow. The variability of through traffic distribution is remarkably lower under high flow conditions than under lesser flow conditions.
- An empirical model is developed that predicts the amount of through traffic in an inside lane based on the subject and opposing turning movement flows. However, the empirical field model is limited to two-lane approaches with shared through/right and through/left-turn lanes that operate with permissive phasing.
- An analysis of the HCM LUF shows that the default value of 0.95 appears reasonable at low flow conditions. Under higher flow conditions, the Lane Utilization Factors for the field data range between 0.70-0.90.

5.0 SUBGROUP LANE DISTRIBUTION MODEL EVALUATION

This chapter provides an evaluation of six lane distribution strategies. The results of the evaluation will be used to determine a recommended strategy for the subgroup lane distribution model. This chapter attempts to answer the following questions:

- 1) Based on the field data collected, which lane distribution strategy provides the best lane flow predictions?
- 2) What are the implications of using one lane distribution strategy versus another?
- 3) How do the lane distribution strategies perform under increasing levels of traffic flow and impedances?

The results of the subgroup lane distribution model analysis are presented in three parts. First, a statistical analysis summarizing the performance of six lane distribution strategies versus field data is shown. Based on the literature review, the comparison of lane distribution strategies against field data is the first of its kind. The strategies are evaluated under various flow regimes to gain insight into the performance of the strategies under a variety of traffic flow conditions.

Second, a comparison of lane delays predicted by the lane distribution criteria is provided to show the implications of using one strategy versus another.

Third, results from a parametric analysis are summarized to show how the lane distribution strategies respond under increasing levels of opposing flow, conflicting pedestrians, bus stops, and green time.

5.1 Evaluation of Lane Distribution Strategies

This section shows how six lane distribution strategies perform versus the field data summarized in the previous chapter. The six lane distribution criteria include: equal

average back of queue, the Bonneson method, equal lane delay, equal lane flow ratio, equal cycle-average queue, and equal lane volume.

The subgroup method is carried out using a software program developed using Visual Basic and Excel. The program allows the user to input volume and geometric characteristics of the intersection, signal timing data and provides the user with lane performance measures including lane saturation flow, delay, level of service, average queue, and average back of queue. The software program calculates individual lane flow based on a specified lane distribution criterion and the turning movement volumes for each approach. Appendix D includes the output for all analyses.

Two tests are used to evaluate the six lane distribution strategies: the Root Mean Squared Error (RMSE) test and the Mean Absolute Percentage Error (MAPE) test. The RMSE statistic returns the absolute difference of a measure between the predicted and observed values. The MAPE statistic returns the absolute *percentage* difference of error between the predicted and observed values. Thus, the RMSE statistic is insensitive to changes in magnitude, so data with low through flows will likely have lower errors values than data with high through flows. For this reason, the MAPE error is the primary statistical value used to evaluate the lane distribution strategies.

The prediction of the amount of through traffic in the inside lane is the measure used to evaluate each strategy in this chapter. The predictions of through traffic in the inside lane are developed for each strategy and compared to the field data for each observation. The RMSE and MAPE values are used to evaluate the performance of the lane distribution strategies. In general terms, the RMSE values represent difference in vehicles per hour between the predicted value and the observed value of through traffic in the inside lane. The MAPE values represent the percentage difference between the predicted and observed values of through traffic in the inside lane.

Analyses were performed for 73 observations for each of the six criteria. It is important to note that the saturation flow rates calculated using the subgroup model were not validated in the field. Thus, the evaluation presented in this chapter focuses on the

relative performance of each strategy in comparison with the field data. Field calibration of the subgroup model, particularly the subgroup headway equivalency factors, is not addressed in this analysis. Field calibration, though, could improve the accuracy of the equivalency factors and reduce the RMSE and MAPE values reported in this analysis.

Figure 5.01 provides a summary of the RMSE and MAPE values for the six criteria for all data sets. As mentioned earlier, the RMSE is representative of the difference in the number of through vehicles in the inside lane in comparison to the observed field values. The MAPE values represents the percentage difference in the number of through vehicles in the inside lane.

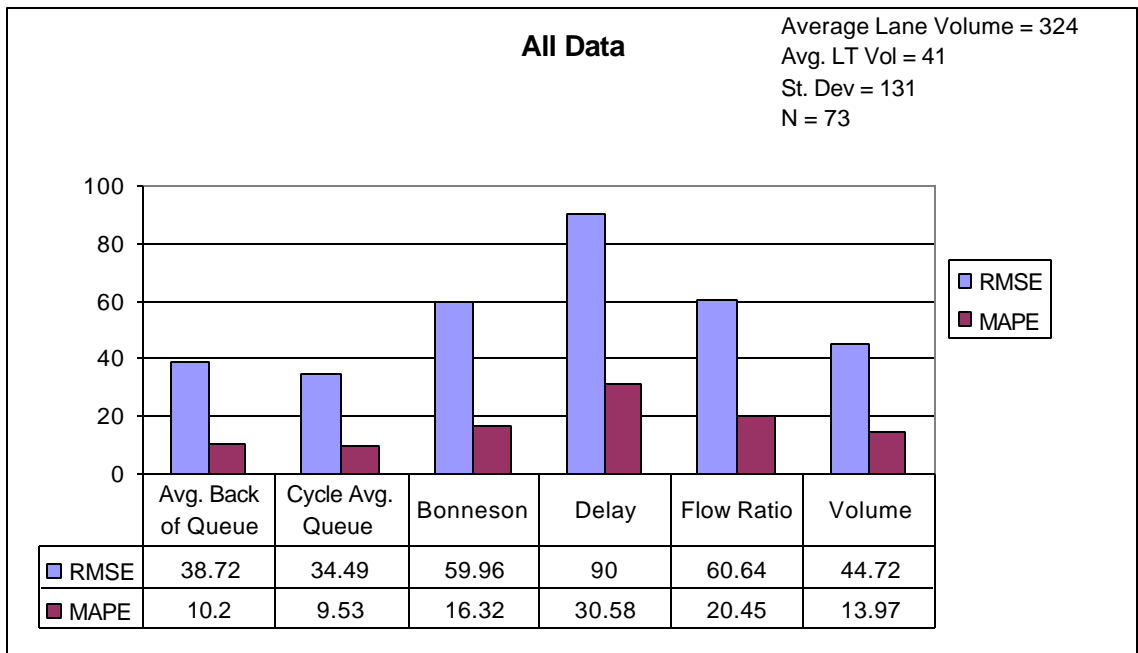


FIGURE 5.01. RMSE/MAPE Comparison for All Data

As shown in Figure 5.01, the average back of queue and cycle-average queue strategies produce the lowest RMSE and MAPE error values when compared for all data sets. A review of the RMSE and MAPE error values for each individual intersection (shown in Appendix E) indicate the same trends as shown in Figure 5.01. The MAPE

values for the two queue-based strategies indicate that the lane flow predictions are within 10% of the observed field values. The equal volume strategy performs slightly better than the Bonneson strategy, and significantly better than the equal delay and flow ratio strategies.

A lane distribution strategy should, at a minimum, perform better than the equal volume strategy. The equal volume strategy is assumed in the Set Initial Volume step of the lane flow allocation process (Step #2). Thus, the iterative process used to achieve a lane distribution criterion is futile if the result is worse than what was initially assumed.

An interesting point is that the three current lane-by-lane analysis procedures (Australia, Canada, and Sweden) all employ an equal flow-ratio model. Based on the results of the analysis summarized in Figure 5.01, the equal flow ratio strategy results in a MAPE error value that is nearly twice that of the average back of queue and cycle-average queue strategies. Further, the flow-ratio strategy performs much worse than the equal volume strategy.

The following figures provide results of an analysis comparing the MAPE error values for the six criteria based on various levels of left-turn flow, subject approach flow, and opposing flow. Each flow type (left-turn, subject, and opposing) includes three regimes. These regimes are depicted in Figures 4.02, 4.03, and 4.04, respectively. The regimes represent logical breakpoints in the data and they include a relatively equal number of samples in each regime. Figures 5.02, 5.03, and 5.04 present the results of this analysis.

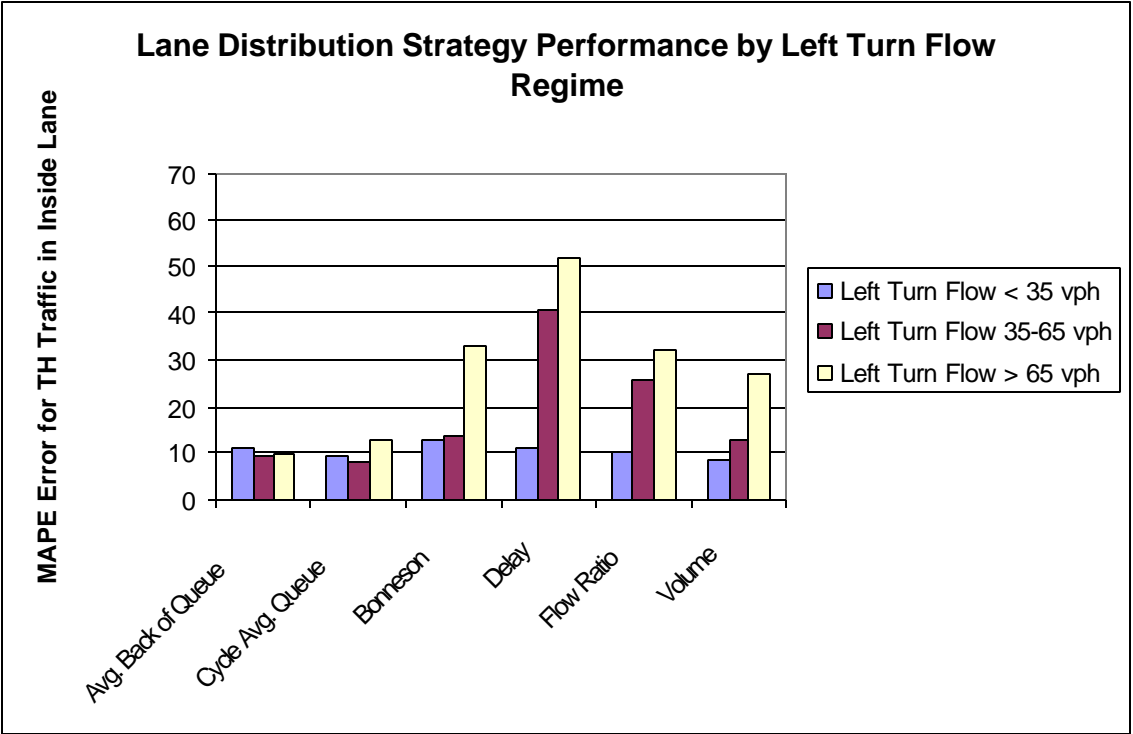


FIGURE 5.02. Comparison of MAPE values by Left Turn Flow Regime

Figure 5.02 shows that under the lowest left-turn flow condition all strategies perform equally well. The Bonneson, delay, flow ratio, and volume strategies perform increasingly worse as left-turn flow increases. The queue strategies perform similarly under each left-turn flow regime.

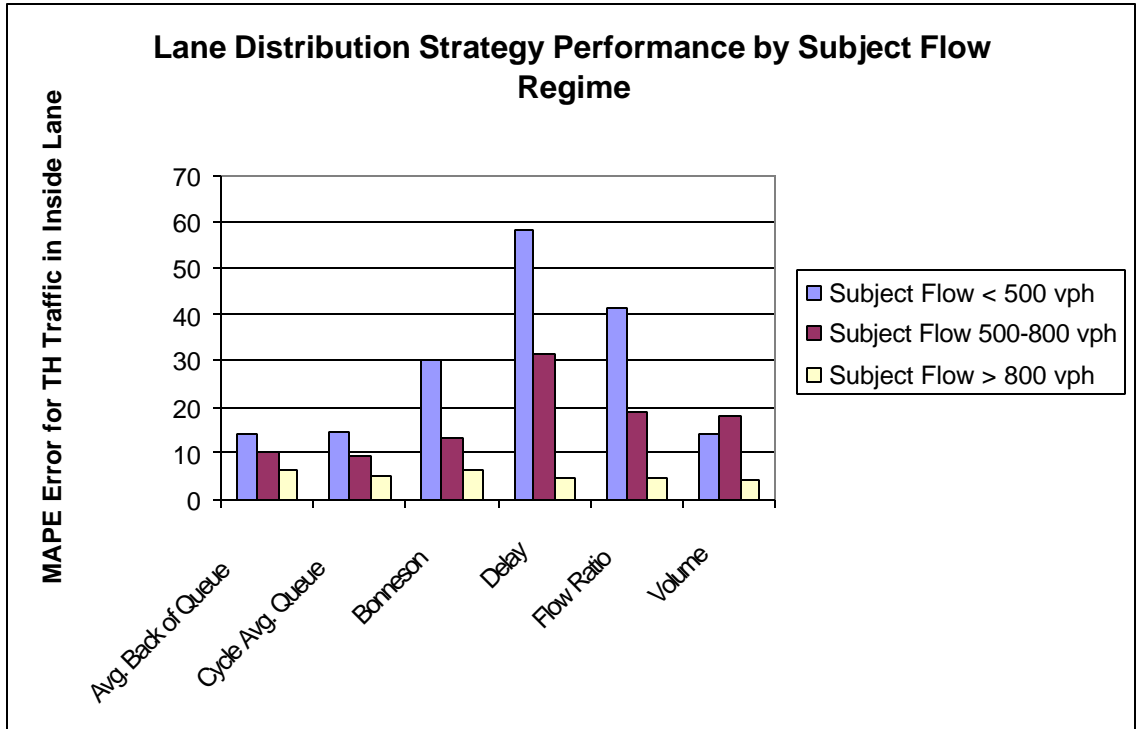


FIGURE 5.03. Comparison of MAPE values by Subject Flow Regime

Based on the subject (approach) flow regimes, the MAPE error value decreases as subject flow increases for all strategies. Under the heaviest flow condition all strategies perform equally well. The queue strategies perform noticeably better than the Bonneson, delay, and flow ratio strategies under the low and medium flow regimes.

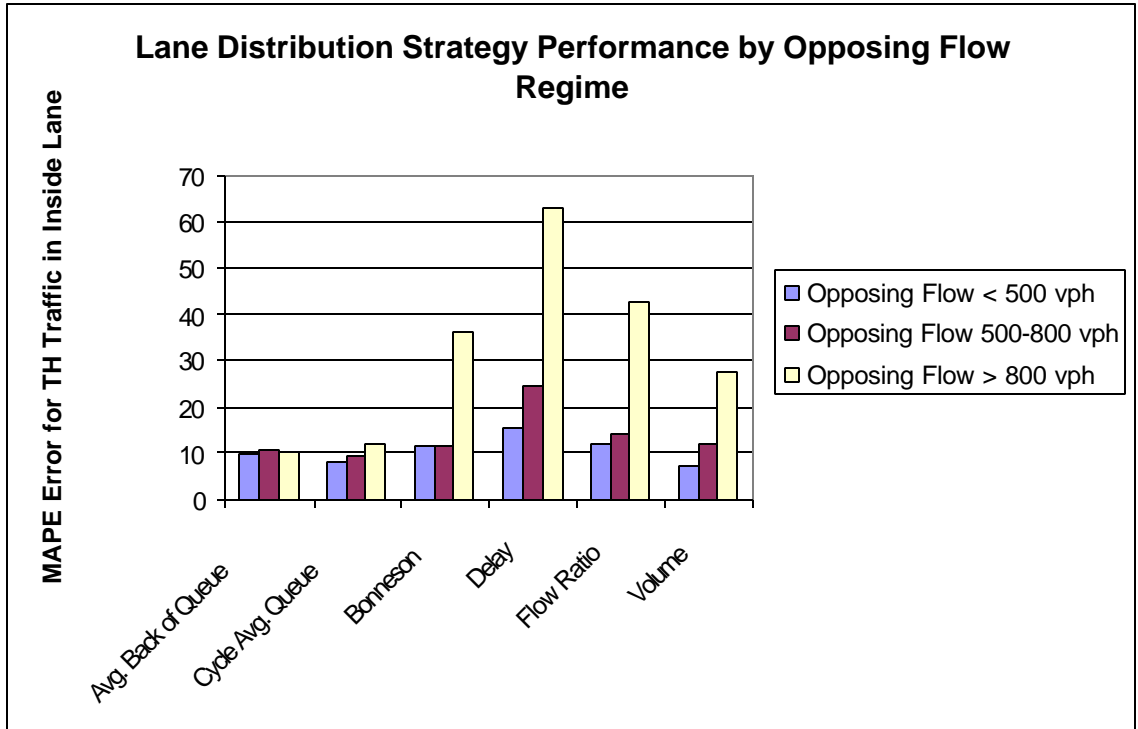


FIGURE 5.04. Comparison of MAPE values by Opposing Flow Regime

Similar to the results of the left-turn flow regime comparison, all strategies, with the exception of the queue strategies, perform increasingly worse as the opposing flow increases. The queue strategies perform similarly under all cases of opposing flow.

The results shown in Figures 5.02-5.04 show that the trends experienced by the equal flow ratio, equal delay, and Bonneson methods are similar under all flow regimes. Likewise, the average back of queue and cycle-average queue strategies perform similarly. In order to gain insight into how these strategies perform under each observation, the prediction of percent through traffic in the inside lane is shown for the field data and the flow ratio and back of queue strategies. The remaining strategies were omitted in order to reduce the amount of clutter in the graph. However, based on the previous analyses, the equal flow ratio strategy is representative of the delay strategy and Bonneson method, and the equal back of queue strategy is representative of the cycle-

average queue strategy. Figure 5.05 presents the results, which show the percentage of through traffic in the inside lane versus the product of opposing and left-turn flow.

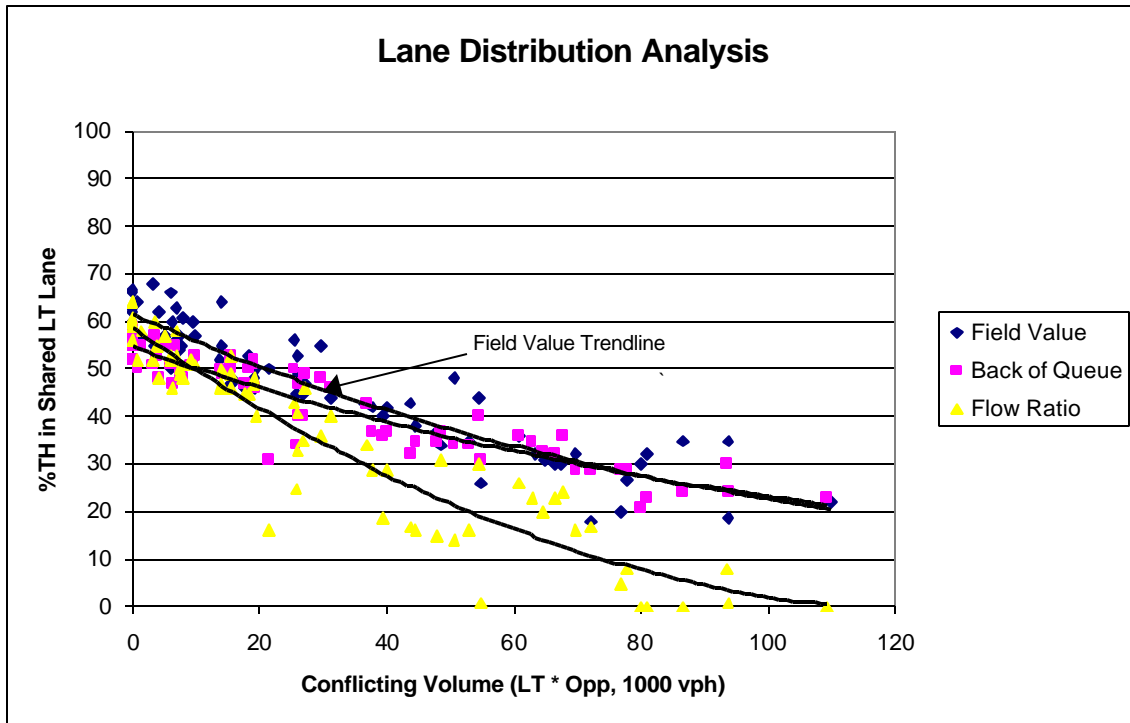


FIGURE 5.05. Lane Distribution Strategy Comparison

As shown in the figure, the equal back of queue strategy represents the distribution of through traffic more accurately than the equal flow ratio strategy. The flow ratio strategy consistently under-estimates the amount of through traffic in the inside lane, particularly under high levels of opposing and conflicting flow. This results in a prediction of defacto turn lanes under much lighter conditions than the back of queue strategy.

Based on the results of the analysis summarized in Figures 5.02-5.05 the equal average back of queue and cycle-average queue criteria provide the best estimation of lane flow (based on the available data) under all levels of left-turn, subject approach, and opposing flows. What stands out from this analysis is that the Bonneson, delay, and flow ratio strategies perform increasingly worse as opposing and left-turn flow increase. The

reason for the worsening is that as these volumes increase, the saturation flow of the inside lane decreases. As this is happening, the saturation flow of the outside lane remains relatively constant, thus the relative difference of saturation flow increases. The Bonneson, delay, and flow ratio strategies essentially assume that the shift in distribution of through traffic is proportional to the difference in saturation flows across the two lanes. Based on the field data collected, this trend is not evident (see Figure 5.05). Rather, the rate that traffic shifts to the outside lane levels off somewhat under higher flow conditions and drivers appear more willing to choose the inside lane, even though it may afford them greater delays. In summary, the Bonneson, delay, and flow ratio methods appear over-sensitive to impedances caused by left-turning vehicles and underestimate the amount of through traffic in the inside lane.

5.2 Implications of Selecting a Lane Distribution Strategy

The first question asked in this chapter (“Which strategy provides the best lane flow predictions?”) has been answered. The average back of queue and cycle-average strategies are superior to the remaining strategies based on the available data. The purpose of this section is to show the implication in terms of critical lane delay for using either the flow ratio, delay, or volume strategies. The Bonneson method is excluded from this analysis because only the percentage of left-turning traffic in the inside lane is calculated for the procedure.

Figures 5.6-5.8 provide critical lane delay comparisons for the flow ratio, delay, and volume strategies versus the back of queue strategy. The purpose of this analysis is to show the differences in critical lane delay that can result from using either the flow ratio, delay, or volume strategies as compared to the equal back of queue strategy.

It is important to note that the critical lane delays summarized in Figures 5.06-5.08 represent a 50% growth rate in the traffic volumes observed in the field. A 50% growth rate is assumed in order to provide results over all level of service regimes. The

critical lane delays using the observed field data only range from 4-25 seconds per vehicle.

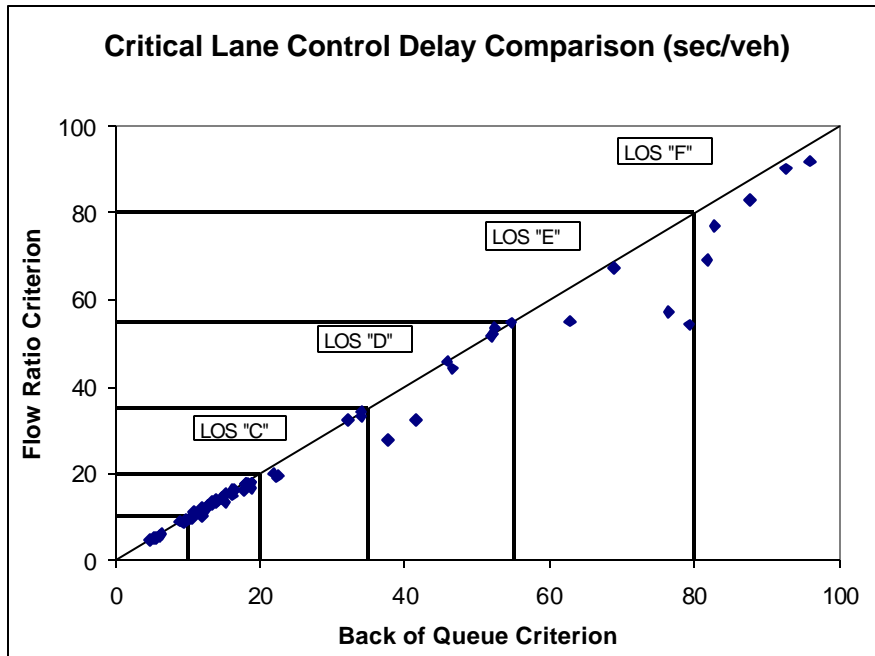


FIGURE 5.06. Critical Lane Delay Comparison: Flow Ratio vs. Back of Queue Strategy

Figure 5.06 shows that the difference in critical lane delays is minimal under LOS “A”, “B” and “C” conditions between the flow ratio and back of queue criteria. However, under LOS “D” and “E” conditions, significant differences begin to emerge between the results predicted from the two strategies. The flow ratio strategy consistently predicts lower lane delays since, theoretically, it is the more efficient measure. The fact that the back of queue strategy predicts higher delays indicates that drivers under this strategy do not fully minimize their delay at an approach. Thus, drivers will choose a lane that may experience greater delays than the adjacent lane.

Under LOS “F” conditions, the delay values appear to coincide, similar to the low delay conditions. The explanation is that under low delays (LOS “A-C”), the approach volumes are at a level where the assignment of through traffic does not significantly

impact delay since both lanes operate well below capacity. Under the LOS “D” and “E” regimes though, the assignment of through traffic is critical and can lead to significant differences in delay. Under the worst conditions (LOS “F”), the assignment of traffic is similar as both strategies approach de-facto left-turn lanes.

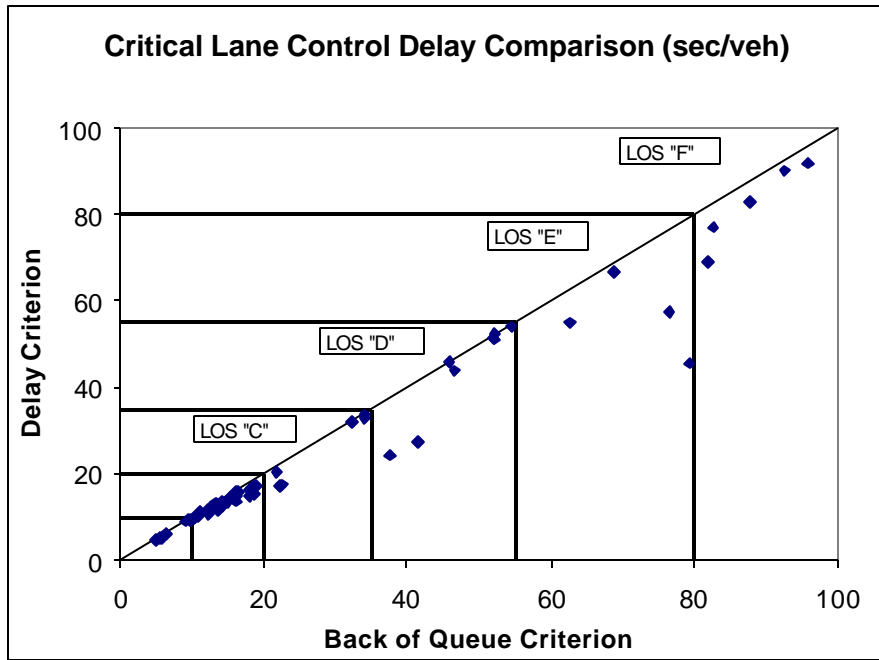


FIGURE 5.07. Critical Lane Delay Comparison: Delay vs. Back of Queue Strategy

The critical lane delay results using the equal delay criterion are similar to the results under the flow ratio strategy, although the differences in delay are greater under the equal delay strategy. Again, minimal differences are found under the extreme low and high delay conditions. Under LOS “D” and “E” conditions though, significant differences in delay are found.

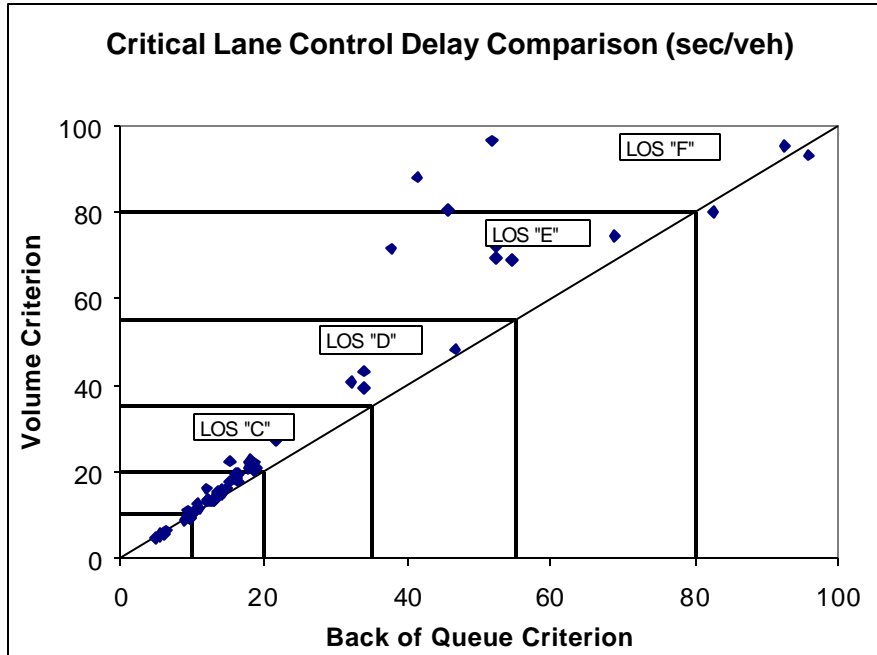


FIGURE 5.08. Critical Lane Delay Comparison: Volume vs. Back of Queue Strategy

The equal volume strategy shows that the critical lane delays, as compared to the equal back of queue criterion, are similar under cases of very low or very high delay. Under the LOS “D” and “E” regimes the equal lane volume strategy predicts significantly higher delays as compared to the back of queue strategy. This is because the equal volume strategy assigns more through traffic to the inside lane which, due to the permissive left-turning movement, experiences much greater delays than the outside lane.

In summary, under low and extremely high delay conditions, the differences in critical lane delays predicted using both methods are negligible. The largest difference in delay predictions occurs in the LOS “D” and “E” regimes. Under these conditions, the equal flow ratio and delay criteria predict significantly lower delays than the back of queue criteria.

As stated earlier, the delay analysis assumes a 50% growth in traffic volumes. An analysis of the observed field data shows that delays range between 4 and 25 seconds per

vehicle for all strategies. Based on the lane distribution strategy evaluation that was performed in Section 5.1, the back of queue and cycle average queue strategies perform the best under the observed conditions which happen to be low delay conditions (< 25 seconds/vehicle). Further data collection is required to show which lane distribution strategy performs the best under higher delay conditions since the lane choice behavior of drivers may change. Furthermore, the back of queue strategy results in higher lane delays in the LOS “D” and “E” regimes than the flow ratio and delay strategies. Whether this behavior is reflected in the field under these conditions is unknown. What is known is that the selection of a lane distribution criterion is most critical under LOS “D” and “E” conditions.

5.3 Parametric Analysis

The final part of the lane distribution evaluation is to show how the lane distribution strategies respond under increasing levels of impedances. This analysis focuses on three criteria: equal back of queue, equal delay, and equal flow ratio. The percentage of through traffic in the inside lane is predicted for each strategy under increasing levels of opposing traffic, pedestrians, bus stops, and green time.

The parametric analysis is performed for a two-lane approach that includes shared, permitted turns. The cycle length is 75 seconds and the subject approach has a displayed green time of 40 seconds. The lost time is equal to the yellow + all red time, thus the effective green time is equal to the displayed green time. Under the default scenario there are no impedances (pedestrians, bus, parking, grade = 0). For simplicity, no heavy trucks are assumed and a peak hour factor of 1.0 is used. The subject approach has a left-turn volume of 125 vph, a through volume of 1000 vph, and a right-turn volume of 150 vph. The opposing approach has a right-turn volume of 175 vph, a through volume of 800 vph and a left-turn volume of 40 vph.

The first parametric analysis shows the effect of increasing levels of opposing traffic on the distribution of through traffic using the back of queue, delay, and flow ratio

strategies. In this analysis, all parameters are held fixed with the exception of the opposing traffic flow (opposing through + right-turn volume) which ranges from 275 to 1475 vph. Figure 5.09 provides the results of this analysis.

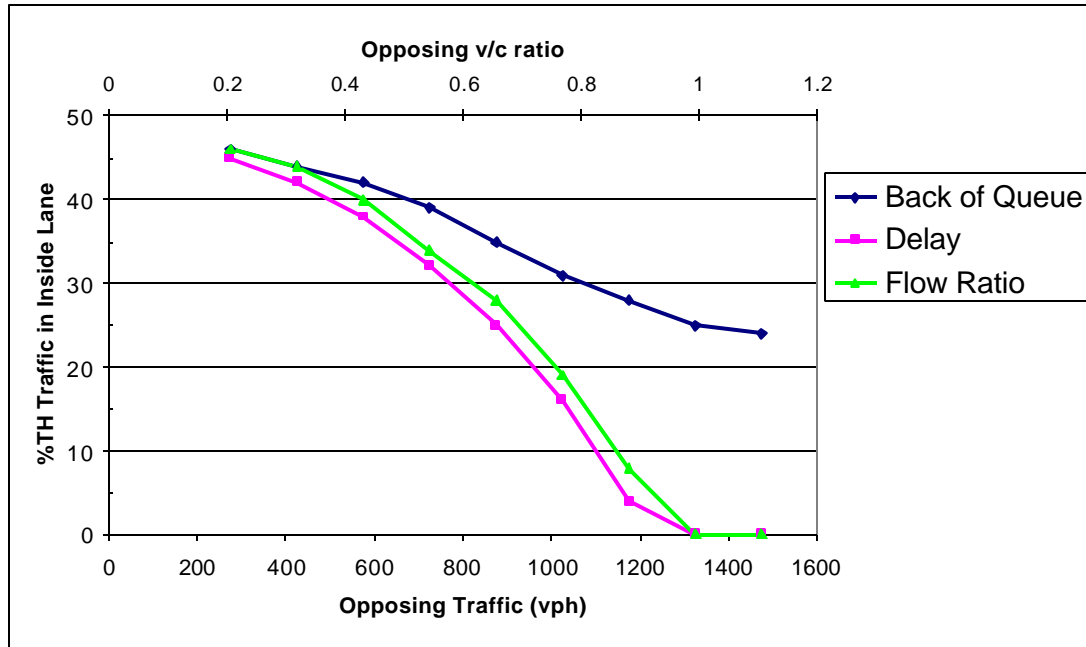


FIGURE 5.09 Effect of Opposing Traffic on Lane Distribution

As shown in Figure 5.09, the delay and flow ratio strategies display nearly a linear decline in the percentage of through traffic that is in the inside lane as opposing traffic increases. Both the delay and flow ratio strategies predict defacto turn lanes at opposing flow levels between and 1,200-1,300 vph, which correspond to an opposing v/c ratio of 1.0. It is interesting to note that Bonneson and Lieberman both conclude from a similar analysis that defacto left-turn lanes were found to occur at an opposing flow of 1,200 vehicles per hour.

The equal back of queue strategy performs quite differently from the delay and flow ratio strategies. The rate of decline of the percentage of through vehicles in the inside lane is much less gradual and plateaus at approximately 25% when the opposing

flow reaches 1,200-1,300 vehicles per hour. This indicates that a certain percentage of drivers would continue to use the inside lane even when the permissive left-turn movement experiences extremely high delays.

The second parametric analysis, shown in Figure 5.10, illustrates the effect that increasing levels of conflicting pedestrians have on the distribution of through traffic. As the level of pedestrians increase, the saturation flow of the right-turning traffic decreases thus disuading through vehicles from using the lane.

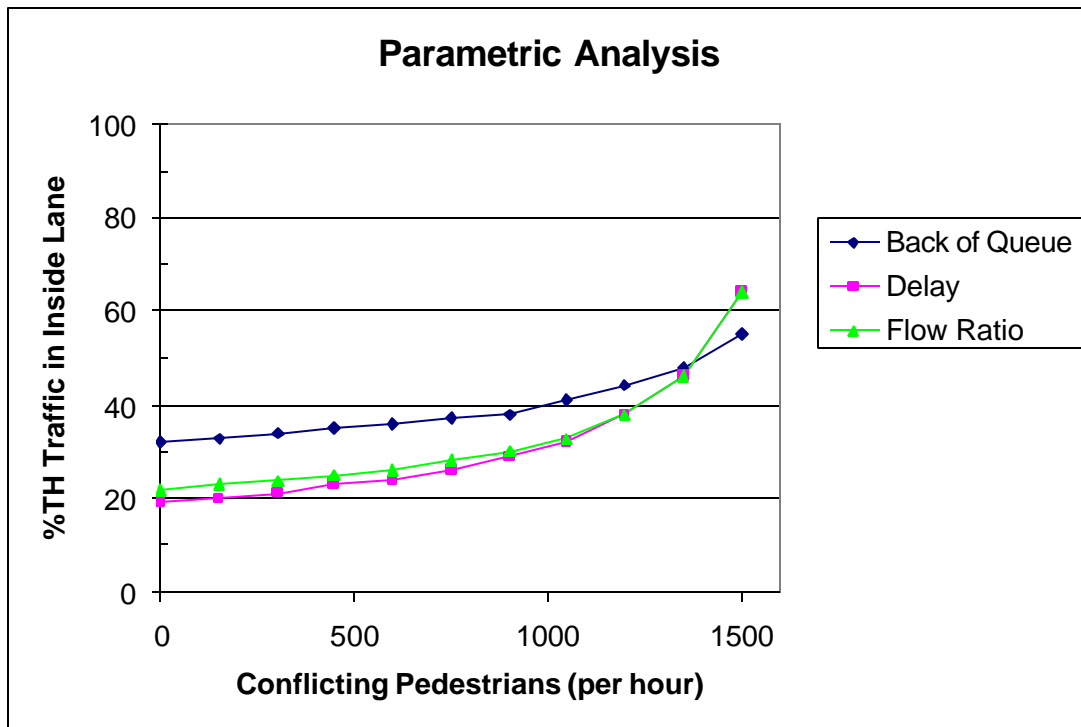


FIGURE 5.10. Effect of Conflicting Pedestrians on Lane Distribution

Figure 5.10 shows that the effect that conflicting pedestrians have on the distribution of through traffic is less sensitive for the back of queue strategy than for the delay and flow ratio strategies. However, when the pedestrian volume is less than 1,400 (which is nearly always the case), the back of queue strategy predicts that more traffic will use the inside lane than do the other two strategies.

The third parametric analysis presented in Figure 5.11 illustrates the effect that bus stops have on lane distribution. As the number of bus stops increase, the saturation flow in the outside lane decreases and the inside lane becomes more attractive. For reference purposes, there are approximately 50 cycles in an hour. Thus, a bus volume of 100 vph represents two bus stops each cycle.

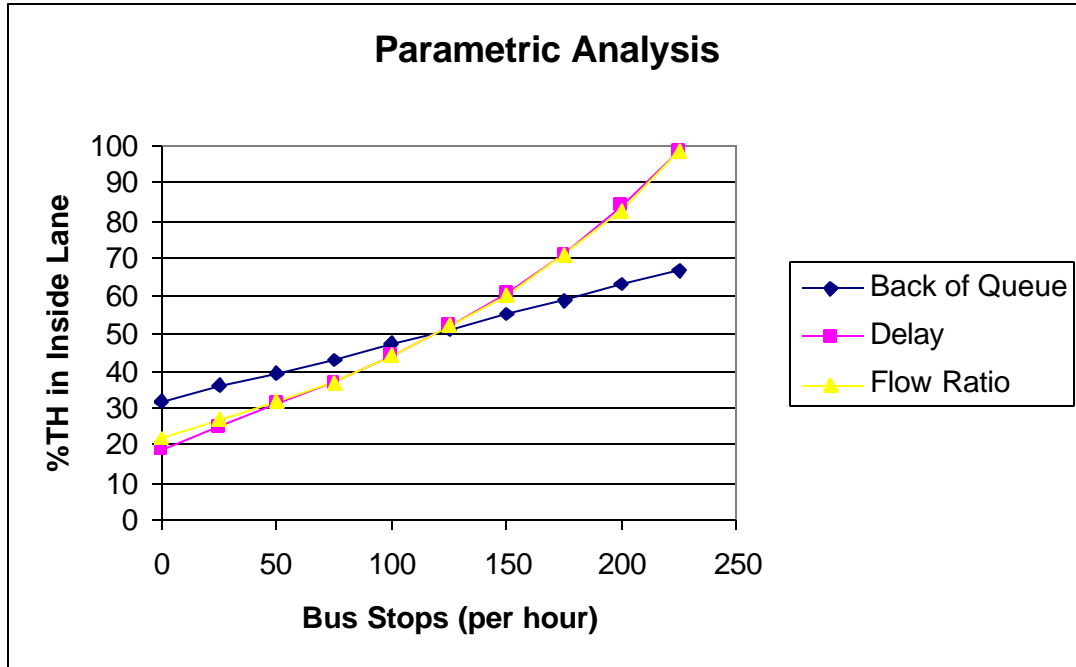


FIGURE 5.11. Effect of Bus Stops on Lane Distribution

Similar to conflicting pedestrians, increasing levels of bus stops have a more profound effect on the distribution of through traffic under the delay and flow ratio strategies as compared to the back of queue strategy. Under low volumes of bus stops, the back of queue strategy predicts more traffic in the inside lane (less on the outside lane). For bus stop volumes greater than 125, the back of queue strategy predicts that less traffic will use the inside lane, thus a higher volume of traffic would be willing to travel in the outside lane even though the frequency of bus stops is high.

The last analysis shows the effect that increasing green time has on the distribution of through traffic. For this analysis, the cycle length is fixed at 75 seconds. Thus, the increase in green time results in a direct increase in the effective green ratio (g/C). Figure 5.12 presents the results of this analysis.

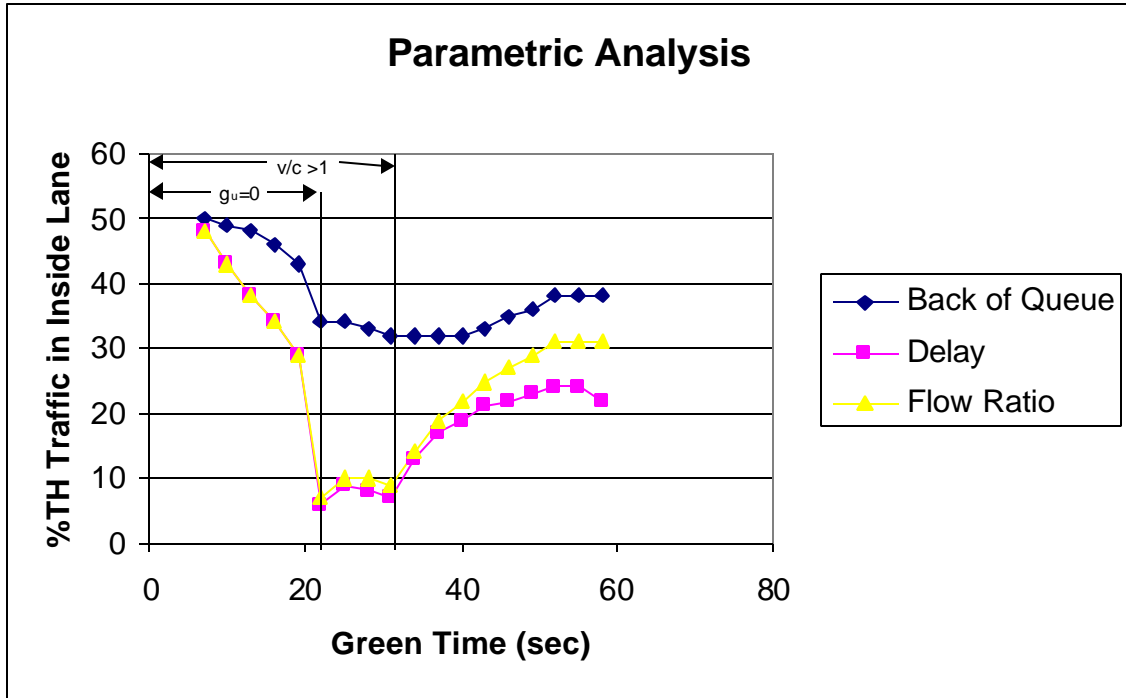


FIGURE 5.12. Effect of Green Time on Lane Distribution

Figure 5.12 shows that there are three distinct intervals over which the distribution of through traffic is affected by the green time. In the first interval, all three strategies experience a steep decline in the percentage of through traffic in the inside lane, with the delay and flow ratio strategies experiencing the most severe drop. A review of the output shows that during this interval the opposing queue does not clear and thus the unopposed green time for the left-turn movement (g_l) is zero. Thus, only sneakers are able to clear the intersection during these cycles, so the added green time in this interval only benefits

the outside lane and thus every increase in green time results in a shift of through traffic to the outside lane.

At the point where the opposing queue begins to clear (green time = 22 seconds), the percentage of through traffic in the inside lane levels out until the volume-to-capacity ratio of the opposing approach drops to 1.0. Theoretically, the volume-to-capacity ratio at this point (22 seconds) should equal 1.0 since an over-capacity condition indicates that the queue for the approach does not clear. As shown in Figure 5.12 however, this is not the case. A review of the HCM shows that a saturation flow of 1800 vph is assumed in the calculation of opposing queue clearance time. In this example, the opposing approach experiences a saturation flow less than 1800 vph, hence the discrepancy between the two values.

From the point that the opposing v/c ratio is less than one, every amount of added green time results in a shift of traffic to the inside lane until the green time is equal to approximately 50-55 seconds. The flow ratio strategy experiences the most dramatic shift during this interval, followed by the delay and back of queue strategies.

In summary, the results of the parametric analysis show that the back of queue strategy is less sensitive to increases in opposing traffic, conflicting pedestrians, bus stops, and green time than the delay and flow ratio strategies. The queue strategy indicates that the shift of through traffic from one lane to another is not directly proportional to the change in the lane saturation flow. The back of queue strategy predicts that although one lane may experience a lower saturation flow rate than another, a percentage of drivers will not change lanes even though it would minimize their travel time and/or delay. This principle is similar to Bonneson's lane change probability theory that drivers, at least under low and high congestion conditions, are less likely to change lanes.

6.0 CONCLUSIONS AND RECOMMENDATIONS

This thesis presents a methodology for analyzing signalized intersections by traffic subgroups. A subgroup is defined as a group of vehicles of unique vehicle type making a single directional movement from one lane. The subgroup method provides the user with greater flexibility than traditional analysis methods such as the HCM. Subgroup results can be aggregated at any level – turning movement, vehicle type, lane, or lane group.

The most critical element of the subgroup model is the estimation of individual lane volumes for cases where a choice lane exists. This thesis provides a summary of lane volume data collected from three intersections. In addition, six potential lane distribution criteria are evaluated against field data.

6.1 Conclusions

The following items summarize the conclusions of this thesis.

- When applied using the same assumptions, the subgroup method produces similar saturation flow rates as the HCM at the lane group level. The similarities give credibility to the subgroup method for estimating performance not only at the lane group level, but at the individual lane level as well.
- Differences between the HCM and subgroup saturation models were found in the right-turn, left-turn, and bus factors. These differences are primarily attributable to two erroneous assumptions made within the HCM: 1) for single lane approaches, the effect of left turn vehicles are assumed to be independent of right turn vehicles, and 2) multilane approaches with bus and parking impedances have equal lane volumes.
- Analyses of the field data show that the distribution of through traffic is most heavily dependent upon the amount of left-turn traffic on the approach and opposing traffic

flow. Defacto left turn lanes did not occur over any of the 73 15-minute periods observed.

- Of the six lane distributions strategies evaluated, the equal average back of queue and cycle-average queue strategies produce results most consistent with the observed field data. The queue strategies outperform the remaining strategies under every level of left-turn, subject, and opposing flow analyzed.
- In general, the back of queue strategy is less sensitive to increases in opposing flow, pedestrian volumes, bus stops, and green time than the flow ratio and delay strategies.
- The equal queue strategies predict that drivers are more likely to choose a lane with lower saturation flow (and thus higher delay and queue clearance time) than the delay and flow ratio strategies. This behavior is reflective in the observed field data.
- The selection of a lane distribution model is most critical under high volume conditions. Under these conditions, the control delay across the models can vary up to 20 seconds/vehicle.

6.2 Recommendations for Future Research

This thesis serves as the first step in the development and evaluation of a subgroup saturation flow model. Further data collection and evaluation is still needed. The items below indicate areas for future research.

Validate the Multiplicative Form of the Saturation Flow Model

The subgroup method provides the opportunity to re-evaluate the multiplicative form of the saturation flow model. The 1997 HCM as well as the Australian, Canadian, and Swedish capacity guides use a multiplicative model to estimate saturation flow. A multiplicative model indicates that a separate adjustment factor is estimated for each non-ideal condition. Then, all the adjustment factors are multiplied together to determine the lane or lane group saturation flow. One alternative is to develop a single unique headway equivalency factor for each subgroup. Using a single headway equivalency

factor for each subgroup would simplify the process of estimating saturation flow by reducing the number of factors in the model. In addition, there is the potential that the effects of various non-ideal conditions are highly correlated. If this is true, the effect of one non-ideal condition (i.e., narrow lanes) could be applied to account for the effect of other non-ideal conditions (i.e., truck movements, right-turn movements, etc.) for all applicable subgroups.

Validate the Headway Adjustment Factors

The subgroup method utilizes the 1997 HCM adjustment factors to estimate the Headway Equivalency Factors (HEF's) for each non-ideal condition. The non-ideal conditions, particularly the bus factor, should be evaluated to determine the impact it has not only on saturation flow but on lane volume distribution. The HEF's could be calibrated by assuming a lane distribution strategy, measuring the lane volumes, and working backwards to determine the lane saturation flow and thus the equivalency factor of bus stops. Anecdotal evidence shows that frequent bus activity on the outside lane tends to force vehicles toward inner travel lanes.

Evaluate Lane Distribution Strategies Under Conditions Not Covered in this Thesis

The analysis presented in this thesis shows that based on the available field data the back of queue and cycle-average queue strategies are the most accurate predictors of lane flow. The data collection and analysis should be expanded to include approaches with three "choice" lanes and minor-street approaches. In addition, data should be collected for approaches that experience high levels of congestion. Evaluation of the lane distribution strategies under these conditions will confirm whether the equal queue strategies remain the best strategies.

Calibrate the Under Utilization Factor

Another element of the lane distribution model that requires field data collection is the under-utilization factor. The under-utilization factor accounts for pre-positioning due to upstream or downstream influences. Examples of such influences are freeway on-

ramps and downstream lane drops. Field data are required to calibrate these factors and estimate the effect they have on lane volume distribution.

7.0 REFERENCES

1. Transportation Research Board. *Highway Capacity Manual*. Special Report Number 209. 1997 Update.
2. Teply, S., D.I. Allingham, D.B. Richardson, B.W. Stephenson. *Canadian Capacity Guide for Signalized Intersections, Second Edition*. Institute of Transportation Engineers; District 7 – Canada. June 1995.
3. Peterson, B.E., A. Hansson, and K.L. Bang. CAPCAL 2 – Model description of Intersection with Signal Control. *Swedish National Road Administration*. 1995
4. Akcelik, R. *Traffic signals: Capacity and Timing Analysis*. Research Report ARR No. 123. ARRB Transport Research Ltd, Vermont South, Australia. 1981.
5. Lieberman, A.B. “Determining the Lateral Deployment of Traffic on an Approach to an Intersection.” *Transportation Research Record 772*, Transportation Research Board, Washington, D.C.
6. Bonneson, J. “Lane Volume and Saturation Flow Rate for Multilane Intersection Approach.” *Journal of Transportation Engineering Volume 124 No. 3*, American Society of Civil Engineers. May/June 1998.
7. Transportation Research Board. *Highway Capacity Manual*. Special Report Number 209. 2000 Update.
8. Akcelik, R. Capacity of a Shared Lane. *Proceeding of the 14th ARRB Conference, Part 2*. Australian Road Research Board. 1988
9. Akcelik, R. *Calibrating SIDRA*. Australian Road Research Ltd. ARR 180. Vermont South, Australia. 1990.
10. Akcelik, R. On the Estimation of Lane Flows for Intersection Analysis. *Australian Road Research*. 1989.
11. Papacostas, C.S., Prevedouros, P. D. *Transportation Engineering and Planning, Third Edition*. Prentice Hall. 2001.
12. Akcelik, R. *SIDRA-2 Does It Lane By Lane*. *Proceedings of 12th ARRB Conference*. 1984.
13. Bonneson, J.A., Messer, C.J. Capacity Analysis of Interchange Ramp Terminals. NCHRP Project 3-47. April 1997.

14. Kaman Sciences Corporation. *TSIS User's Guide*. Federal Highway Administration. January 1996.
15. Federal Highway Administration. *Manual on Uniform Traffic Control Devices*. 1988.

APPENDIX A

SUBGROUP WORKSHEETS FOR HCM EXAMPLES

Intersection: Third/Main
Analysis Year: 1994
Scenario: HCM #1
Time Period: 4-6 p.m.

Project: -
Analyst: BLN
Date: 7/24/00
Sheetname: HCM #1

Avg Int Control Delay = 44.41
 LOS = D

Approach	Geometry	Adj. Vol	Sat Flow	v/s	g/c	Capacity	v/c	Control Delay	LOS	Cycle-Average Queue	Average Back of Queue	95th Percentile Queue
NB	LTR	466	1371	0.34	0.51	705	0.66	17.3	B	2.2	1.4	3.3
EB	TR	620	1550	0.4	0.37	576	1.08	80.2	F	13.8	10.4	17.9
EB	LT	179	494	0.362	0.37	184	0.97	80.1	F	4	3.3	7.1
SB	LTR	667	1475	0.452	0.51	759	0.88	28.8	C	5.3	4.2	8.5
WB	TR	496	1557	0.319	0.37	578	0.86	37.8	D	5.2	3	6.5
WB	LT	337	1119	0.301	0.37	416	0.81	37.7	D	3.5	3.3	7

Subgroup	Lane	Move.	Veh Type	Adj Vol	Vol Frac	LW	HV	Grade	Park (rt)	Park (lt)	Bus	AT	RT	LT	TH	HEF
NBSub1	1	R	car	20	0.043	0.909	1.000	1.000	1.000	1.000	1.000	1.111	1.246	1.000	1.000	1.259
NBSub2	1	R	truck	2	0.004	0.909	2.000	1.000	1.000	1.000	1.000	1.111	1.246	1.000	1.000	2.518
NBSub3	1	T	car	378	0.811	0.909	1.000	1.000	1.000	1.000	1.000	1.111	1.000	1.000	1.000	1.010
NBSub4	1	T	truck	33	0.071	0.909	2.000	1.000	1.000	1.000	1.000	1.111	1.000	1.000	1.000	2.020
NBSub5	1	L	car	30	0.064	0.909	1.000	1.000	1.000	1.000	1.000	1.111	1.000	4.596	1.000	4.642
NBSub6	1	L	truck	3	0.006	0.909	2.000	1.000	1.000	1.000	1.000	1.111	1.000	4.596	1.000	9.285
EBSub1	1	R	car	37	0.060	1.034	1.000	1.000	1.000	1.000	1.000	1.111	1.246	1.000	1.000	1.433
EBSub2	1	R	truck	2	0.003	1.034	2.000	1.000	1.000	1.000	1.000	1.111	1.246	1.000	1.000	2.865
EBSub3	1	T	car	552	0.890	1.034	1.000	1.000	1.000	1.000	1.000	1.111	1.000	1.000	1.000	1.149
EBSub4	1	T	truck	29	0.047	1.034	2.000	1.000	1.000	1.000	1.000	1.111	1.000	1.000	1.000	2.299
EBSub5	2	T	car	102	0.570	1.034	1.000	1.000	1.000	1.000	1.000	1.111	1.000	1.000	1.358	1.561
EBSub6	2	T	truck	5	0.028	1.034	2.000	1.000	1.000	1.000	1.000	1.111	1.000	1.000	1.358	3.122
EBSub7	2	L	car	68	0.380	1.034	1.000	1.000	1.000	1.000	1.000	1.111	1.000	5.873	1.000	6.750
EBSub8	2	L	truck	4	0.022	1.034	2.000	1.000	1.000	1.000	1.000	1.111	1.000	5.873	1.000	13.501
SBSub1	1	R	car	52	0.078	0.909	1.000	1.000	1.000	1.000	1.000	1.111	1.246	1.000	1.000	1.259
SBSub2	1	R	truck	4	0.006	0.909	2.000	1.000	1.000	1.000	1.000	1.111	1.246	1.000	1.000	2.518
SBSub3	1	T	car	522	0.783	0.909	1.000	1.000	1.000	1.000	1.000	1.111	1.000	1.000	1.000	1.010
SBSub4	1	T	truck	45	0.067	0.909	2.000	1.000	1.000	1.000	1.000	1.111	1.000	1.000	1.000	2.020
SBSub5	1	L	car	40	0.060	0.909	1.000	1.000	1.000	1.000	1.000	1.111	1.000	3.410	1.000	3.445
SBSub6	1	L	truck	4	0.006	0.909	2.000	1.000	1.000	1.000	1.000	1.111	1.000	3.410	1.000	6.889
WBSub1	1	R	car	21	0.042	1.034	1.000	1.000	1.000	1.000	1.000	1.111	1.246	1.000	1.000	1.433
WBSub2	1	R	truck	1	0.002	1.034	2.000	1.000	1.000	1.000	1.000	1.111	1.246	1.000	1.000	2.865
WBSub3	1	T	car	450	0.907	1.034	1.000	1.000	1.000	1.000	1.000	1.111	1.000	1.000	1.000	1.149
WBSub4	1	T	truck	24	0.048	1.034	2.000	1.000	1.000	1.000	1.000	1.111	1.000	1.000	1.000	2.299
WBSub5	2	T	car	289	0.858	1.034	1.000	1.000	1.000	1.000	1.000	1.111	1.000	1.000	1.000	1.149
WBSub6	2	T	truck	15	0.045	1.034	2.000	1.000	1.000	1.000	1.000	1.111	1.000	1.000	1.000	2.299
WBSub7	2	L	car	31	0.092	1.034	1.000	1.000	1.000	1.000	1.000	1.111	1.000	5.113	1.000	5.877
WBSub8	2	L	truck	2	0.006	1.034	2.000	1.000	1.000	1.000	1.000	1.111	1.000	5.113	1.000	11.755

Intersection: Sixth St/Western Blvd
Analysis Year: 1993
Scenario: HCM #2
Time Period: AM

Project: -
Analyst: BLN
Date: 7/24/00
Sheetname: HCM #2

Avg Int Control Delay = 23.93
 LOS = C

Approach	Geometry	Adj. Vol	Sat Flow	v/s	g/c	Capacity	v/c	Control Delay	LOS	Cycle-Average Queue	Average Back of Queue	95th Percentile Queue
NB	TR	449	1536	0.292	0.39	599	0.75	26.8	C	3.3	1.8	4.2
NB	LT	445	1524	0.292	0.39	594	0.75	26.8	C	3.3	3.4	7.1
EB	T	490	1589	0.308	0.5	788	0.62	16.5	B	2.3	1.3	3.1
EB	T	542	1728	0.314	0.5	857	0.63	16.5	B	2.5	2.8	6
EB	L	126	544	0.231	0.5	270	0.47	17.3	B	0.6	1	2.3
WB	TR	387	1515	0.255	0.34	509	0.76	31	C	3.3	1.7	3.9
WB	T	454	1729	0.263	0.34	580	0.78	31	C	3.9	3.8	7.8

Subgroup	Lane	Move.	Veh Type	Adj Vol	Vol Frac	LW	HV	Grade	Park (rt)	Park (lt)	Bus	AT	RT	LT	TH	HEF
NBSub1	1	R	car	25	0.056	1.000	1.000	0.990	1.176	1.000	1.000	1.000	1.210	1.000	1.000	1.410
NBSub2	1	R	truck	1	0.002	1.000	2.000	0.990	1.176	1.000	1.000	1.000	1.210	1.000	1.000	2.820
NBSub3	1	T	car	402	0.895	1.000	1.000	0.990	1.176	1.000	1.000	1.000	1.000	1.000	1.000	1.165
NBSub4	1	T	truck	21	0.047	1.000	2.000	0.990	1.176	1.000	1.000	1.000	1.000	1.000	1.000	2.330
NBSub5	2	T	car	383	0.861	1.000	1.000	0.990	1.000	1.176	1.000	1.000	1.000	1.000	1.000	1.165
NBSub6	2	T	truck	20	0.045	1.000	2.000	0.990	1.000	1.176	1.000	1.000	1.000	1.000	1.000	2.330
NBSub7	2	L	car	40	0.090	1.000	1.000	0.990	1.000	1.176	1.000	1.000	1.000	1.210	1.000	1.410
NBSub8	2	L	truck	2	0.004	1.000	2.000	0.990	1.000	1.176	1.000	1.000	1.000	1.210	1.000	2.820
EBSub1	1	T	car	441	0.900	1.000	1.000	1.000	1.000	1.000	1.087	1.000	1.000	1.000	1.000	1.087
EBSub2	1	T	truck	49	0.100	1.000	2.000	1.000	1.000	1.000	1.087	1.000	1.000	1.000	1.000	2.174
EBSub3	2	T	car	488	0.900	1.000	1.000	1.000	1.000	1.000	1.000	1.000	1.000	1.000	1.000	1.000
EBSub4	2	T	truck	54	0.100	1.000	2.000	1.000	1.000	1.000	1.000	1.000	1.000	1.000	1.000	2.000
EBSub5	3	L	car	113	0.897	1.000	1.000	1.000	1.000	1.000	1.000	1.000	1.000	3.164	1.000	3.164
EBSub6	3	L	truck	13	0.103	1.000	2.000	1.000	1.000	1.000	1.000	1.000	1.000	3.164	1.000	6.328
WBSub1	1	R	car	94	0.243	1.000	1.000	1.000	1.000	1.000	1.087	1.000	1.176	1.000	1.000	1.279
WBSub2	1	R	truck	11	0.028	1.000	2.000	1.000	1.000	1.000	1.087	1.000	1.176	1.000	1.000	2.558
WBSub3	1	T	car	254	0.656	1.000	1.000	1.000	1.000	1.000	1.087	1.000	1.000	1.000	1.000	1.087
WBSub4	1	T	truck	28	0.072	1.000	2.000	1.000	1.000	1.000	1.087	1.000	1.000	1.000	1.000	2.174
WBSub5	2	T	car	409	0.901	1.000	1.000	1.000	1.000	1.000	1.000	1.000	1.000	1.000	1.000	1.000
WBSub6	2	T	truck	45	0.099	1.000	2.000	1.000	1.000	1.000	1.000	1.000	1.000	1.000	1.000	2.000

Intersection: 5th Avenue/12th Street
Analysis Year: 1999
Scenario:
Time Period: 5-6 p.m.

Project:
Analyst: BLN
Date: 8/27/00
Sheetname: HCM #3

Avg Int Control Delay = 45.99
LOS = D

Approach	Geometry	Adj. Vol	Sat Flow	v/s	g/c	Capacity	v/c	Control Delay	LOS	Cycle-Average Queue	Average Back of Queue	95th Percentile Queue
NB	TR	856	1641	0.522	0.56	924	0.93	34.3	C	8.2	7.3	13.4
NB	T	877	1676	0.523	0.56	944	0.93	34.5	C	8.4	11.9	20.1
NB	L	133	517	0.257	0.7	361	0.37	8.4	A	0.3	0.9	2.3
EB	TR	171	1110	0.154	0.21	237	0.72	50.2	D	2.4	1	2.3
EB	T	253	1518	0.167	0.21	324	0.78	50.4	D	3.5	2.8	6.1
EB	L	71	315	0.226	0.21	67	1.06	162	F	3.2	2.4	5.3
SB	TR	494	1622	0.305	0.56	914	0.54	14.6	B	2	1.2	2.9
SB	T	516	1677	0.308	0.56	945	0.55	14.7	B	2.1	2.5	5.6
SB	L	194	278	0.698	0.7	194	1	78.3	E	4.2	5.1	10.1
WB	TR	285	1296	0.22	0.21	276	1.03	97.7	F	7.7	4.6	9.3
WB	T	339	1520	0.223	0.21	324	1.05	97.8	F	9.2	7.6	13.9
WB	L	118	560	0.211	0.21	119	0.99	114.4	F	3.7	3.3	7

Subgroup Summary (HCM #3 Cont)

Subgroup	Lane	Move.	Veh Type	Adj Vol	Vol Frac	LW	HV	Grade	Park (rt)	Park (lt)	Bus	AT	RT	LT	TH	HEF
NBSub1	1	R	car	87	0.102	1.000	1.000	1.000	1.000	1.000	1.000	1.111	1.210	1.000	1.000	1.345
NBSub2	1	R	truck	2	0.002	1.000	2.000	1.000	1.000	1.000	1.000	1.111	1.210	1.000	1.000	2.690
NBSub3	1	T	car	752	0.879	1.000	1.000	1.000	1.000	1.000	1.000	1.111	1.000	1.000	1.000	1.111
NBSub4	1	T	truck	15	0.018	1.000	2.000	1.000	1.000	1.000	1.000	1.111	1.000	1.000	1.000	2.222
NBSub5	2	T	car	859	0.979	1.000	1.000	1.000	1.000	1.000	1.000	1.111	1.000	1.000	1.000	1.111
NBSub6	2	T	truck	18	0.021	1.000	2.000	1.000	1.000	1.000	1.000	1.111	1.000	1.000	1.000	2.222
NBSub7	3	L	car	130	0.977	1.000	1.000	1.000	1.000	1.000	1.000	1.111	1.000	3.233	1.000	3.592
NBSub8	3	L	truck	3	0.023	1.000	2.000	1.000	1.000	1.000	1.000	1.111	1.000	3.233	1.000	7.184
EBSub1	1	R	car	101	0.591	1.071	1.000	1.000	1.143	1.000	1.000	1.111	1.325	1.000	1.000	1.803
EBSub2	1	R	truck	5	0.029	1.071	2.000	1.000	1.143	1.000	1.000	1.111	1.325	1.000	1.000	3.605
EBSub3	1	T	car	62	0.363	1.071	1.000	1.000	1.143	1.000	1.000	1.111	1.000	1.000	1.000	1.361
EBSub4	1	T	truck	3	0.018	1.071	2.000	1.000	1.143	1.000	1.000	1.111	1.000	1.000	1.000	2.721
EBSub5	2	T	car	240	0.949	1.071	1.000	1.000	1.000	1.000	1.000	1.111	1.000	1.000	1.000	1.190
EBSub6	2	T	truck	13	0.051	1.071	2.000	1.000	1.000	1.000	1.000	1.111	1.000	1.000	1.000	2.381
EBSub7	3	L	car	67	0.944	1.071	1.000	1.000	1.000	1.000	1.000	1.111	1.000	4.800	1.000	5.714
EBSub8	3	L	truck	4	0.056	1.071	2.000	1.000	1.000	1.000	1.000	1.111	1.000	4.800	1.000	11.429
SBSub1	1	R	car	76	0.154	1.000	1.000	1.000	1.000	1.000	1.000	1.111	1.210	1.000	1.000	1.345
SBSub2	1	R	truck	2	0.004	1.000	2.000	1.000	1.000	1.000	1.000	1.111	1.210	1.000	1.000	2.690
SBSub3	1	T	car	408	0.826	1.000	1.000	1.000	1.000	1.000	1.000	1.111	1.000	1.000	1.000	1.111
SBSub4	1	T	truck	8	0.016	1.000	2.000	1.000	1.000	1.000	1.000	1.111	1.000	1.000	1.000	2.222
SBSub5	2	T	car	506	0.981	1.000	1.000	1.000	1.000	1.000	1.000	1.111	1.000	1.000	1.000	1.111
SBSub6	2	T	truck	10	0.019	1.000	2.000	1.000	1.000	1.000	1.000	1.111	1.000	1.000	1.000	2.222
SBSub7	3	L	car	190	0.979	1.000	1.000	1.000	1.000	1.000	1.000	1.111	1.000	6.029	1.000	6.699
SBSub8	3	L	truck	4	0.021	1.000	2.000	1.000	1.000	1.000	1.000	1.111	1.000	6.029	1.000	13.398
WBSub1	1	R	car	23	0.081	1.071	1.000	1.000	1.143	1.000	1.000	1.111	1.325	1.000	1.000	1.803
WBSub2	1	R	truck	1	0.004	1.071	2.000	1.000	1.143	1.000	1.000	1.111	1.325	1.000	1.000	3.605
WBSub3	1	T	car	248	0.870	1.071	1.000	1.000	1.143	1.000	1.000	1.111	1.000	1.000	1.000	1.361
WBSub4	1	T	truck	13	0.046	1.071	2.000	1.000	1.143	1.000	1.000	1.111	1.000	1.000	1.000	2.721
WBSub5	2	T	car	322	0.950	1.071	1.000	1.000	1.000	1.000	1.000	1.111	1.000	1.000	1.000	1.190
WBSub6	2	T	truck	17	0.050	1.071	2.000	1.000	1.000	1.000	1.000	1.111	1.000	1.000	1.000	2.381
WBSub7	3	L	car	112	0.949	1.071	1.000	1.000	1.000	1.000	1.000	1.111	1.000	2.712	1.000	3.228
WBSub8	3	L	truck	6	0.051	1.071	2.000	1.000	1.000	1.000	1.000	1.111	1.000	2.712	1.000	6.457

APPENDIX B

LANE VOLUME FIELD DATA PER CYCLE

Intersection: Grand/Franklin
 Date: 5/25/00

Time Beg.	Cycle	WB RT	WB TH (rt lane)	WB TH (lt lane)	WB LT	EB RT	EB TH (rt lane)	EB TH (lt lane)	EB LT
6:59:40 AM	1	0	2	10	0	1	0	4	0
7:00:55 AM	2	1	5	5	1	0	2	1	2
7:02:10 AM	3	2	1	4	0	0	3	2	1
7:03:25 AM	4	0	4	6	0	0	3	2	1
7:04:40 AM	5	0	4	6	0	0	2	1	2
7:05:55 AM	6	1	4	12	0	0	3	2	0
7:07:10 AM	7	2	1	4	0	1	2	2	1
7:08:25 AM	8	0	5	6	0	0	2	2	0
7:09:40 AM	9	1	0	3	0	0	3	6	0
7:10:55 AM	10	0	2	2	0	1	3	1	2
7:12:10 AM	11	1	2	3	0	0	2	3	4
7:13:25 AM	12	1	4	0	0	0	2	1	0
7:14:40 AM	13	1	3	6	0	0	7	4	0
7:15:55 AM	14	0	4	3	0	0	5	5	1
7:17:10 AM	15	2	1	5	0	0	5	3	2
7:18:25 AM	16	0	3	7	0	0	4	3	1
7:19:40 AM	17	0	4	9	0	0	5	3	2
7:20:55 AM	18	0	3	8	0	0	1	1	2
7:22:10 AM	19	3	2	8	0	0	6	4	1
7:23:25 AM	20	1	5	9	0	0	0	1	0
7:24:40 AM	21	1	2	5	0	0	3	2	1
7:25:55 AM	22	2	4	5	0	0	7	5	2
7:27:10 AM	23	0	4	5	0	0	2	4	1
7:28:25 AM	24	1	2	6	0	0	3	5	0
7:29:40 AM	25	0	6	9	1	0	2	3	2
7:30:55 AM	26	0	5	9	0	0	5	2	2
7:32:10 AM	27	0	5	8	0	1	2	4	0
7:33:25 AM	28	2	5	8	0	1	2	1	1
7:34:40 AM	29	0	4	7	0	0	4	5	1
7:35:55 AM	30	1	4	6	0	0	4	3	1
7:37:10 AM	31	1	7	11	0	0	2	5	0
7:38:25 AM	32	1	12	11	0	0	7	1	2
7:39:40 AM	33	1	4	10	1	1	7	3	3
7:40:55 AM	34	2	3	8	0	0	9	4	2
7:42:10 AM	35	1	4	8	0	1	2	0	2
7:43:25 AM	36	0	3	5	1	0	2	5	0
7:44:40 AM	37	0	3	5	1	0	5	1	1
7:45:55 AM	38	1	4	11	0	1	7	3	2
7:47:10 AM	39	0	4	6	0	0	3	4	0
7:48:25 AM	40	2	4	7	1	1	1	4	1
7:49:40 AM	41	0	4	6	0	0	4	8	0
7:50:55 AM	42	0	3	8	0	0	9	6	1
7:52:10 AM	43	1	5	5	0	0	5	5	2
7:53:25 AM	44	0	8	4	1	0	9	5	1
7:54:40 AM	45	1	3	6	0	0	8	5	1
7:55:55 AM	46	1	7	7	0	2	7	10	0
7:57:10 AM	47	2	4	7	0	1	5	4	1
7:58:25 AM	48	1	4	6	0	0	6	2	2
7:59:40 AM	49	2	4	9	0	0	9	2	3
8:00:55 AM	50	2	8	4	1	0	8	3	1
8:02:10 AM	51	2	5	7	0	1	3	1	2
8:03:25 AM	52	0	14	1	1	1	8	3	2
8:04:40 AM	53	3	5	9	0	0	7	1	2
8:05:55 AM	54	2	10	7	1	0	8	8	1
8:07:10 AM	55	0	4	8	0	0	3	2	0
8:08:25 AM	56	0	8	5	2	2	3	7	0
8:09:40 AM	57	1	6	4	0	0	5	6	0
8:10:55 AM	58	2	9	5	1	0	11	6	2
8:12:10 AM	59	0	4	5	3	0	2	2	1
8:13:25 AM	60	3	5	5	0	2	1	8	0
8:14:40 AM	61	2	7	5	0	0	14	2	2
8:15:55 AM	62	0	6	7	0	1	13	4	4
8:17:10 AM	63	1	5	8	1	1	8	1	1

Intersection: Grand/Franklin
 Date: 5/25/00

Time Beg.	Cycle	WB RT	WB TH (rt lane)	WB TH (lt lane)	WB LT	EB RT	EB TH (rt lane)	EB TH (lt lane)	EB LT
8:18:25 AM	64	0	6	8	0	0	5	7	0
8:19:40 AM	65	2	10	4	1	1	8	4	2
8:20:55 AM	66	1	3	12	0	1	5	4	3
8:22:10 AM	67	3	7	9	0	0	14	0	2
8:23:25 AM	68	0	5	0	1	0	2	8	0
8:24:40 AM	69	2	7	13	0	0	7	6	0
8:25:55 AM	70	2	4	9	0	1	7	3	3
8:27:10 AM	71	3	3	6	0	2	11	4	1
8:28:25 AM	72	0	2	6	0	1	3	8	0
8:33:25 AM	73	1	3	11	0	0	12	2	2
8:34:40 AM	74	4	3	12	0	0	12	0	1
8:35:55 AM	75	0	3	4	0	0	13	1	4
8:37:10 AM	76	1	7	3	2	1	7	2	2
8:38:25 AM	77	1	8	7	2	0	5	7	1
8:39:40 AM	78	2	6	14	0	1	15	2	3
8:40:55 AM	79	1	4	3	1	1	6	7	3
8:42:10 AM	80	2	4	12	1	0	0	7	1
8:43:25 AM	81	0	2	3	0	0	8	5	3
8:44:40 AM	82	1	3	10	0	2	9	5	1
8:45:55 AM	83	4	5	9	0	0	8	1	3
8:47:10 AM	84	3	4	6	0	0	3	3	1
8:48:25 AM	85	1	8	9	1	0	9	0	2
8:49:40 AM	86	2	4	9	0	0	9	4	2
8:50:55 AM	87	1	6	11	0	0	6	8	0
8:52:10 AM	88	2	3	4	1	1	9	2	2
8:53:25 AM	89	1	6	7	0	0	7	0	3
8:54:40 AM	90	1	6	10	0	0	12	1	3
8:55:55 AM	91	1	3	7	1	0	5	2	3
8:57:10 AM	92	0	7	11	0	1	4	3	2
8:58:25 AM	93	1	6	6	0	0	11	1	3
8:59:40 AM	94	2	3	14	0	0	13	0	2
9:00:55 AM	95	0	9	6	0	0	9	1	1
9:02:10 AM	96	2	3	8	1	0	8	1	2
9:03:25 AM	97	2	4	8	0	0	8	1	2
9:04:40 AM	98	2	5	4	0	1	3	3	2
9:05:55 AM	99	3	5	7	0	0	9	0	3
9:07:10 AM	100	0	1	6	0	1	10	1	3
9:08:25 AM	101	2	4	11	1	1	6	6	1
9:09:40 AM	102	1	5	11	0	1	2	11	0
9:10:55 AM	103	4	11	12	0	1	9	5	1
9:12:10 AM	104	0	7	8	0	0	5	1	3
9:13:25 AM	105	5	5	7	1	0	6	2	3
9:14:40 AM	106	2	7	6	2	0	8	5	2
9:15:55 AM	107	2	2	4	1	1	4	2	3
9:17:10 AM	108	1	4	6	0	0	7	0	2
9:18:25 AM	109	0	9	9	0	0	4	5	0
9:19:40 AM	110	3	3	7	0	1	4	3	4
9:20:55 AM	111	4	3	12	0	1	12	8	1
9:22:10 AM	112	1	4	15	1	1	5	1	0
9:23:25 AM	113	1	4	8	0	0	5	3	2
9:24:40 AM	114	2	4	6	0	0	10	6	1
9:25:55 AM	115	4	1	6	0	0	11	2	2
9:27:10 AM	116	0	8	6	0	2	0	1	2
9:28:25 AM	117	3	2	8	0	0	6	6	0
9:29:40 AM	118	2	4	8	1	2	4	3	1
9:30:55 AM	119	0	7	5	1	0	3	4	1
9:32:10 AM	120	0	1	7	0	0	3	6	1
9:33:25 AM	121	2	1	5	0	1	5	4	2
9:34:40 AM	122	1	4	4	0	0	4	3	1
9:35:55 AM	123	0	6	5	0	1	1	0	1
9:37:10 AM	124	1	5	9	1	0	2	1	0
9:38:25 AM	125	0	5	8	0	0	6	3	2

Intersection: Grand/Franklin
 Date: 5/25/00

Time Beg.	Cycle	WB RT	WB TH (rt lane)	WB TH (lt lane)	WB LT	EB RT	EB TH (rt lane)	EB TH (lt lane)	EB LT
9:39:40 AM	126	1	4	5	0	1	3	5	0
9:40:55 AM	127	1	3	4	0	0	5	5	3
9:42:10 AM	128	2	4	4	0	1	1	8	0
9:43:25 AM	129	2	1	9	0	1	3	7	0
9:44:40 AM	130	2	1	6	1	2	5	5	2
9:45:55 AM	131	2	0	15	0	2	2	3	0
9:47:10 AM	132	1	4	8	0	0	10	1	1
9:48:25 AM	133	3	1	9	0	2	7	2	1
9:49:40 AM	134	1	2	2	0	1	4	5	1
9:50:55 AM	135	0	7	10	0	0	4	5	1
9:52:10 AM	136	2	10	8	1	0	7	0	1
9:53:25 AM	137	0	5	10	1	0	7	0	2
9:54:40 AM	138	1	5	17	0	1	9	3	1
9:55:55 AM	139	2	3	7	0	0	6	3	3
9:57:10 AM	140	3	7	2	1	2	3	6	0
9:58:25 AM	141	1	2	11	1	0	4	2	1
3:30:40 PM	142	0	7	12	1	2	11	1	2
3:31:55 PM	143	2	8	11	1	0	4	5	0
3:33:10 PM	144	2	3	13	0	0	4	2	0
3:34:25 PM	145	5	7	12	0	0	2	4	0
3:35:40 PM	146	4	9	13	0	0	6	0	1
3:36:55 PM	147	5	9	10	1	0	6	0	3
3:38:10 PM	148	1	8	12	0	0	4	2	0
3:39:25 PM	149	1	11	11	1	0	1	7	0
3:40:40 PM	150	1	8	12	0	1	8	1	2
3:41:55 PM	151	1	12	14	0	0	3	7	0
3:43:10 PM	152	4	11	4	3	2	2	5	0
3:44:25 PM	153	0	9	2	2	0	7	1	3
3:45:40 PM	154	1	10	2	1	1	8	1	3
3:46:55 PM	155	2	9	9	0	3	5	1	1
3:48:10 PM	156	2	10	8	1	2	4	4	0
3:49:25 PM	157	5	10	11	1	0	4	2	2
3:50:40 PM	158	2	5	11	0	1	5	5	2
3:51:55 PM	159	2	9	12	0	0	4	4	0
3:53:10 PM	160	1	10	10	0	0	8	0	3
3:54:25 PM	161	1	7	13	0	1	8	4	1
3:55:40 PM	162	5	4	11	0	0	5	0	2
3:56:55 PM	163	1	11	12	1	0	7	1	3
3:58:10 PM	164	3	5	12	0	1	6	4	1
3:59:25 PM	165	1	6	10	0	0	9	1	2
4:00:40 PM	166	1	13	6	1	1	8	4	2
4:01:55 PM	167	0	8	9	0	1	2	3	0
4:03:10 PM	168	2	11	13	0	0	8	1	3
4:04:25 PM	169	2	7	11	0	0	4	5	0
4:05:40 PM	170	0	12	8	0	0	3	1	4
4:06:55 PM	171	2	10	11	0	0	2	2	0
4:08:10 PM	172	4	9	12	2	0	0	4	0
4:09:25 PM	173	1	12	10	0	1	5	2	1
4:10:40 PM	174	3	6	11	0	1	1	8	0
4:11:55 PM	175	6	6	14	1	0	2	3	0
4:13:10 PM	176	4	11	6	1	3	8	6	1
4:14:25 PM	177	4	10	9	1	0	4	4	1
4:15:40 PM	178	1	10	9	0	1	3	0	1
4:16:55 PM	179	1	15	12	1	0	4	2	1
4:18:10 PM	180	1	12	12	0	0	0	5	0
4:19:25 PM	181	2	7	1	1	0	4	6	0
4:20:40 PM	182	2	8	11	0	1	8	0	2
4:21:55 PM	183	3	7	14	0	0	4	4	0
4:23:10 PM	184	3	7	8	0	0	9	2	1
4:24:25 PM	185	2	9	7	1	1	4	5	1
4:25:40 PM	186	1	8	8	0	0	3	8	0
4:26:55 PM	187	3	7	8	0	0	6	1	2

Intersection: Grand/Franklin
 Date: 5/25/00

Time Beg.	Cycle	WB RT	WB TH (rt lane)	WB TH (lt lane)	WB LT	EB RT	EB TH (rt lane)	EB TH (lt lane)	EB LT
4:28:10 PM	188	1	12	8	1	1	3	1	2
4:29:25 PM	189	5	9	12	0	0	5	2	0
4:30:40 PM	190	0	12	10	1	0	8	2	2
4:31:55 PM	191	2	11	10	0	1	7	0	1
4:33:10 PM	192	1	5	14	0	1	3	0	7
4:34:25 PM	193	1	11	13	0	0	13	0	2
4:35:40 PM	194	5	6	12	0	0	11	1	2
4:36:55 PM	195	1	11	11	0	0	5	0	2
4:38:10 PM	196	3	8	12	0	0	0	6	0
4:39:25 PM	197	1	7	12	0	1	4	8	0
4:40:40 PM	198	0	15	14	1	0	10	0	2
4:41:55 PM	199	1	10	6	0	1	10	0	1
4:43:10 PM	200	5	5	7	2	1	7	4	1
4:44:25 PM	201	1	12	11	0	0	13	0	2
4:45:40 PM	202	3	10	14	1	2	6	4	2
4:46:55 PM	203	3	14	14	1	0	4	0	2
4:48:10 PM	204	3	11	13	1	0	4	0	2
4:49:25 PM	205	3	10	4	1	0	5	5	1
4:50:40 PM	206	7	6	13	0	2	11	0	2
4:51:55 PM	207	3	15	15	0	0	8	5	2
4:53:10 PM	208	6	11	13	1	1	3	5	1
4:54:25 PM	209	2	9	10	0	0	4	6	1
4:55:40 PM	210	2	9	7	1	0	6	0	2
4:56:55 PM	211	2	10	13	2	0	3	0	1
4:58:10 PM	212	4	9	13	1	0	3	2	1
4:59:25 PM	213	1	9	6	2	0	0	0	0
5:00:40 PM	214	1	9	9	0	0	0	0	0
5:01:53 PM	215	4	13	14	0	0	2	0	4
5:03:08 PM	216	5	10	12	0	1	7	2	1
5:04:23 PM	217	2	8	14	0	0	7	7	1
5:05:38 PM	218	1	7	12	0	0	2	0	3
5:06:53 PM	219	5	4	14	0	0	2	4	0
5:08:08 PM	220	3	9	12	0	2	7	1	2
5:09:23 PM	221	2	8	7	1	0	7	8	1
5:10:38 PM	222	4	9	20	0	1	4	7	1
5:11:53 PM	223	4	13	11	0	1	4	3	1
5:13:08 PM	224	4	10	9	0	1	10	0	2
5:14:23 PM	225	3	13	15	0	1	7	0	2
5:15:38 PM	226	7	11	11	1	0	5	3	0
5:16:53 PM	227	5	10	12	0	0	1	10	0
5:18:08 PM	228	4	9	14	0	1	3	7	0
5:19:23 PM	229	5	7	11	0	1	11	0	2
5:20:38 PM	230	1	12	12	0	0	9	0	2
5:21:53 PM	231	1	8	11	0	0	7	0	1
5:23:08 PM	232	3	8	13	1	0	4	6	0
5:24:23 PM	233	3	11	13	1	0	1	5	0
5:25:38 PM	234	3	13	14	0	0	6	2	1
5:26:53 PM	235	5	8	15	0	0	2	1	1
5:28:08 PM	236	3	6	10	0	2	5	3	1
5:29:23 PM	237	2	8	10	0	1	8	0	2
5:30:38 PM	238	3	9	14	0	0	3	10	0
5:31:53 PM	239	2	9	11	1	0	9	0	1
5:33:08 PM	240	3	5	9	0	1	3	7	0
5:34:23 PM	241	5	11	12	1	1	7	1	1
5:35:38 PM	242	1	7	11	0	1	6	2	2
5:36:53 PM	243	2	8	13	0	1	3	1	3
5:38:08 PM	244	4	3	17	0	1	3	5	1
5:39:23 PM	245	4	8	14	1	0	6	2	0
5:40:38 PM	246	5	5	10	0	0	10	0	1
5:41:53 PM	247	6	6	13	0	0	5	0	1
5:43:08 PM	248	6	11	14	0	0	3	5	0
5:44:23 PM	249	3	4	8	1	1	8	2	2
5:45:38 PM	250	4	12	12	0	0	6	0	2

Intersection: Grand/Franklin
 Date: 5/25/00

Time Beg.	Cycle	WB RT	WB TH (rt lane)	WB TH (lt lane)	WB LT	EB RT	EB TH (rt lane)	EB TH (lt lane)	EB LT
5:46:53 PM	251	5	10	10	0	0	5	0	2
5:48:08 PM	252	2	11	13	0	0	3	4	1
5:49:23 PM	253	5	14	8	1	4	14	0	1
5:50:38 PM	254	4	11	13	1	0	10	0	2
5:51:53 PM	255	6	7	17	0	0	6	3	0
5:53:08 PM	256	5	10	8	0	1	3	3	0
5:54:23 PM	257	5	6	10	0	3	6	1	3
5:55:38 PM	258	5	10	16	0	1	12	1	2
5:56:53 PM	259	5	6	13	0	0	7	0	2
5:58:08 PM	260	1	13	10	0	0	4	3	1
5:59:23 PM	261	3	3	7	0	1	6	6	0
6:00:38 PM	262	0	7	11	0	0	7	1	0
6:01:53 PM	263	0	11	12	0	0	3	2	0
6:03:08 PM	264	0	11	12	0	0	8	0	0
6:04:24 PM	265	3	6	7	0	1	4	2	1
6:05:39 PM	266	1	8	3	1	1	9	1	5
6:06:54 PM	267	3	12	13	0	0	2	2	1
6:08:09 PM	268	5	6	8	0	1	3	3	0
6:09:24 PM	269	2	6	9	1	0	0	5	0
6:10:39 PM	270	7	8	14	0	2	7	0	2
6:11:54 PM	271	4	11	12	1	0	3	0	2
6:13:09 PM	272	3	9	15	0	0	4	0	2
6:14:24 PM	273	2	10	13	0	0	4	3	0
6:15:39 PM	274	1	10	10	0	0	6	1	3
6:16:54 PM	275	2	9	8	0	1	6	0	3
6:18:09 PM	276	6	9	4	3	0	6	1	1
6:19:24 PM	277	0	12	9	2	0	2	5	0
6:20:39 PM	278	2	10	10	0	3	6	3	6
6:21:54 PM	279	3	7	9	0	1	1	1	2
6:23:09 PM	280	2	6	12	0	0	3	2	1
6:24:24 PM	281	0	13	13	0	1	2	2	1
6:25:39 PM	282	3	3	9	1	2	1	1	2
6:26:54 PM	283	1	2	11	0	1	6	1	1
6:28:09 PM	284	2	8	12	1	2	0	0	0
6:29:24 PM	285	2	7	11	0	1	1	0	1

Intersection: Poole/Beverly
 Date: 9/18/00

Time	Cycle	WB TH (rt lane)	WB TH (lt lane)	WB LT (lt lane)	EB RT	EB TH (rt lane)	EB TH (lt lane)
3:57:24 PM	1	5	6	2	1	7	11
3:59:05 PM	2	11	4	2	5	5	7
4:01:33 PM	4	9	1	2	3	2	8
4:02:33 PM	5	4			1	8	12
4:03:40 PM	6	10	5	2	3	9	13
4:05:10 PM	7	11	6	5	3	7	19
4:07:42 PM	9	11	3	2	3	4	8
4:09:03 PM	10	16	10	3	4	17	18
4:11:53 PM	12	10	5	2	5	1	13
4:13:54 PM	13	16	9	1	5	12	14
4:21:04 PM	16	8	8		4	8	13
4:23:12 PM	17	7	7	1	3	2	5
4:24:15 PM	18	11		3	1	11	15
4:25:30 PM	19	19	2	4	8	10	20
4:28:14 PM	21	2	3	1	0	5	9
4:29:23 PM	22	8	7		3	8	8
4:31:22 PM	23	9	5	5	3	3	12
4:32:58 PM	24	3	4		4	2	5
4:33:56 PM	25	8	1	2	1	1	7
4:34:46 PM	26	12	3	3	4	6	15
4:36:13 PM	27	10	2	2	2	4	5
4:37:52 PM	29	19	5	3	3	14	12
4:39:47 PM	30	6	5		2	6	6
4:40:54 PM	31	11	4	4	3	9	8
4:42:15 PM	32	9	1	1	2	3	11
4:43:08 PM	33	8	7		5	6	17
4:45:39 PM	35	6	4	2	2	5	6
4:46:56 PM	36	7	6	1	1	4	6
4:48:31 PM	38	14	11	1	6	4	12
4:50:18 PM	39	5	2		1	4	9
4:51:11 PM	40	8	6	2	4	7	17
4:52:23 PM	41	3	7	1	2	4	5
4:53:13 PM	42	8	3	2	5	7	10
4:54:47 PM	43	9	8	1	1	2	9
4:56:41 PM	44	6	4		2	3	8
4:58:05 PM	45	15	3	3	2	11	12
5:00:37 PM	47	11	3	3	6	9	10
5:02:23 PM	48	6	3		1	8	7
5:03:27 PM	49	9	8		1	11	11
5:04:20 PM	50	14	11	2	5	9	16
5:06:10 PM	51	10	2	2	1	5	9
5:07:08 PM	52	6	2		3	4	13
5:08:27 PM	54	25	4	6	5	15	22
5:10:10 PM	55	10	13		7	6	16
5:11:33 PM	56	9	5	3	6	6	14
5:13:28 PM	57	3	1	1	4	10	9
5:16:21 PM	61	6	6		2	9	9
5:17:20 PM	62	9	2	5	5	6	12
5:18:48 PM	63	6	3		6	8	14
5:19:57 PM	64	6	2	2	2	2	3
5:20:47 PM	65	17	8	3	10	13	21
5:23:07 PM	66	10	4	1	5	7	21
5:24:41 PM	67	4		4	3	10	10
5:25:52 PM	68	10	4	2	5	10	9
5:28:00 PM	70	5	4	1	2	2	3
5:35:04 PM	72	7			3	5	8
5:35:54 PM	73	3		2	2	2	6
5:36:48 PM	74	6		2	5	7	15
5:37:47 PM	75	5	2	1	1	7	4
5:42:03 PM	77	4	1	5	4	5	10

Intersection: Peace/St Mary's
 Date: 9/21/00

Time	Cycle	WB LT	WB TH (lt lane)	WB TH (rt lane)	WB RT	EB RT	EB TH (rt lane)	EB TH (lt lane)	EB LT
3:43:18 PM	1	3	2	12	3	1	8	2	
3:43:19 PM	2	3	4	5	3	2	3	2	1
3:43:21 PM	3		9	4	1		1	3	1
3:43:24 PM	4	1	4	5	1	1	12	2	1
3:43:28 PM	5		4	3	1	2	4	2	
3:43:33 PM	6		5	4	1		3	1	
3:43:39 PM	7	1	2		1	3	5	2	1
3:43:46 PM	8		2	1		2	4	5	
3:43:54 PM	9		7	6	1	2	2	4	
3:44:03 PM	10		4	4	2		10	1	1
3:44:13 PM	11	1	6	3	3	3	5	2	
3:44:24 PM	12		4	3	1	1	10	4	
3:44:36 PM	13		7	4	3	3	9	6	1
3:44:49 PM	14	1	6	1	4	2	4	3	1
3:45:03 PM	15		2	1			11	4	
3:45:18 PM	16	1	3	1	3	3	10	6	
3:45:34 PM	17	3	1	4	3	1	9	4	
3:45:51 PM	18	1	7	6	1	1	6	5	
3:46:09 PM	19		8	4	1		7	4	1
3:46:28 PM	20		6	4	2	2	3	2	1
3:46:48 PM	21		3	2	1	3	7	5	
3:47:09 PM	22	2	2	2	1		8	5	
3:47:31 PM	23	2	3	7	3		8	3	
3:47:54 PM	24	1		6	2	1	11	6	
3:48:18 PM	25	2	6	1		1	7	2	
3:48:43 PM	26		3	3		1	2	1	1
3:49:09 PM	27		9	6	2	1	4	2	1
3:49:36 PM	28	2	2	6	1	1	4	2	1
3:50:04 PM	29		5	4	1	3	3	1	1
3:50:33 PM	30	1	4	5			6	3	1
3:51:03 PM	31		6	3	2	2	11	3	
3:51:34 PM	32		5	3	2	3	9	5	
3:52:06 PM	33	2	7	7	4	1	5	4	
3:52:39 PM	34	2	3	4		2	4	3	2
3:53:13 PM	35	4	1	7	1	2	3	3	
3:53:48 PM	36		6	4	1	3	6	3	1
3:54:24 PM	37	1	5	3	2	2	7	4	1
3:55:01 PM	38		9	3	1	1	7	4	1
3:55:39 PM	39		8	1	1	4	8	1	1
3:56:18 PM	40		7	5	3		10	7	
3:56:58 PM	41		3	5	1	3	9	8	
3:57:39 PM	42	1	1	8	4	2	14	10	
3:58:21 PM	43		6	5	1	2	5	6	
3:59:04 PM	44		8	4	2		2	7	
3:59:48 PM	45	1	5	5		1	6	5	
4:00:33 PM	46		9	4	3		5	5	
4:01:19 PM	47	1	4	6	4	2	1	1	
4:02:06 PM	48		3	2	2	1	2	3	
4:02:54 PM	49	1	4	4	2	3	3	2	
4:03:43 PM	50		4	3	2	1	8	4	
4:04:33 PM	51		4	7	2		7	4	
4:05:24 PM	52		10	7	4	2	6	3	
4:06:16 PM	53	2	5	4			9	3	1
4:07:09 PM	54	2	5	1		1	5	5	
4:08:03 PM	55		7	7	1		4		1
4:08:58 PM	56		9	8	2		10	3	1
4:09:54 PM	57	1	5	10		2	7	7	

Intersection: Peace/St Mary's
 Date: 9/21/00

Time	Cycle	WB LT	WB TH (lt lane)	WB TH (rt lane)	WB RT	EB RT	EB TH (rt lane)	EB TH (lt lane)	EB LT
4:10:51 PM	58	1	5	3	2	1	11	2	1
4:11:49 PM	59		2	1	1	4	7	3	2
4:12:48 PM	60		5	3	1		2	3	
4:13:48 PM	61	2	4	7	3	1	3	3	
4:14:49 PM	62	1	12	7	3	2	4	4	
4:15:51 PM	63	1	1	7	4	1	10	4	1
4:16:54 PM	64	2	4	7	3	1	12	2	3
4:17:58 PM	65		2	4			6	4	1
4:19:03 PM	66		11	7	6	3	7	7	
4:20:09 PM	67		5	8	1	1	8	8	
4:21:16 PM	68	1	8	8	1		8	4	
4:22:24 PM	69	2	7	6	1	1	6	3	
4:23:33 PM	70	2	5	7	1	2	9	9	
4:24:43 PM	71	3	3	8	2	1	5	5	
4:25:54 PM	72	4	4	12	3	3	8	1	1
4:27:06 PM	73	1	1	5	2		11	5	2
4:28:19 PM	74	1	12	11	2		7	4	1
4:29:33 PM	75	4	4	5	1		8	3	
4:30:48 PM	76	2	4	10	1	1	8	6	2
4:32:04 PM	77	2	5	6	1	2	8	5	2
4:33:21 PM	78	2	12	5	3		7	2	1
4:34:39 PM	79	1	3	2	2	1	11	3	
4:35:58 PM	80		4	1			9	4	1
4:37:18 PM	81								

Intersection: Peace/St Mary's
 Date: 16/16/00

Time	Cycle	WB LT	WB TH (lt lane)	WB TH (rt lane)	WB RT	EB RT	EB TH (rt lane)	EB TH (lt lane)	EB LT
4:23:33 PM	1	2	1	5		3	10	3	1
4:24:51 PM	2	4	4	4	2		9	2	
4:26:12 PM	3	1	3	8		1	8	8	1
4:27:32 PM	4	1	1	3	1	1	11	4	
4:28:52 PM	5	1	8	8	2	1	11	4	
4:30:12 PM	6	3		12		1	8	5	1
4:31:31 PM	7		7	3	3	2	4	4	
4:32:52 PM	8		6	8	2	2	7	3	1
4:34:12 PM	9	1	5	5	1		6	4	
4:35:31 PM	10	1	9	12			10	3	
4:36:53 PM	11	1	9	2	1	1	11	1	
4:38:13 PM	12		5	2	4	1	13	4	1
4:39:32 PM	13	2	4	2	1	1	12	8	
4:40:52 PM	14	1	1	8	2	3	8	4	2
4:43:31 PM	15		3	5	2	1	12	6	
4:44:51 PM	16	1	4	4		2	6	2	
4:46:11 PM	17	1	6	5		1	2	5	
4:47:31 PM	18		7	6	4	1	7		3
4:48:51 PM	19	5	7	10	1	3	6	1	
4:50:11 PM	20	1	2	9	2	3	8	3	
4:51:31 PM	21	1	6	9		3	6	6	
4:52:51 PM	22		10	10	2	1	11	5	1
4:54:12 PM	23	1		8	1	3	7	8	1
4:55:32 PM	24	1	6	5	3	2	5	6	
4:56:52 PM	25	1	9	5	1	1	11	2	1
4:58:11 PM	26	1		8	4	2	3	6	1
4:59:31 PM	27	1		4	1	1	4	6	3
5:00:51 PM	28		8	2	2	4	7	4	
5:02:11 PM	29		10	9	3	1	7	5	
5:03:31 PM	30		9	6	2	3	9	6	
5:04:50 PM	31		1	7		1	12	8	1
5:06:11 PM	32	1	6	5	4	2	5	5	
5:07:31 PM	33		6	3	4	4	6	4	3
5:08:51 PM	34	1	8	9	2	4	7	6	
5:10:14 PM	35		10	7	2	2	9	12	
5:11:32 PM	36	1	4	7	3	3	9	3	1
5:12:51 PM	37	1	4	6	5	3	9	2	
5:14:11 PM	38		5	6	3		8	4	
5:15:30 PM	39	2	7	4	4	2	4	4	
5:16:51 PM	40		9	3	4	2	14	1	3
5:18:11 PM	41	1	4	7	1		6	2	
5:19:31 PM	42	1	5	15	2	1	10	4	
5:20:51 PM	43	1	1	4		2	4	3	
5:22:14 PM	44		8	9	1		5	2	1
5:23:31 PM	45		8	8	3	1	6	4	
5:24:51 PM	46	1	4		3	2	7	6	
5:26:14 PM	47		11	9	4	2	9	9	
5:27:32 PM	48	1	1	9	1	2	5	5	
5:28:51 PM	49	2	6	12	4		9	5	
5:30:11 PM	50		9	3	2	2	10	2	1
5:31:33 PM	51	3	6	10	3	1	5	10	
5:32:51 PM	52	1	8	7		3	4	7	
5:34:12 PM	53	2	2	8			14	6	
5:35:32 PM	54		7	7	2	1	3	1	
5:36:51 PM	55	1	9	7	3	2	3	2	
5:39:32 PM	56		5	3	8	1	7	4	1
5:40:54 PM	57	3	6	2		1	4	3	1
5:42:11 PM	58		6	5	1		5	4	1

Intersection: Peace/St Mary's
 Date: 16/16/00

Time	Cycle	WB LT	WB TH (lt lane)	WB TH (rt lane)	WB RT	EB RT	EB TH (rt lane)	EB TH (lt lane)	EB LT
5:43:31 PM	59	3	8	6	2	1	9	5	1
5:44:51 PM	60		8	4			7	4	
5:46:12 PM	61		8	4	4	1	6	2	
5:47:30 PM	62	2	2	5		1	4	3	1
5:48:50 PM	63	1	6	11			8	4	
5:54:11 PM	64	1	4	5	2	1	8	5	1
5:55:32 PM	65	1	6	5	1	1	3	4	
5:56:51 PM	66	3	2	5	2		4	2	1
5:58:11 PM	67	3	4	6	3	2	13	2	1
5:59:31 PM	68		5	5	2	3	5	6	2
6:00:50 PM	69	1	6	4	4	2	6	4	1
6:02:11 PM	70	1	5	5	2	2	5	3	1
6:03:30 PM	71		4	3	3	2	2	4	
6:04:55 PM	72	4	3	5	1	1	2		
6:06:11 PM	73		8	8	2	1	7	3	1
6:07:31 PM	74		3	2	2	1	5	3	
6:08:51 PM	75		4	3	1	1	7	4	
6:10:11 PM	76		4	8			3		1
6:11:31 PM	77		3	4	1	2	3	2	
6:12:46 PM	78	1	4	3	2		2	1	1
6:13:50 PM	79		5	2	1		5		1
6:14:58 PM	80	3	4	8	4		5	2	
6:16:09 PM	81	1	4	1	1		2	5	
6:17:19 PM	82		3	1			6	3	
6:18:28 PM	83	1	1	3	3	3	5	4	1
6:19:38 PM	84	4	4	3	1		4	3	1
6:20:49 PM	85	1	3	4	5		3	2	
6:21:58 PM	86	1	5	3	4		4	5	
6:23:08 PM	87		4	1	1	2	4	2	1
6:24:20 PM	88	2	7	6	2	1	6	5	

Intersection: Hillsborough/McDowell
 Date: 9/25/00

Time	Cycle	EB RT	EB TH (rt lane)	EB TH (lt lane)	EB LT	WB LT	WB TH (lt lane)	WB TH (rt lane)	WB RT
4:14:12 PM	1		5	2	3				
4:15:32 PM	2		2	2	2		1	0	1
4:16:53 PM	3		2	6	3				1
4:18:12 PM	4		4	2	7				
4:19:32 PM	5		2	6	4				
4:20:52 PM	6		4		6			1	
4:22:12 PM	7		3	2	3		1		
4:23:32 PM	8		3	1	5				
4:24:52 PM	9		5	3	3				
4:26:12 PM	10		4	4	4				1
4:27:32 PM	11		3	1	2				
4:28:53 PM	12		2	2	5		2		1
4:30:17 PM	13		1	2	4				
4:31:33 PM	14		2	2	3				2
4:32:53 PM	15		4	3	2				2
4:34:12 PM	16		5	3	4		1	1	
4:35:32 PM	17		5	3	3		3		
4:36:53 PM	18		4	4	2			1	
4:38:12 PM	19		3	2	3		1	1	
4:39:32 PM	20		5	1	7		2		
4:40:54 PM	21		4	3	3			1	2
4:42:12 PM	22		7	4	4		1	2	1
4:43:37 PM	23		2	1	5				3
4:44:53 PM	24		7		6				1
4:46:13 PM	25		4	1	5				
4:47:32 PM	26		2	1	8		3		
4:48:52 PM	27		4		4		2		
4:50:13 PM	28		2	2			1	2	1
4:51:32 PM	29		3	2	4		2		
4:52:52 PM	30		2	3	2		1		1
4:54:13 PM	31		5	4	3		1	1	
4:55:32 PM	32		1	3	4				
4:56:55 PM	33		5		10		1		1
4:58:12 PM	34		3	3	5		1	1	1
4:59:32 PM	35		3	2	4		1	1	1
5:00:52 PM	36		4	1	5		2	1	
5:02:13 PM	37		3		8				4
5:03:32 PM	38		4	2	5		2		3
5:04:52 PM	39		9		9		1	1	3
5:06:14 PM	40		5	1	3		3	3	
5:07:32 PM	41		3	1	9				4
5:08:52 PM	42		4	3	7		2		1
5:10:13 PM	43		6		4		5	1	1
5:11:32 PM	44		1		6		1	3	1
5:12:53 PM	45		2	2	7		2		2
5:14:13 PM	46		4	1	7		1		2
5:15:32 PM	47		4	1	7			1	1
5:16:52 PM	48		4	1	4		2	1	1
5:18:12 PM	49		1	3	5		1	1	
5:19:34 PM	50		3	3	5		3	1	
5:20:52 PM	51		3	1	6		1		2
5:22:12 PM	52		3	1	10		2	1	1
5:23:33 PM	53		3	2	2		1	1	
5:24:53 PM	54		4	3	4		1	1	
5:26:12 PM	55		4	2	2		1	1	2
5:27:33 PM	56		2	3	4		2		1
5:28:52 PM	57		2		1		2		1
5:30:13 PM	58		3	3	3				

Intersection: Hillsborough/McDowell
Date: 9/25/00

Time	Cycle	EB RT	EB TH (rt lane)	EB TH (lt lane)	EB LT	WB LT	WB TH (lt lane)	WB TH (rt lane)	WB RT
5:31:31 PM	59		2	3	4				1
5:32:52 PM	60		5	1	5		1	2	1
5:34:12 PM	61		8		5		3		2
5:35:32 PM	62		3	4	3				1
5:36:51 PM	63		4	2	4				
5:38:13 PM	64		1	2	6				1
5:39:32 PM	65		2	1	4		1	2	1
5:40:52 PM	66		2	1	2		4		
5:42:13 PM	67		1	2	3				
5:43:32 PM	68		1	2	4				

APPENDIX C

LANE VOLUME DATA PER 15 MINUTES

INTERSECTION: Grand/Franklin

DATE: 5/25/00

Time Beginning	WB RT	WB TH (rt lane)	WB TH (lt lane)	WB LT	EB RT	EB TH (rt lane)	EB TH (lt lane)	EB LT
7:00 AM	36	136	244	4	12	108	108	52
7:15 AM	44	148	304	0	0	192	160	52
7:30 AM	36	248	400	12	16	192	144	64
7:45 AM	36	212	312	12	20	276	228	48
8:00 AM	68	328	276	36	24	272	196	56
8:15 AM	64	260	348	12	32	388	204	72
8:30 AM	80	208	376	24	20	392	168	100
8:45 AM	56	256	408	16	8	408	92	100
9:00 AM	96	240	360	20	24	308	148	100
9:15 AM	80	200	388	12	28	268	192	60
9:30 AM	60	152	328	8	36	188	180	48
9:45 AM	104	408	504	36	20	232	140	44
3:30 PM	104	384	484	16	36	292	108	80
3:45 PM	116	460	480	24	28	188	172	48
4:00 PM	100	444	440	16	16	212	144	40
4:15 PM	84	452	528	16	20	364	84	88
4:30 PM	156	492	540	44	20	228	108	68
4:45 PM	152	452	596	4	28	236	128	72
5:00 PM	168	444	584	12	20	248	148	40
5:15 PM	176	344	584	16	24	264	140	48
5:30 PM	200	452	548	8	40	328	84	64
5:45 PM	120	420	516	12	20	216	76	52
6:00 PM	96	384	472	28	48	160	68	84

INTERSECTION: Poole/Beverly
DATE: 9/18/00

Time Beginning	WB RT	WB TH (rt lane)	WB TH (lt lane)	WB LT	EB RT	EB TH (rt lane)	EB TH (lt lane)	EB LT
3:30 PM	0	375	178	76	120	262	447	0
3:45 PM	0	363	167	79	129	234	455	0
4:00 PM	0	430	243	69	134	284	462	0
4:15 PM	0	455	195	73	122	321	485	0
4:30 PM	0	351	193	83	220	338	566	0
4:45 PM	0	343	94	111	189	326	471	0

INTERSECTION: Peace/StMary's
DATE: 9/21/00

Time Beginning	WB RT	WB TH (rt lane)	WB TH (lt lane)	WB LT	EB RT	EB TH (rt lane)	EB TH (lt lane)	EB LT
3:45 PM	83	213	237	35	79	300	142	23
4:00 PM	81	150	181	50	54	352	189	11
4:15 PM	57	212	208	45	77	233	122	32
4:30 PM	90	200	265	16	69	302	237	12
4:45 PM	69	229	249	28	49	294	147	16
5:00 PM	98	265	249	36	53	298	184	28
5:15 PM	73	294	233	90	40	372	192	40

INTERSECTION: Peace/St Mary's
DATE: 11/16/00

Time Beginning	WB RT	WB TH (rt lane)	WB TH (lt lane)	WB LT	EB RT	EB TH (rt lane)	EB TH (lt lane)	EB LT
4:30 PM	49	286	216	61	45	388	167	16
4:45 PM	73	286	225	49	81	372	180	28
5:00 PM	102	253	225	24	98	310	245	40
5:15 PM	110	315	265	32	77	347	175	20
5:30 PM	102	327	290	45	65	306	233	4
5:45 PM	81	225	249	57	28	265	163	28
6:00 PM	85	216	200	36	69	237	126	28
6:15 PM	112	163	205	65	28	215	149	23

INTERSECTION: Hillsborough/McDowell
DATE: 9/25/00

Time Beginning	WB RT	WB TH (rt lane)	WB TH (lt lane)	WB LT	EB RT	EB TH (rt lane)	EB TH (lt lane)	EB LT
4:15 PM	12	4	8	0	0	151	118	171
4:30 PM	32	24	40	0	0	171	118	163
4:45 PM	28	12	45	0	0	151	69	208
5:00 PM	77	45	73	0	0	184	53	265
5:15 PM	45	32	61	0	0	143	81	241
5:30 PM	36	16	53	0	0	139	81	167

APPENDIX D

LANE DISTRIBUTION MODEL EVALUATION OUTPUT

Intersection	Run			TH Vol	TH Vol	Lane 1	Lane 2	%TH in	Opp	Conf Vol	Sub Vol		
	Number	Approach	Criterion									RT Vol	(rt lane)
Grand/Franklin	1	EB	Field Value	12	108	108	52	120	160	50	416	21.6	280
Grand/Franklin	1	EB	Delay	12	216	0	52	228	52	0	416	21.6	280
Grand/Franklin	1	EB	Queue	12	128	88	52	140	140	41	416	21.6	280
Grand/Franklin	1	EB	Volume	12	128	88	52	140	140	41	416	21.6	280
Grand/Franklin	1	EB	Flow Ratio	12	181	35	52	193	87	16	416	21.6	280
Grand/Franklin	1	EB	Back of Queue	12	148	68	52	160	120	31	416	21.6	280
Grand/Franklin	1	EB	Bonneson	12	132	84	52	144	136	39	384	20.0	280
Grand/Franklin	1	WB	Field Value	36	136	244	4	172	248	64	228	0.9	420
Grand/Franklin	1	WB	Delay	36	190	190	4	226	194	50	228	0.9	420
Grand/Franklin	1	WB	Queue	36	175	205	4	211	209	54	228	0.9	420
Grand/Franklin	1	WB	Volume	36	174	206	4	210	210	54	228	0.9	420
Grand/Franklin	1	WB	Flow Ratio	36	182	198	4	218	202	52	228	0.9	420
Grand/Franklin	1	WB	Back of Queue	36	190	190	4	226	194	50	228	0.9	420
Grand/Franklin	1	WB	Bonneson	36	164	216	4	200	220	57	268	1.1	420
Grand/Franklin	2	EB	Field Value	0	192	160	52	192	212	45	496	25.8	404
Grand/Franklin	2	EB	Delay	0	311	41	52	311	93	12	496	25.8	404
Grand/Franklin	2	EB	Queue	0	221	131	52	221	183	37	496	25.8	404
Grand/Franklin	2	EB	Volume	0	202	150	52	202	202	43	496	25.8	404
Grand/Franklin	2	EB	Flow Ratio	0	263	89	52	263	141	25	496	25.8	404
Grand/Franklin	2	EB	Back of Queue	0	231	121	52	231	173	34	496	25.8	404
Grand/Franklin	2	EB	Bonneson	0	212	140	52	212	192	40	452	23.5	404
Grand/Franklin	2	WB	Field Value	44	148	304	0	192	304	67	352	0.0	496
Grand/Franklin	2	WB	Delay	44	196	256	0	240	256	57	352	0.0	496
Grand/Franklin	2	WB	Queue	44	206	246	0	250	246	54	352	0.0	496
Grand/Franklin	2	WB	Volume	44	204	248	0	248	248	55	352	0.0	496
Grand/Franklin	2	WB	Flow Ratio	44	198	254	0	242	254	56	352	0.0	496
Grand/Franklin	2	WB	Back of Queue	44	216	236	0	260	236	52	352	0.0	496
Grand/Franklin	2	WB	Bonneson	44	452	0	0	496	0	0	404	0.0	496
Grand/Franklin	3	EB	Field Value	16	192	144	64	208	208	43	684	43.8	416
Grand/Franklin	3	EB	Delay	16	336	0	64	352	64	0	684	43.8	416
Grand/Franklin	3	EB	Queue	16	228	108	64	244	172	32	684	43.8	416
Grand/Franklin	3	EB	Volume	16	192	144	64	208	208	43	684	43.8	416
Grand/Franklin	3	EB	Flow Ratio	16	280	56	64	296	120	17	684	43.8	416
Grand/Franklin	3	EB	Back of Queue	16	228	108	64	244	172	32	684	43.8	416
Grand/Franklin	3	EB	Bonneson	16	240	96	64	256	160	29	660	42.2	416
Grand/Franklin	3	WB	Field Value	36	248	400	12	284	412	62	352	4.2	696
Grand/Franklin	3	WB	Delay	36	344	304	12	380	316	47	352	4.2	696
Grand/Franklin	3	WB	Queue	36	324	324	12	360	336	50	352	4.2	696
Grand/Franklin	3	WB	Volume	36	312	336	12	348	348	52	352	4.2	696
Grand/Franklin	3	WB	Flow Ratio	36	336	312	12	372	324	48	352	4.2	696
Grand/Franklin	3	WB	Back of Queue	36	339	309	12	375	321	48	352	4.2	696
Grand/Franklin	3	WB	Bonneson	36	298	350	12	334	362	54	400	4.8	696
Grand/Franklin	4	EB	Field Value	20	276	228	48	296	276	45	560	26.9	572
Grand/Franklin	4	EB	Delay	20	360	144	48	380	192	29	560	26.9	572
Grand/Franklin	4	EB	Queue	20	292	212	48	312	260	42	560	26.9	572
Grand/Franklin	4	EB	Volume	20	266	238	48	286	286	47	560	26.9	572
Grand/Franklin	4	EB	Flow Ratio	20	329	175	48	349	223	35	560	26.9	572
Grand/Franklin	4	EB	Back of Queue	20	302	202	48	322	250	40	560	26.9	572
Grand/Franklin	4	EB	Bonneson	20	283	221	48	303	269	44	536	25.7	572
Grand/Franklin	4	WB	Field Value	36	212	312	12	248	324	60	524	6.3	572
Grand/Franklin	4	WB	Delay	36	292	232	12	328	244	44	524	6.3	572
Grand/Franklin	4	WB	Queue	36	262	262	12	298	274	50	524	6.3	572
Grand/Franklin	4	WB	Volume	36	250	274	12	286	286	52	524	6.3	572
Grand/Franklin	4	WB	Flow Ratio	36	281	243	12	317	255	46	524	6.3	572
Grand/Franklin	4	WB	Back of Queue	36	277	247	12	313	259	47	524	6.3	572
Grand/Franklin	4	WB	Bonneson	36	239	285	12	275	297	54	552	6.6	572
Grand/Franklin	5	EB	Field Value	24	272	196	56	296	252	42	672	37.6	548
Grand/Franklin	5	EB	Delay	24	389	79	56	413	135	17	672	37.6	548
Grand/Franklin	5	EB	Queue	24	289	179	56	313	235	38	672	37.6	548
Grand/Franklin	5	EB	Volume	24	250	218	56	274	274	47	672	37.6	548
Grand/Franklin	5	EB	Flow Ratio	24	332	136	56	356	192	29	672	37.6	548
Grand/Franklin	5	EB	Back of Queue	24	294	174	56	318	230	37	672	37.6	548
Grand/Franklin	5	EB	Bonneson	24	299	169	56	323	225	36	640	35.8	548
Grand/Franklin	5	WB	Field Value	68	328	276	36	396	312	46	492	17.7	708
Grand/Franklin	5	WB	Delay	68	350	254	36	418	290	42	492	17.7	708
Grand/Franklin	5	WB	Queue	68	302	302	36	370	338	50	492	17.7	708
Grand/Franklin	5	WB	Volume	68	286	318	36	354	354	53	492	17.7	708
Grand/Franklin	5	WB	Flow Ratio	68	332	272	36	400	308	45	492	17.7	708
Grand/Franklin	5	WB	Back of Queue	68	322	282	36	390	318	47	492	17.7	708
Grand/Franklin	5	WB	Bonneson	68	283	321	36	351	357	53	524	18.9	708
Grand/Franklin	6	EB	Field Value	32	388	204	72	420	276	34	672	48.4	696
Grand/Franklin	6	EB	Delay	32	451	141	72	483	213	24	672	48.4	696
Grand/Franklin	6	EB	Queue	32	363	229	72	395	301	39	672	48.4	696
Grand/Franklin	6	EB	Volume	32	316	276	72	348	348	47	672	48.4	696
Grand/Franklin	6	EB	Flow Ratio	32	407	185	72	439	257	31	672	48.4	696
Grand/Franklin	6	EB	Back of Queue	32	371	221	72	403	293	37	672	48.4	696
Grand/Franklin	6	EB	Bonneson	32	398	194	72	430	266	33	620	44.6	696
Grand/Franklin	6	WB	Field Value	64	260	348	12	324	360	57	624	7.5	684
Grand/Franklin	6	WB	Delay	64	324	284	12	388	296	47	624	7.5	684
Grand/Franklin	6	WB	Queue	64	289	319	12	353	331	52	624	7.5	684
Grand/Franklin	6	WB	Volume	64	278	330	12	342	342	54	624	7.5	684
Grand/Franklin	6	WB	Flow Ratio	64	311	297	12	375	309	49	624	7.5	684

Intersection	Run		Criterion	RT Vol	TH Vol	TH Vol	Lane 1		Lane 2	%TH in	Opp	Conf Vol	Sub Vol
	Number	Approach			(rt lane)	(lt lane)	LT Vol	Vol	Vol	LT Lane	Vol		
Grand/Franklin	6	WB	Back of Queue	64	309	299	12	373	311	49	624	7.5	684
Grand/Franklin	6	WB	Bonneson	64	265	343	12	329	355	56	664	8.0	684
Grand/Franklin	7	EB	Field Value	20	392	168	100	412	268	30	664	66.4	680
Grand/Franklin	7	EB	Delay	20	495	65	100	515	165	12	664	66.4	680
Grand/Franklin	7	EB	Queue	20	380	180	100	400	280	32	664	66.4	680
Grand/Franklin	7	EB	Volume	20	320	240	100	340	340	43	664	66.4	680
Grand/Franklin	7	EB	Flow Ratio	20	431	129	100	451	229	23	664	66.4	680
Grand/Franklin	7	EB	Back of Queue	20	381	179	100	401	279	32	664	66.4	680
Grand/Franklin	7	EB	Bonneson	20	453	107	100	473	207	19	608	60.8	680
Grand/Franklin	7	WB	Field Value	80	208	376	24	288	400	64	580	13.9	688
Grand/Franklin	7	WB	Delay	80	323	261	24	403	285	45	580	13.9	688
Grand/Franklin	7	WB	Queue	80	284	300	24	364	324	51	580	13.9	688
Grand/Franklin	7	WB	Volume	80	264	320	24	344	344	55	580	13.9	688
Grand/Franklin	7	WB	Flow Ratio	80	307	277	24	387	301	47	580	13.9	688
Grand/Franklin	7	WB	Back of Queue	80	299	285	24	379	309	49	580	13.9	688
Grand/Franklin	7	WB	Bonneson	80	257	327	24	337	351	56	660	15.8	688
Grand/Franklin	8	EB	Field Value	8	408	92	100	416	192	18	720	72.0	608
Grand/Franklin	8	EB	Delay	8	500	0	100	508	100	0	720	72.0	608
Grand/Franklin	8	EB	Queue	8	350	150	100	358	250	30	720	72.0	608
Grand/Franklin	8	EB	Volume	8	296	204	100	304	304	41	720	72.0	608
Grand/Franklin	8	EB	Flow Ratio	8	417	83	100	425	183	17	720	72.0	608
Grand/Franklin	8	EB	Back of Queue	8	355	145	100	363	245	29	720	72.0	608
Grand/Franklin	8	EB	Bonneson	8	432	68	100	440	168	14	680	68.0	608
Grand/Franklin	8	WB	Field Value	56	256	408	16	312	424	61	508	8.1	736
Grand/Franklin	8	WB	Delay	56	357	307	16	413	323	46	508	8.1	736
Grand/Franklin	8	WB	Queue	56	332	332	16	388	348	50	508	8.1	736
Grand/Franklin	8	WB	Volume	56	312	352	16	368	368	53	508	8.1	736
Grand/Franklin	8	WB	Flow Ratio	56	346	318	16	402	334	48	508	8.1	736
Grand/Franklin	8	WB	Back of Queue	56	344	320	16	400	336	48	508	8.1	736
Grand/Franklin	8	WB	Bonneson	56	299	365	16	355	381	55	600	9.6	736
Grand/Franklin	9	EB	Field Value	24	308	148	100	332	248	32	696	69.6	580
Grand/Franklin	9	EB	Delay	24	456	0	100	480	100	0	696	69.6	580
Grand/Franklin	9	EB	Queue	24	321	135	100	345	235	30	696	69.6	580
Grand/Franklin	9	EB	Volume	24	266	190	100	290	290	42	696	69.6	580
Grand/Franklin	9	EB	Flow Ratio	24	382	74	100	406	174	16	696	69.6	580
Grand/Franklin	9	EB	Back of Queue	24	323	133	100	347	233	29	696	69.6	580
Grand/Franklin	9	EB	Bonneson	24	392	64	100	416	164	14	620	62.0	580
Grand/Franklin	9	WB	Field Value	96	240	360	20	336	380	60	480	9.6	716
Grand/Franklin	9	WB	Delay	96	300	300	20	396	320	50	480	9.6	716
Grand/Franklin	9	WB	Queue	96	280	320	20	376	340	53	480	9.6	716
Grand/Franklin	9	WB	Volume	96	262	338	20	358	358	56	480	9.6	716
Grand/Franklin	9	WB	Flow Ratio	96	292	308	20	388	328	51	480	9.6	716
Grand/Franklin	9	WB	Back of Queue	96	293	307	20	389	327	51	480	9.6	716
Grand/Franklin	9	WB	Bonneson	96	251	349	20	347	369	58	556	11.1	716
Grand/Franklin	10	EB	Field Value	28	268	192	60	296	252	42	668	40.1	548
Grand/Franklin	10	EB	Delay	28	380	80	60	408	140	17	668	40.1	548
Grand/Franklin	10	EB	Queue	28	285	175	60	313	235	38	668	40.1	548
Grand/Franklin	10	EB	Volume	28	246	214	60	274	274	47	668	40.1	548
Grand/Franklin	10	EB	Flow Ratio	28	328	132	60	356	192	29	668	40.1	548
Grand/Franklin	10	EB	Back of Queue	28	290	170	60	318	230	37	668	40.1	548
Grand/Franklin	10	EB	Bonneson	28	296	164	60	324	224	36	600	36.0	548
Grand/Franklin	10	WB	Field Value	80	200	388	12	280	400	66	488	5.9	680
Grand/Franklin	10	WB	Delay	80	294	294	12	374	306	50	488	5.9	680
Grand/Franklin	10	WB	Queue	80	274	314	12	354	326	53	488	5.9	680
Grand/Franklin	10	WB	Volume	80	260	328	12	340	340	56	488	5.9	680
Grand/Franklin	10	WB	Flow Ratio	80	283	305	12	363	317	52	488	5.9	680
Grand/Franklin	10	WB	Back of Queue	80	287	301	12	367	313	51	488	5.9	680
Grand/Franklin	10	WB	Bonneson	80	246	342	12	326	354	58	520	6.2	680
Grand/Franklin	11	EB	Field Value	36	188	180	48	224	228	49	540	25.9	452
Grand/Franklin	11	EB	Delay	36	284	84	48	320	132	23	540	25.9	452
Grand/Franklin	11	EB	Queue	36	214	154	48	250	202	42	540	25.9	452
Grand/Franklin	11	EB	Volume	36	190	178	48	226	226	48	540	25.9	452
Grand/Franklin	11	EB	Flow Ratio	36	248	120	48	284	168	33	540	25.9	452
Grand/Franklin	11	EB	Back of Queue	36	220	148	48	256	196	40	540	25.9	452
Grand/Franklin	11	EB	Bonneson	36	202	166	48	238	214	45	488	23.4	452
Grand/Franklin	11	WB	Field Value	60	152	328	8	212	336	68	404	3.2	548
Grand/Franklin	11	WB	Delay	60	240	240	8	300	248	50	404	3.2	548
Grand/Franklin	11	WB	Queue	60	220	260	8	280	268	54	404	3.2	548
Grand/Franklin	11	WB	Volume	60	214	266	8	274	274	55	404	3.2	548
Grand/Franklin	11	WB	Flow Ratio	60	230	250	8	290	258	52	404	3.2	548
Grand/Franklin	11	WB	Back of Queue	60	235	245	8	295	253	51	404	3.2	548
Grand/Franklin	11	WB	Bonneson	60	202	278	8	262	286	58	416	3.3	548
Grand/Franklin	12	EB	Field Value	20	232	140	44	252	184	38	1016	44.7	436
Grand/Franklin	12	EB	Delay	20	372	0	44	392	44	0	1016	44.7	436
Grand/Franklin	12	EB	Queue	20	246	126	44	266	170	34	1016	44.7	436
Grand/Franklin	12	EB	Volume	20	198	174	44	218	218	47	1016	44.7	436
Grand/Franklin	12	EB	Flow Ratio	20	311	61	44	331	105	16	1016	44.7	436
Grand/Franklin	12	EB	Back of Queue	20	241	131	44	261	175	35	1016	44.7	436
Grand/Franklin	12	EB	Bonneson	20	272	100	44	292	144	27	948	41.7	436
Grand/Franklin	12	WB	Field Value	104	408	504	36	512	540	55	392	14.1	1052
Grand/Franklin	12	WB	Delay	104	463	449	36	567	485	49	392	14.1	1052
Grand/Franklin	12	WB	Queue	104	446	466	36	550	502	51	392	14.1	1052
Grand/Franklin	12	WB	Volume	104	422	490	36	526	526	54	392	14.1	1052
Grand/Franklin	12	WB	Flow Ratio	104	456	456	36	560	492	50	392	14.1	1052

Intersection	Run		Criterion	RT Vol	TH Vol	TH Vol	Lane 1		Lane 2	%TH in	Opp	Conf Vol	Sub Vol
	Number	Approach			(rt lane)	(lt lane)	LT Vol	Vol	Vol	LT Lane	Vol		
Grand/Franklin	12	WB	Back of Queue	104	463	449	36	567	485	49	392	14.1	1052
Grand/Franklin	12	WB	Bonneson	104	408	504	36	512	540	55	416	15.0	1052
Grand/Franklin	13	EB	Field Value	36	292	108	80	328	188	27	972	77.8	516
Grand/Franklin	13	EB	Delay	36	400	0	80	436	80	0	972	77.8	516
Grand/Franklin	13	EB	Queue	36	295	105	80	331	185	26	972	77.8	516
Grand/Franklin	13	EB	Volume	36	222	178	80	258	258	45	972	77.8	516
Grand/Franklin	13	EB	Flow Ratio	36	368	32	80	404	112	8	972	77.8	516
Grand/Franklin	13	EB	Back of Queue	36	283	117	80	319	197	29	972	77.8	516
Grand/Franklin	13	EB	Bonneson	36	365	35	80	401	115	9	884	70.7	516
Grand/Franklin	13	WB	Field Value	104	384	484	16	488	500	56	436	7.0	988
Grand/Franklin	13	WB	Delay	104	419	449	16	523	465	52	436	7.0	988
Grand/Franklin	13	WB	Queue	104	404	464	16	508	480	53	436	7.0	988
Grand/Franklin	13	WB	Volume	104	390	478	16	494	494	55	436	7.0	988
Grand/Franklin	13	WB	Flow Ratio	104	412	456	16	516	472	53	436	7.0	988
Grand/Franklin	13	WB	Back of Queue	104	424	444	16	528	460	51	436	7.0	988
Grand/Franklin	13	WB	Bonneson	104	370	498	16	474	514	57	480	7.7	988
Grand/Franklin	14	EB	Field Value	28	188	172	48	216	220	48	1056	50.7	436
Grand/Franklin	14	EB	Delay	28	360	0	48	388	48	0	1056	50.7	436
Grand/Franklin	14	EB	Queue	28	240	120	48	268	168	33	1056	50.7	436
Grand/Franklin	14	EB	Volume	28	190	170	48	218	218	47	1056	50.7	436
Grand/Franklin	14	EB	Flow Ratio	28	311	49	48	339	97	14	1056	50.7	436
Grand/Franklin	14	EB	Back of Queue	28	237	123	48	265	171	34	1056	50.7	436
Grand/Franklin	14	EB	Bonneson	28	275	85	48	303	133	24	964	46.3	436
Grand/Franklin	14	WB	Field Value	116	460	480	24	576	504	51	388	9.3	1080
Grand/Franklin	14	WB	Delay	116	453	487	24	569	511	52	388	9.3	1080
Grand/Franklin	14	WB	Queue	116	435	505	24	551	529	54	388	9.3	1080
Grand/Franklin	14	WB	Volume	116	424	516	24	540	540	55	388	9.3	1080
Grand/Franklin	14	WB	Flow Ratio	116	447	493	24	563	517	52	388	9.3	1080
Grand/Franklin	14	WB	Back of Queue	116	459	481	24	575	505	51	388	9.3	1080
Grand/Franklin	14	WB	Bonneson	116	404	536	24	520	560	57	408	9.8	1080
Grand/Franklin	15	EB	Field Value	16	212	144	40	228	184	40	984	39.4	412
Grand/Franklin	15	EB	Delay	16	356	0	40	372	40	0	984	39.4	412
Grand/Franklin	15	EB	Queue	16	218	138	40	234	178	39	984	39.4	412
Grand/Franklin	15	EB	Volume	16	190	166	40	206	206	47	984	39.4	412
Grand/Franklin	15	EB	Flow Ratio	16	290	66	40	306	106	19	984	39.4	412
Grand/Franklin	15	EB	Back of Queue	16	228	128	40	244	168	36	984	39.4	412
Grand/Franklin	15	EB	Bonneson	16	246	110	40	262	150	31	900	36.0	412
Grand/Franklin	15	WB	Field Value	100	444	440	16	544	456	50	372	6.0	1000
Grand/Franklin	15	WB	Delay	100	425	459	16	525	475	52	372	6.0	1000
Grand/Franklin	15	WB	Queue	100	412	472	16	512	488	53	372	6.0	1000
Grand/Franklin	15	WB	Volume	100	400	484	16	500	500	55	372	6.0	1000
Grand/Franklin	15	WB	Flow Ratio	100	418	466	16	518	482	53	372	6.0	1000
Grand/Franklin	15	WB	Back of Queue	100	432	452	16	532	468	51	372	6.0	1000
Grand/Franklin	15	WB	Bonneson	100	379	505	16	479	521	57	396	6.3	1000
Grand/Franklin	16	EB	Field Value	20	364	84	88	384	172	19	1064	93.6	556
Grand/Franklin	16	EB	Delay	20	448	0	88	468	88	0	1064	93.6	556
Grand/Franklin	16	EB	Queue	20	359	89	88	379	177	20	1064	93.6	556
Grand/Franklin	16	EB	Volume	20	258	190	88	278	278	42	1064	93.6	556
Grand/Franklin	16	EB	Flow Ratio	20	444	4	88	464	92	1	1064	93.6	556
Grand/Franklin	16	EB	Back of Queue	20	340	108	88	360	196	24	1064	93.6	556
Grand/Franklin	16	EB	Bonneson	20	446	2	88	466	90	0	996	87.6	556
Grand/Franklin	16	WB	Field Value	84	452	528	16	536	544	54	468	7.5	1080
Grand/Franklin	16	WB	Delay	84	490	490	16	574	506	50	468	7.5	1080
Grand/Franklin	16	WB	Queue	84	475	505	16	559	521	52	468	7.5	1080
Grand/Franklin	16	WB	Volume	84	456	524	16	540	540	53	468	7.5	1080
Grand/Franklin	16	WB	Flow Ratio	84	490	490	16	574	506	50	468	7.5	1080
Grand/Franklin	16	WB	Back of Queue	84	495	485	16	579	501	49	468	7.5	1080
Grand/Franklin	16	WB	Bonneson	84	435	545	16	519	561	56	536	8.6	1080
Grand/Franklin	17	EB	Field Value	20	228	108	68	248	176	32	1188	80.8	424
Grand/Franklin	17	EB	Delay	20	336	0	68	356	68	0	1188	80.8	424
Grand/Franklin	17	EB	Queue	20	288	48	68	308	116	14	1188	80.8	424
Grand/Franklin	17	EB	Volume	20	192	144	68	212	212	43	1188	80.8	424
Grand/Franklin	17	EB	Flow Ratio	20	336	0	68	356	68	0	1188	80.8	424
Grand/Franklin	17	EB	Back of Queue	20	260	76	68	280	144	23	1188	80.8	424
Grand/Franklin	17	EB	Bonneson	20	329	7	68	349	75	2	1076	73.2	424
Grand/Franklin	17	WB	Field Value	156	492	540	44	648	584	52	356	15.7	1232
Grand/Franklin	17	WB	Delay	156	493	539	44	649	583	52	356	15.7	1232
Grand/Franklin	17	WB	Queue	156	481	551	44	637	595	53	356	15.7	1232
Grand/Franklin	17	WB	Volume	156	460	572	44	616	616	55	356	15.7	1232
Grand/Franklin	17	WB	Flow Ratio	156	487	545	44	643	589	53	356	15.7	1232
Grand/Franklin	17	WB	Back of Queue	156	501	531	44	657	575	51	356	15.7	1232
Grand/Franklin	17	WB	Bonneson	156	443	589	44	599	633	57	404	17.8	1232
Grand/Franklin	18	EB	Field Value	28	236	128	72	264	200	35	1200	86.4	464
Grand/Franklin	18	EB	Delay	28	364	0	72	392	72	0	1200	86.4	464
Grand/Franklin	18	EB	Queue	28	302	62	72	330	134	17	1200	86.4	464
Grand/Franklin	18	EB	Volume	28	204	160	72	232	232	44	1200	86.4	464
Grand/Franklin	18	EB	Flow Ratio	28	364	0	72	392	72	0	1200	86.4	464
Grand/Franklin	18	EB	Back of Queue	28	277	87	72	305	159	24	1200	86.4	464
Grand/Franklin	18	EB	Bonneson	28	356	8	72	384	80	2	1052	75.7	464
Grand/Franklin	18	WB	Field Value	152	452	596	4	604	600	57	392	1.6	1204
Grand/Franklin	18	WB	Delay	152	443	605	4	595	609	58	392	1.6	1204
Grand/Franklin	18	WB	Queue	152	444	604	4	596	608	58	392	1.6	1204
Grand/Franklin	18	WB	Volume	152	450	598	4	602	602	57	392	1.6	1204
Grand/Franklin	18	WB	Flow Ratio	152	444	604	4	596	608	58	392	1.6	1204

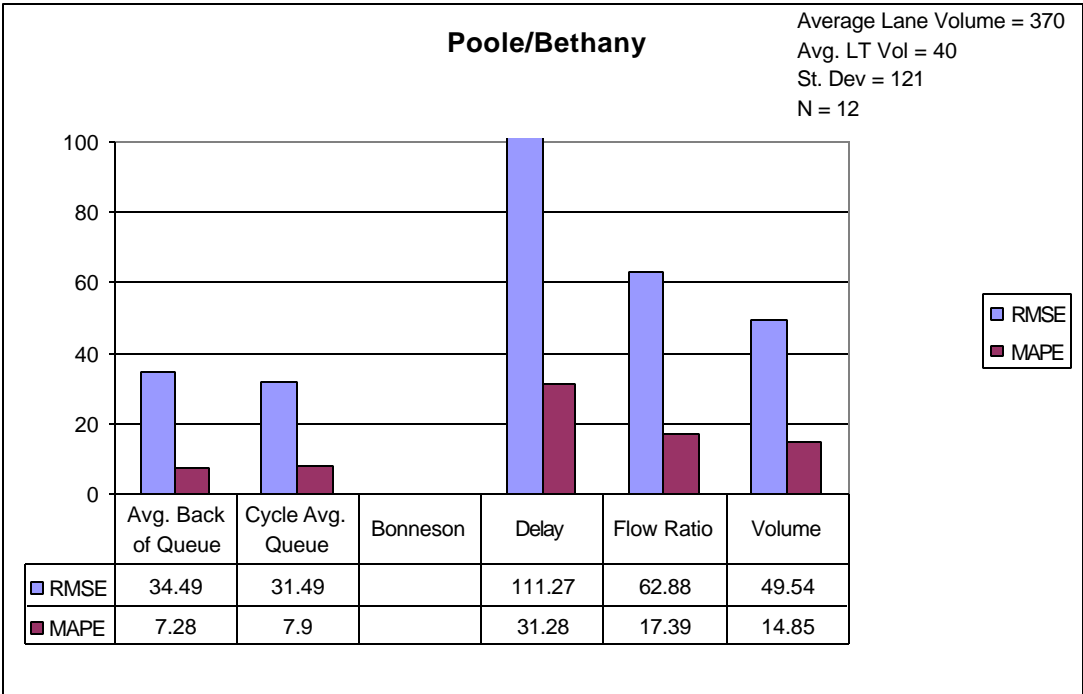
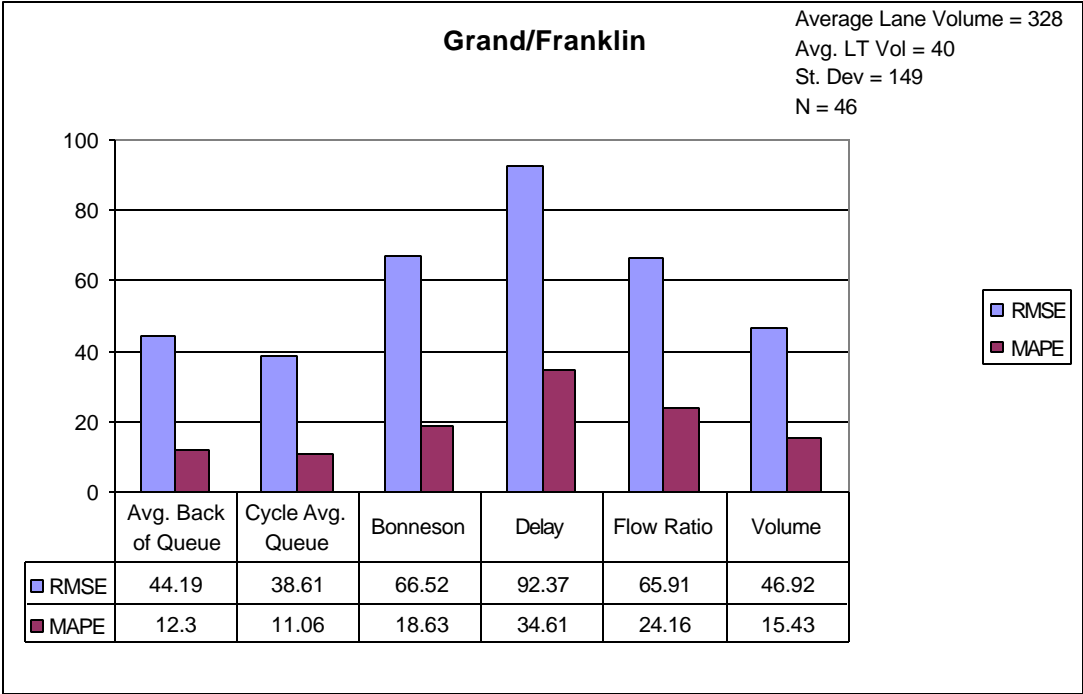
Intersection	Run		Criterion	RT Vol	TH Vol	TH Vol	LT Vol	Lane 1	Lane 2	%TH in	Opp	Conf Vol	Sub Vol
	Number	Approach			(rt lane)	(lt lane)		Vol	Vol	LT Lane			
Grand/Franklin	18	WB	Back of Queue	152	470	578	4	622	582	55	392	1.6	1204
Grand/Franklin	18	WB	Bonneson	152	420	628	4	572	632	60	436	1.7	1204
Grand/Franklin	19	EB	Field Value	20	248	148	40	268	188	37	1196	47.8	456
Grand/Franklin	19	EB	Delay	20	396	0	40	416	40	0	1196	47.8	456
Grand/Franklin	19	EB	Queue	20	258	138	40	278	178	35	1196	47.8	456
Grand/Franklin	19	EB	Volume	20	208	188	40	228	228	47	1196	47.8	456
Grand/Franklin	19	EB	Flow Ratio	20	337	59	40	357	99	15	1196	47.8	456
Grand/Franklin	19	EB	Back of Queue	20	258	138	40	278	178	35	1196	47.8	456
Grand/Franklin	19	EB	Bonneson	20	304	92	40	324	132	23	1040	41.6	456
Grand/Franklin	19	WB	Field Value	168	444	584	12	612	596	57	416	5.0	1208
Grand/Franklin	19	WB	Delay	168	445	583	12	613	595	57	416	5.0	1208
Grand/Franklin	19	WB	Queue	168	441	587	12	609	599	57	416	5.0	1208
Grand/Franklin	19	WB	Volume	168	436	592	12	604	604	58	416	5.0	1208
Grand/Franklin	19	WB	Flow Ratio	168	443	585	12	611	597	57	416	5.0	1208
Grand/Franklin	19	WB	Back of Queue	168	464	564	12	632	576	55	416	5.0	1208
Grand/Franklin	19	WB	Bonneson	168	408	620	12	576	632	60	436	5.2	1208
Grand/Franklin	20	EB	Field Value	24	264	140	48	288	188	35	1104	53.0	476
Grand/Franklin	20	EB	Delay	24	404	0	48	428	48	0	1104	53.0	476
Grand/Franklin	20	EB	Queue	24	272	132	48	296	180	33	1104	53.0	476
Grand/Franklin	20	EB	Volume	24	214	190	48	238	238	47	1104	53.0	476
Grand/Franklin	20	EB	Flow Ratio	24	341	63	48	365	111	16	1104	53.0	476
Grand/Franklin	20	EB	Back of Queue	24	266	138	48	290	186	34	1104	53.0	476
Grand/Franklin	20	EB	Bonneson	24	314	90	48	338	138	22	944	45.3	476
Grand/Franklin	20	WB	Field Value	176	344	584	16	520	600	63	428	6.8	1120
Grand/Franklin	20	WB	Delay	176	397	531	16	573	547	57	428	6.8	1120
Grand/Franklin	20	WB	Queue	176	389	539	16	565	555	58	428	6.8	1120
Grand/Franklin	20	WB	Volume	176	384	544	16	560	560	59	428	6.8	1120
Grand/Franklin	20	WB	Flow Ratio	176	394	534	16	570	550	58	428	6.8	1120
Grand/Franklin	20	WB	Back of Queue	176	413	515	16	589	531	55	428	6.8	1120
Grand/Franklin	20	WB	Bonneson	176	359	569	16	535	585	61	452	7.2	1120
Grand/Franklin	21	EB	Field Value	40	328	84	64	368	148	20	1200	76.8	516
Grand/Franklin	21	EB	Delay	40	412	0	64	452	64	0	1200	76.8	516
Grand/Franklin	21	EB	Queue	40	305	107	64	345	171	26	1200	76.8	516
Grand/Franklin	21	EB	Volume	40	218	194	64	258	258	47	1200	76.8	516
Grand/Franklin	21	EB	Flow Ratio	40	391	21	64	431	85	5	1200	76.8	516
Grand/Franklin	21	EB	Back of Queue	40	291	121	64	331	185	29	1200	76.8	516
Grand/Franklin	21	EB	Bonneson	40	373	39	64	413	103	9	1008	64.5	516
Grand/Franklin	21	WB	Field Value	200	452	548	8	652	556	55	452	3.6	1208
Grand/Franklin	21	WB	Delay	200	399	601	8	599	609	60	452	3.6	1208
Grand/Franklin	21	WB	Queue	200	401	599	8	601	607	60	452	3.6	1208
Grand/Franklin	21	WB	Volume	200	404	596	8	604	604	60	452	3.6	1208
Grand/Franklin	21	WB	Flow Ratio	200	400	600	8	600	608	60	452	3.6	1208
Grand/Franklin	21	WB	Back of Queue	200	425	575	8	625	583	57	452	3.6	1208
Grand/Franklin	21	WB	Bonneson	200	374	626	8	574	634	63	476	3.8	1208
Grand/Franklin	22	EB	Field Value	20	216	76	52	236	128	26	1056	54.9	364
Grand/Franklin	22	EB	Delay	20	292	0	52	312	52	0	1056	54.9	364
Grand/Franklin	22	EB	Queue	20	206	86	52	226	138	29	1056	54.9	364
Grand/Franklin	22	EB	Volume	20	162	130	52	182	182	45	1056	54.9	364
Grand/Franklin	22	EB	Flow Ratio	20	290	2	52	310	54	1	1056	54.9	364
Grand/Franklin	22	EB	Back of Queue	20	202	90	52	222	142	31	1056	54.9	364
Grand/Franklin	22	EB	Bonneson	20	238	54	52	258	106	18	948	49.3	364
Grand/Franklin	22	WB	Field Value	120	420	516	12	540	528	55	312	3.7	1068
Grand/Franklin	22	WB	Delay	120	427	509	12	547	521	54	312	3.7	1068
Grand/Franklin	22	WB	Queue	120	418	518	12	538	530	55	312	3.7	1068
Grand/Franklin	22	WB	Volume	120	414	522	12	534	534	56	312	3.7	1068
Grand/Franklin	22	WB	Flow Ratio	120	425	511	12	545	523	55	312	3.7	1068
Grand/Franklin	22	WB	Back of Queue	120	443	493	12	563	505	53	312	3.7	1068
Grand/Franklin	22	WB	Bonneson	120	390	546	12	510	558	58	344	4.1	1068
Grand/Franklin	23	EB	Field Value	48	160	68	84	208	152	30	952	80.0	360
Grand/Franklin	23	EB	Delay	48	228	0	84	276	84	0	952	80.0	360
Grand/Franklin	23	EB	Queue	48	194	34	84	242	118	15	952	80.0	360
Grand/Franklin	23	EB	Volume	48	132	96	84	180	180	42	952	80.0	360
Grand/Franklin	23	EB	Flow Ratio	48	228	0	84	276	84	0	952	80.0	360
Grand/Franklin	23	EB	Back of Queue	48	179	49	84	227	133	21	952	80.0	360
Grand/Franklin	23	EB	Bonneson	48	228	0	84	276	84	0	884	74.3	360
Grand/Franklin	23	WB	Field Value	96	384	472	28	480	500	55	276	7.7	980
Grand/Franklin	23	WB	Delay	96	428	428	28	524	456	50	276	7.7	980
Grand/Franklin	23	WB	Queue	96	408	448	28	504	476	52	276	7.7	980
Grand/Franklin	23	WB	Volume	96	394	462	28	490	490	54	276	7.7	980
Grand/Franklin	23	WB	Flow Ratio	96	417	439	28	513	467	51	276	7.7	980
Grand/Franklin	23	WB	Back of Queue	96	428	428	28	524	456	50	276	7.7	980
Grand/Franklin	23	WB	Bonneson	96	378	478	28	474	506	56	312	8.7	980
Peace/St Mary's	1	WB	Field Value	83	213	237	35	296	272	53	521	18.2	568
Peace/St Mary's	1	WB	Delay	83	265	185	35	348	220	41	521	18.2	568
Peace/St Mary's	1	WB	Queue	83	215	235	35	298	270	52	521	18.2	568
Peace/St Mary's	1	WB	Volume	83	201	249	35	284	284	55	521	18.2	568
Peace/St Mary's	1	WB	Flow Ratio	83	246	204	35	329	239	45	521	18.2	568
Peace/St Mary's	1	WB	Back of Queue	83	225	225	35	308	260	50	521	18.2	568
Peace/St Mary's	1	WB	Bonneson	83	199	251	35	282	286	56	465	16.3	568
Peace/St Mary's	2	WB	Field Value	81	150	181	50	231	231	55	595	29.8	463
Peace/St Mary's	2	WB	Delay	81	246	86	50	327	136	26	594	29.7	463
Peace/St Mary's	2	WB	Queue	81	166	166	50	247	216	50	594	29.7	463
Peace/St Mary's	2	WB	Volume	81	150	182	50	231	232	55	594	29.7	463
Peace/St Mary's	2	WB	Flow Ratio	81	213	119	50	294	169	36	594	29.7	463

Intersection	Run		Criterion	RT Vol	TH Vol	TH Vol	Lane 1		Lane 2		%TH in	Opp	Conf Vol	Sub Vol
	Number	Approach			(rt lane)	(lt lane)	LT Vol	Vol	Vol	LT Lane	Vol			
Peace/St Mary's	2	WB	Back of Queue	81	172	160	50	253	210	48	594	29.7	463	
Peace/St Mary's	2	WB	Bonneson	81	157	174	50	238	224	53	552	27.6	462	
Peace/St Mary's	3	WB	Field Value	57	212	208	45	269	253	50	432	19.4	522	
Peace/St Mary's	3	WB	Delay	57	270	150	45	327	195	36	433	19.5	522	
Peace/St Mary's	3	WB	Queue	57	210	210	45	267	255	50	433	19.5	522	
Peace/St Mary's	3	WB	Volume	57	204	216	45	261	261	51	433	19.5	522	
Peace/St Mary's	3	WB	Flow Ratio	57	251	169	45	308	214	40	433	19.5	522	
Peace/St Mary's	3	WB	Back of Queue	57	225	195	45	282	240	46	433	19.5	522	
Peace/St Mary's	3	WB	Bonneson	57	205	215	45	262	260	51	387	17.4	522	
Peace/St Mary's	4	WB	Field Value	90	200	265	16	290	281	57	608	9.7	571	
Peace/St Mary's	4	WB	Delay	90	232	232	16	322	248	50	609	9.7	570	
Peace/St Mary's	4	WB	Queue	90	212	252	16	302	268	54	609	9.7	570	
Peace/St Mary's	4	WB	Volume	90	195	269	16	285	285	58	609	9.7	570	
Peace/St Mary's	4	WB	Flow Ratio	90	227	237	16	317	253	51	609	9.7	570	
Peace/St Mary's	4	WB	Back of Queue	90	216	248	16	306	264	53	609	9.7	570	
Peace/St Mary's	4	WB	Bonneson	90	186	279	16	276	295	60	551	8.8	571	
Peace/St Mary's	5	WB	Field Value	69	229	249	28	298	277	52	490	13.7	575	
Peace/St Mary's	5	WB	Delay	69	269	209	28	338	237	44	489	13.7	575	
Peace/St Mary's	5	WB	Queue	69	239	239	28	308	267	50	489	13.7	575	
Peace/St Mary's	5	WB	Volume	69	218	260	28	287	288	54	489	13.7	575	
Peace/St Mary's	5	WB	Flow Ratio	69	257	221	28	326	249	46	489	13.7	575	
Peace/St Mary's	5	WB	Back of Queue	69	239	239	28	308	267	50	489	13.7	575	
Peace/St Mary's	5	WB	Bonneson	69	213	265	28	282	293	55	457	12.8	575	
Peace/St Mary's	6	WB	Field Value	98	265	249	36	363	285	48	535	19.3	648	
Peace/St Mary's	6	WB	Delay	98	288	226	36	386	262	44	535	19.3	648	
Peace/St Mary's	6	WB	Queue	98	242	272	36	340	308	53	535	19.3	648	
Peace/St Mary's	6	WB	Volume	98	226	288	36	324	324	56	535	19.3	648	
Peace/St Mary's	6	WB	Flow Ratio	98	272	242	36	370	278	47	535	19.3	648	
Peace/St Mary's	6	WB	Back of Queue	98	252	262	36	350	298	51	535	19.3	648	
Peace/St Mary's	6	WB	Bonneson	98	223	291	36	321	327	57	510	18.4	648	
Peace/St Mary's	7	WB	Field Value	73	294	233	90	367	323	44	604	54.4	690	
Peace/St Mary's	7	WB	Delay	73	410	118	90	483	208	22	604	54.4	691	
Peace/St Mary's	7	WB	Queue	73	304	224	90	377	314	42	604	54.4	691	
Peace/St Mary's	7	WB	Volume	73	273	255	90	346	345	48	604	54.4	691	
Peace/St Mary's	7	WB	Flow Ratio	73	367	161	90	440	251	30	604	54.4	691	
Peace/St Mary's	7	WB	Back of Queue	73	315	213	90	388	303	40	604	54.4	691	
Peace/St Mary's	7	WB	Bonneson	73	312	215	90	385	305	41	604	54.4	690	
Peace/St Mary's	8	WB	Field Value	49	286	216	61	335	277	43	600	36.6	612	
Peace/St Mary's	8	WB	Delay	49	359	143	61	408	204	28	601	36.7	612	
Peace/St Mary's	8	WB	Queue	49	271	231	61	320	292	46	601	36.7	612	
Peace/St Mary's	8	WB	Volume	49	257	245	61	306	306	49	601	36.7	612	
Peace/St Mary's	8	WB	Flow Ratio	49	330	172	61	379	233	34	601	36.7	612	
Peace/St Mary's	8	WB	Back of Queue	49	288	214	61	337	275	43	601	36.7	612	
Peace/St Mary's	8	WB	Bonneson	49	272	230	61	321	291	46	571	34.8	612	
Peace/St Mary's	9	WB	Field Value	73	286	225	49	359	274	44	633	31.0	633	
Peace/St Mary's	9	WB	Delay	73	336	176	49	409	225	34	633	31.0	634	
Peace/St Mary's	9	WB	Queue	73	266	246	49	339	295	48	633	31.0	634	
Peace/St Mary's	9	WB	Volume	73	244	268	49	317	317	52	633	31.0	634	
Peace/St Mary's	9	WB	Flow Ratio	73	309	203	49	382	252	40	633	31.0	634	
Peace/St Mary's	9	WB	Back of Queue	73	275	237	49	348	286	46	633	31.0	634	
Peace/St Mary's	9	WB	Bonneson	73	252	259	49	325	308	51	580	28.4	633	
Peace/St Mary's	10	WB	Field Value	102	253	225	24	355	249	47	653	15.7	604	
Peace/St Mary's	10	WB	Delay	102	259	219	24	361	243	46	654	15.7	604	
Peace/St Mary's	10	WB	Queue	102	214	264	24	316	288	55	654	15.7	604	
Peace/St Mary's	10	WB	Volume	102	200	278	24	302	302	58	654	15.7	604	
Peace/St Mary's	10	WB	Flow Ratio	102	244	234	24	346	258	49	654	15.7	604	
Peace/St Mary's	10	WB	Back of Queue	102	224	254	24	326	278	53	654	15.7	604	
Peace/St Mary's	10	WB	Bonneson	102	194	284	24	296	308	59	595	14.3	604	
Peace/St Mary's	11	WB	Field Value	110	315	265	32	425	297	46	599	19.2	722	
Peace/St Mary's	11	WB	Delay	110	315	265	32	425	297	46	599	19.2	722	
Peace/St Mary's	11	WB	Queue	110	270	310	32	380	342	53	599	19.2	722	
Peace/St Mary's	11	WB	Volume	110	251	329	32	361	361	57	599	19.2	722	
Peace/St Mary's	11	WB	Flow Ratio	110	299	281	32	409	313	48	599	19.2	722	
Peace/St Mary's	11	WB	Back of Queue	110	280	300	32	390	332	52	599	19.2	722	
Peace/St Mary's	11	WB	Bonneson	110	246	334	32	356	366	58	542	17.3	722	
Peace/St Mary's	12	WB	Field Value	102	327	290	45	429	335	47	604	27.2	764	
Peace/St Mary's	12	WB	Delay	102	353	263	45	455	308	43	605	27.2	763	
Peace/St Mary's	12	WB	Queue	102	308	308	45	410	353	50	605	27.2	763	
Peace/St Mary's	12	WB	Volume	102	279	337	45	381	382	55	605	27.2	763	
Peace/St Mary's	12	WB	Flow Ratio	102	334	282	45	436	327	46	605	27.2	763	
Peace/St Mary's	12	WB	Back of Queue	102	313	303	45	415	348	49	605	27.2	763	
Peace/St Mary's	12	WB	Bonneson	102	282	335	45	384	380	54	543	24.4	764	
Peace/St Mary's	13	WB	Field Value	81	225	249	57	306	306	53	456	26.0	612	
Peace/St Mary's	13	WB	Delay	81	298	176	57	379	233	37	456	26.0	612	
Peace/St Mary's	13	WB	Queue	81	237	237	57	318	294	50	456	26.0	612	
Peace/St Mary's	13	WB	Volume	81	225	249	57	306	306	53	456	26.0	612	
Peace/St Mary's	13	WB	Flow Ratio	81	279	195	57	360	252	41	456	26.0	612	
Peace/St Mary's	13	WB	Back of Queue	81	252	222	57	333	279	47	456	26.0	612	
Peace/St Mary's	13	WB	Bonneson	81	231	243	57	312	300	51	456	26.0	612	
Peace/St Mary's	14	WB	Field Value	85	216	200	36	301	236	48	432	15.6	537	
Peace/St Mary's	14	WB	Delay	85	238	178	36	323	214	43	433	15.6	537	
Peace/St Mary's	14	WB	Queue	85	193	223	36	278	259	54	433	15.6	537	
Peace/St Mary's	14	WB	Volume	85	183	233	36	268	269	56	433	15.6	537	
Peace/St Mary's	14	WB	Flow Ratio	85	224	192	36	309	228	46	433	15.6	537	

Intersection	Run		Criterion	RT Vol	TH Vol	TH Vol	LT Vol	Lane 1	Lane 2	%TH in	Opp	Conf Vol	Sub Vol
	Number	Approach			(rt lane)	(lt lane)		Vol	Vol	LT Lane	Vol		
Peace/St Mary's	14	WB	Back of Queue	85	208	208	36	293	244	50	433	15.6	537
Peace/St Mary's	14	WB	Bonneson	85	180	236	36	265	272	57	391	14.1	537
Peace/St Mary's	15	WB	Field Value	112	163	205	65	275	270	56	392	25.5	545
Peace/St Mary's	15	WB	Delay	112	229	139	65	341	204	38	392	25.5	545
Peace/St Mary's	15	WB	Queue	112	169	199	65	281	264	54	392	25.5	545
Peace/St Mary's	15	WB	Volume	112	160	208	65	272	273	57	392	25.5	545
Peace/St Mary's	15	WB	Flow Ratio	112	209	159	65	321	224	43	392	25.5	545
Peace/St Mary's	15	WB	Back of Queue	112	184	184	65	296	249	50	392	25.5	545
Peace/St Mary's	15	WB	Bonneson	112	168	200	65	280	265	54	387	25.2	545
Poole/Beverly	1	EB	Field Value	120	262	447	0	382	447	63	553	0.0	829
Poole/Beverly	1	EB	Delay	120	274	434	0	394	434	61	552	0.0	828
Poole/Beverly	1	EB	Queue	120	314	394	0	434	394	56	552	0.0	828
Poole/Beverly	1	EB	Volume	120	294	414	0	414	414	58	552	0.0	828
Poole/Beverly	1	EB	Flow Ratio	120	283	425	0	403	425	60	552	0.0	828
Poole/Beverly	1	EB	Back of Queue	120	314	394	0	434	394	56	552	0.0	828
Poole/Beverly	1	WB	Field Value	0	375	178	76	375	255	32	829	63.3	629
Poole/Beverly	1	WB	Delay	0	516	36	76	516	112	7	828	62.9	628
Poole/Beverly	1	WB	Queue	0	356	196	76	356	272	36	828	62.9	628
Poole/Beverly	1	WB	Volume	0	314	238	76	314	314	43	828	62.9	628
Poole/Beverly	1	WB	Flow Ratio	0	427	125	76	427	201	23	828	62.9	628
Poole/Beverly	1	WB	Back of Queue	0	361	191	76	361	267	35	828	62.9	628
Poole/Beverly	2	EB	Field Value	129	234	455	0	363	455	66	530	0.0	818
Poole/Beverly	2	EB	Delay	129	264	424	0	393	424	62	530	0.0	817
Poole/Beverly	2	EB	Queue	129	269	419	0	398	419	61	530	0.0	817
Poole/Beverly	2	EB	Volume	129	279	409	0	408	409	59	530	0.0	817
Poole/Beverly	2	EB	Flow Ratio	129	268	420	0	397	420	61	530	0.0	817
Poole/Beverly	2	EB	Back of Queue	129	299	389	0	428	389	57	530	0.0	817
Poole/Beverly	2	WB	Field Value	0	363	167	79	363	246	31	818	64.8	609
Poole/Beverly	2	WB	Delay	0	530	0	79	530	79	0	817	64.5	609
Poole/Beverly	2	WB	Queue	0	350	180	79	350	259	34	817	64.5	609
Poole/Beverly	2	WB	Volume	0	305	225	79	305	304	42	817	64.5	609
Poole/Beverly	2	WB	Flow Ratio	0	422	108	79	422	187	20	817	64.5	609
Poole/Beverly	2	WB	Back of Queue	0	355	175	79	355	254	33	817	64.5	609
Poole/Beverly	3	EB	Field Value	134	284	462	0	418	462	62	673	0.0	880
Poole/Beverly	3	EB	Delay	134	293	453	0	427	453	61	672	0.0	880
Poole/Beverly	3	EB	Queue	134	313	433	0	447	433	58	672	0.0	880
Poole/Beverly	3	EB	Volume	134	306	440	0	440	440	59	672	0.0	880
Poole/Beverly	3	EB	Flow Ratio	134	295	451	0	429	451	60	672	0.0	880
Poole/Beverly	3	EB	Back of Queue	134	327	419	0	461	419	56	672	0.0	880
Poole/Beverly	3	WB	Field Value	0	430	243	69	430	312	36	880	60.6	742
Poole/Beverly	3	WB	Delay	0	596	76	69	596	145	11	880	60.7	741
Poole/Beverly	3	WB	Queue	0	427	245	69	427	314	36	880	60.7	741
Poole/Beverly	3	WB	Volume	0	371	301	69	371	370	45	880	60.7	741
Poole/Beverly	3	WB	Flow Ratio	0	494	178	69	494	247	26	880	60.7	741
Poole/Beverly	3	WB	Back of Queue	0	431	241	69	431	310	36	880	60.7	741
Poole/Beverly	4	EB	Field Value	122	321	485	0	443	485	60	650	0.0	929
Poole/Beverly	4	EB	Delay	122	327	479	0	449	479	59	650	0.0	928
Poole/Beverly	4	EB	Queue	122	343	463	0	465	463	57	650	0.0	928
Poole/Beverly	4	EB	Volume	122	342	464	0	464	464	58	650	0.0	928
Poole/Beverly	4	EB	Flow Ratio	122	331	475	0	453	475	59	650	0.0	928
Poole/Beverly	4	EB	Back of Queue	122	363	443	0	485	443	55	650	0.0	928
Poole/Beverly	4	WB	Field Value	0	455	195	73	455	268	30	929	67.4	722
Poole/Beverly	4	WB	Delay	0	605	45	73	605	118	7	928	67.7	723
Poole/Beverly	4	WB	Queue	0	418	232	73	418	305	36	928	67.7	723
Poole/Beverly	4	WB	Volume	0	362	288	73	362	361	44	928	67.7	723
Poole/Beverly	4	WB	Flow Ratio	0	492	158	73	492	231	24	928	67.7	723
Poole/Beverly	4	WB	Back of Queue	0	419	231	73	419	304	36	928	67.7	723
Poole/Beverly	5	EB	Field Value	220	338	566	0	558	566	63	544	0.0	1124
Poole/Beverly	5	EB	Delay	220	317	587	0	537	587	65	544	0.0	1124
Poole/Beverly	5	EB	Queue	220	352	552	0	572	552	61	544	0.0	1124
Poole/Beverly	5	EB	Volume	220	342	562	0	562	562	62	544	0.0	1124
Poole/Beverly	5	EB	Flow Ratio	220	322	582	0	542	582	64	544	0.0	1124
Poole/Beverly	5	EB	Back of Queue	220	367	537	0	587	537	59	544	0.0	1124
Poole/Beverly	5	WB	Field Value	0	351	193	83	351	277	35	1124	93.7	628
Poole/Beverly	5	WB	Delay	0	544	0	83	544	83	0	1124	93.3	627
Poole/Beverly	5	WB	Queue	0	407	137	83	407	220	25	1124	93.3	627
Poole/Beverly	5	WB	Volume	0	314	230	83	314	313	42	1124	93.3	627
Poole/Beverly	5	WB	Flow Ratio	0	501	43	83	501	126	8	1124	93.3	627
Poole/Beverly	5	WB	Back of Queue	0	382	162	83	382	245	30	1124	93.3	627
Poole/Beverly	6	EB	Field Value	189	326	471	0	514	471	59	437	0.0	986
Poole/Beverly	6	EB	Delay	189	283	513	0	472	513	64	436	0.0	985
Poole/Beverly	6	EB	Queue	189	295	501	0	484	501	63	436	0.0	985
Poole/Beverly	6	EB	Volume	189	303	493	0	492	493	62	436	0.0	985
Poole/Beverly	6	EB	Flow Ratio	189	286	510	0	475	510	64	436	0.0	985
Poole/Beverly	6	EB	Back of Queue	189	323	473	0	512	473	59	436	0.0	985
Poole/Beverly	6	WB	Field Value	0	343	94	111	343	206	22	986	109.8	549
Poole/Beverly	6	WB	Delay	0	437	-1	111	437	110	0	985	109.3	547
Poole/Beverly	6	WB	Queue	0	358	78	111	358	189	18	985	109.3	547
Poole/Beverly	6	WB	Volume	0	274	162	111	274	273	37	985	109.3	547
Poole/Beverly	6	WB	Flow Ratio	0	437	-1	111	437	110	0	985	109.3	547
Poole/Beverly	6	WB	Back of Queue	0	334	102	111	334	213	23	985	109.3	547

APPENDIX E

RMSE/MAPE OUTPUT FOR INDIVIDUAL INTERSECTIONS



Peace/St. Mary's

Average Lane Volume = 277
 Avg. LT Vol = 44
 St. Dev = 29
 N = 15

